

# Dynamics and Control of a Tensegrity System in Low-Earth Orbit

Maria del Carmen Rye

Dissertation submitted to the Faculty of the  
Virginia Polytechnic Institute and State University  
in partial fulfillment of the requirements for the degree of

Doctor of Philosophy

in

Aerospace Engineering

Cornel Sultan, Chair

Craig Woolsey

Michael Philen

Gary Seidel

March 24, 2017

Blacksburg, Virginia

Keywords: Tensegrity, Gravity Gradient, Spacecraft, Flexible Structures

Copyright 2017, Maria Rye

# Dynamics and Control of Tensegrity Systems in Low-Earth Orbit

Maria del Carmen Rye

## ABSTRACT

Low-Earth orbit (LEO) is an environment where the effects of the Earth's gravitational field are still strong enough to produce potentially detrimental distortions of large flexible structures. One such example is a tensegrity system, which is held in balance by an assortment of interconnected bars and cables to form a self-standing but ultimately flexible structure. This thesis derives the dynamics of such a structure in the gravity field of LEO, including the distortion of the structure due to the motions of the individual bars and the changes in attitude of the spacecraft. Methods of linear control are discussed for minimizing or controlling these gravity-induced distortions.

Funding for this research was provided by the Aerospace Department at Virginia Tech, the College of Engineering, the Multicultural Academic Opportunities Program, and the Virginia Space Grant Consortium. This work was also supported by the National Science Foundation under the grant CMMI-0952558.

# Dynamics and Control of Tensegrity Systems in Low-Earth Orbit

Maria del Carmen Rye

GENERAL AUDIENCE ABSTRACT

Tensegrity is the name given to a system of interconnected bars and tendons that can form a flexible self-standing structure. Its flexibility is due to the ability of the bars to move near-independent to each other, movement that can be caused by controlled tension forces in the tendons or external forces such as gravity. However, a balance of sorts must be maintained - if a tendon were to go slack, the entire structure could become unstable and collapse on itself.

This thesis looks at placing a tensegrity structure in orbit around the Earth. As a spacecraft's orbit is moved further away from the Earth, the strength of the Earth's gravity field lessens. Ideally, such a flexible structure would be placed far enough away from the Earth so that the gravity field would have too weak an impact on its individual elements to cause major distortions. However, the author recognizes that altitudes below 2,000 km, where the Earth's gravity field is still very prevalent, are the most common altitudes used by orbiting spacecraft today. The goal of this thesis is to analyze the distortions of the tensegrity structure at these lower altitudes, and also look at methods for controlling these distortions.

Funding for this research was provided by the Aerospace Department at Virginia Tech, the College of Engineering, the Multicultural Academic Opportunities Program, and the Virginia Space Grant Consortium. This work was also supported by the National Science Foundation under the grant CMMI-0952558.

# Acknowledgments

I would like to take this opportunity to extend my sincerest appreciation to all those that have guided me towards the completion of this dissertation.

To my advisor, Dr. Cornel Sultan, who has been of constant support since bringing me on into his graduate group in 2012. His advice and guidance in my research has been invaluable, and his patience with my schedule and outside work has seemed unlimited. Thank you for continuing to push me towards the completion of my degree.

To my committee, Dr. Craig Woolsey, Dr. Michael Philen, and Dr. Gary Seidel, whose advice and suggestions regarding my research have been taken to heart.

To the Multicultural Academic Opportunities Program, for its resources and support; specifically, to Dr. Jody Thompson Marshall, whose counseling throughout the period I was a part of the program was greatly appreciated.

To my parents, who are always pushing me to success, and to my sister, who is always there for me to rant to about my parents always pushing me.

To the Air Transportation Systems Laboratory, and Dr. Antonio Trani, for whom I worked for occasionally throughout my degree. If it weren't for you, my knowledge of MATLAB would never have reached such heights, and my financial situation as a graduate student would have been even more stressful.

And finally, to my good friend Mr. Howard Swingle. Thank you for being there through the entire long hard road of my academic career. It will take many years of IT support for me to ever come close to paying that debt.

# Contents

<b>1</b>	<b>Literature Review</b>	<b>1</b>
<b>2</b>	<b>General Dynamics</b>	<b>11</b>
2.1	Kinetic Energy . . . . .	20
2.1.1	Translational Kinetic Energy . . . . .	20
2.1.2	Rotational Kinetic Energy . . . . .	21
2.1.3	Total Kinetic Energy . . . . .	23
2.2	Gravitational Effects . . . . .	23
2.2.1	Gravity Potential Energy . . . . .	27
2.2.2	Gravity Generalized Forces . . . . .	30
2.3	Elastic Potential Energy . . . . .	36
2.4	Thruster Generalized Forces . . . . .	37

2.5	General Equations of Motion . . . . .	39
<b>3</b>	<b>General Control</b>	<b>40</b>
3.1	Linearization . . . . .	41
3.2	LQR Control . . . . .	47
<b>4</b>	<b>Application to Simple Tensegrity Spacecraft</b>	<b>51</b>
4.1	Spacecraft Base . . . . .	51
4.1.1	Base Kinetic Energy . . . . .	52
4.1.2	Gravitational Effects . . . . .	60
4.1.3	Methods of Passive Control . . . . .	67
4.2	3-Bar Tensegrity Structure . . . . .	76
4.2.1	Kinetic Energy . . . . .	80
4.2.2	Generalized Gravitational Force . . . . .	85
4.2.3	Tensegrity Elastic Potential Energy . . . . .	86
4.2.4	Tensegrity Prestressed Equilibrium . . . . .	87
4.2.5	Desired Configuration . . . . .	98
4.2.6	LQR Control . . . . .	105



4.3	6-Bar Tensegrity Structure . . . . .	120
4.3.1	Kinetic Energy . . . . .	122
4.3.2	Generalized Gravitational Forces . . . . .	128
4.3.3	Tensegrity Elastic Potential Energy . . . . .	129
4.3.4	Desired Configuration . . . . .	130
<b>5</b>	<b>Conclusions</b>	<b>134</b>
5.1	Future Work . . . . .	135
	<b>Bibliography</b>	<b>142</b>

# List of Figures

1.1	The Needle Tower at Hirshhorn Museum and Sculpture Garden in Washington D.C., created by Kenneth Snelson in 1968 using aluminum and stainless steel. The structure itself stands at 60 feet in height.[1]	2
1.2	Sketch of the structure of the Georgia Dome in Atlanta, GA. The dome spans a length of nearly 800 feet and consists of interconnected cables and beams in a triangular truss pattern. It is built to withstand environmental loads such as snow, wind, and temperature.[2]	4
1.3	A generic simple tensegrity structure. Tensegrity consists of a collection of rigid bars (the thicker elements in the diagram) connected by a web of tendons (the thinner elements). The motion of one element of the system impacts the motion and forces on the others.	5
1.4	Tensegrity 1g habitation module proposed by Dr. Skelton and Dr. Longman. This research was rewarded a NASA NIAC 2013 Phase 1 grant to investigate the feasibility of such a structure.[3]	6

1.5	A deployable tensegrity system, in both the collapsed and expanded configurations.[4] The shape of the tensegrity structure is changed by modifying the lengths of the tendons, which can be done, for example, by means of actuators or piezoelectric materials. . . . .	7
1.6	Harris Corporation deployable 18-meter antenna. This specific antenna was used for S-band communications on the TerreStar-1 satellite, launched in 2009.[5]	9
2.1	Earth-centered inertial frame $\{\mathbf{i}\}$ and spacecraft position. The position vector $\mathbf{r}_0$ of the spacecraft relative to the center of the Earth is a function of the orbit radius $R$ and the latitude and longitude angles $\phi$ and $\delta$ . . . . .	17
2.2	Base-centered orbital frame $\{\mathbf{o}\}$ and body frame $\{\mathbf{b}\}$ . The $\{\mathbf{o}_\phi, \mathbf{o}_\lambda, \mathbf{o}_r\}$ axes are the $\{1, 2, 3\}$ axes of the orbital frame. The axes of the body frame lie along the principal axes of the base. . . . .	18
2.3	The bar-centered body frame for the $i$ th bar is defined at the center of mass of the bar. Each bar is oriented an angle $\alpha$ and $\delta$ (referred to as the ascension and declination angles) from the base body frame $\{\mathbf{b}\}$ . An endpoint of the bar (point $A_i$ ) is located at a distance $[x_i, y_i, z_i]^t$ from the center of mass of the base. . . . .	19

2.4	The concept of gravity gradient, as illustrated by Pierre Bely.[6] This diagram shows the gravity forces on two point masses connected via a massless rod, where the force on $m_1$ will be greater than that on $m_2$ and will thus induce a moment. The analysis in this thesis spreads these point masses out to a long rigid body; in the case of a tensegrity structure, the long bars. The gravity force along the length of the bar will vary, and will similarly induce a moment on the bar. . . . .	25
2.5	Parameters defining orbiting rigid body. The vector $\mathbf{R}$ is the position of the center of mass of the body relative to the Earth center, whereas $\mathbf{r}$ is the vector from the mass center of the body to a differential mass $dm$ in the body. $\mathbf{R}$ lies along the orbit radius direction $\mathbf{o}_r$ . The Earth-centered frame pictured is an inertial frame. . . . .	26
4.1	Position vectors and dimensions of rectangular-prism spacecraft base. The base has dimensions along its $\{1, 2, 3\}$ principal axes of $D_1$ , $D_2$ , and $D_3$ , respectively. As the base is considered a rigid body, these dimensions are remain static. . . . .	52
4.2	Dimensions of a rectangular prism base, $\{D_1, D_2, D_3\}$ . . . . .	73

4.3	Stability regions for a rigid body in a circular orbit, where the unshaded regions denote Lyapunov (neutral) stability. It is beneficial to design the rigid body such that its principal moments of inertial lead to Lyapunov stability. The shaded region above the diagonal denotes a body with unstable pitch ( $\theta_3$ ) authority, whereas shaded regions below the diagonal denote unstable roll or yaw ( $\theta_1, \theta_2$ ) authority.[7] . . . . .	74
4.4	Unstable dynamics of an orbiting rigid body where all the conditions for neutral stability are not met; specifically in this case ( $k_2 \not> k_1$ ). The attitude of the rigid body slowly diverges from the desired orientation. . . . .	75
4.5	Dynamics of an orbiting rigid body where all the conditions for neutral stability are met. This system is neutrally stable since it never converges to an equilibrium, but rather fluctuates around the equilibrium. . . . .	75
4.6	A simple 3-bar tensegrity structure mounted to an orbiting rectangular prism base. The moments of inertia of the base are chosen to induce some amount of passive stability (see previous section about Lyapunov stability). The bars are attached to the base at one end; the other ends are constrained by the web of 6 elastic tendons. . . . .	78

4.7	The position vector of the center of mass of the bar with respect to the inertial frame $\{\mathbf{i}\}$ is found by summing the position vector to the base $\mathbf{r}_0$ and the position vector from the base to the $i$ th bar center $\mathbf{r}_i$ . This vector can be further split into a static vector BA (which defines the position of the bar connection points) and the vector AC (whose magnitude remains static, but whose direction is defined by the angles $\alpha_i$ and $\delta_i$ . . . . .	79
4.8	Assigned indices to bars and tendons that make up the 3-bar tensegrity structure. A tendon force $F_j$ means a tendon force in the $j$ th tendon, according to this diagram.[8] . . . . .	93
4.9	Top view looking down along $\mathbf{b}_3$ axis of 3-bar tensegrity structure. The symmetry of the structure is apparent.[8] . . . . .	94
4.10	For a chosen $\delta$ that falls between 0 and $\pi$ , and the symmetric configuration suggested, the limits of $\alpha$ are depicted above. Note the fairly small range of $\alpha$ for which the tensegrity structure will meet the conditions of prestressability (i.e. all tendons in a state of stress). . . . .	95
4.11	Plot of area where tensions in the vertical three tendons $F_{1,2,3}$ are positive. If an angle $\alpha$ or $\delta$ is chosen outside this shaded region, the tendon will be slack and the tensegrity structure will risk collapse. . . . .	96

4.12	Plot of area where tensions in the top three horizontal tendons $F_{4,5,6}$ are positive. If an angle $\alpha$ or $\delta$ is chosen outside this shaded region, the tendon will be slack and the tensegrity structure will risk collapse. . . . .	97
4.13	Desired orbit configuration chosen for tensegrity spacecraft. The orbit is a synchronous one, meaning that the same face of the spacecraft (the bottom of the base) is always pointed along the negative orbital radius vector (i.e. pointed towards the earth). This also means the body frame of the base $\{\mathbf{b}\}$ coincides with the orbital frame $\{\mathbf{o}\}$ (the Euler angles relating the two are all zero). If the spacecraft is in a circular orbit about an assumed-spherical Earth, this means that the spacecraft will be subject to the same gravitational forces throughout its orbit. . . . .	104
4.14	Response for the base attitude angles $\theta_1, \theta_2, \theta_3$ for their perturbation from equilibrium of $1^\circ$ . The base is quickly returned to equilibrium by the thruster controls. . . . .	108
4.15	Response for the bar orientation angles $\alpha_{1,2,3}$ and $\delta_{1,2,3}$ for the perturbed attitude angles. Although the bars are not initially perturbed, their motion is affected by the oscillation of the base. Note how the response of the bars follows that of the base. When the base finally stills about its equilibrium, it is no longer affecting the bars, and therefore the bars stop oscillating as well. . . . .	109
4.16	Zoomed into initial response of Figure 4.14. . . . .	110

4.17	Zoomed into initial response of Figure 4.15. . . . .	111
4.18	Response for the base attitude angles $\theta_1, \theta_2, \theta_3$ for the perturbed bar orientation angles. The steady state response of the base is a continuous oscillation about its equilibrium, which is due to the thruster controls constantly making minute adjustments to the base as it moves about the Earth. The increase in amplitude towards the beginning of the time frame is due to the movement of the bars upon the base, as they work to return from their initial perturbation back to their equilibrium state. . . . .	112
4.19	Response for $\alpha_{1,2,3}$ and $\delta_{1,2,3}$ for a perturbation of $\{0.1, 0.2, 0.3\}^\circ$ , respectively. The bars are quickly returned to their equilibrium configuration. . . . .	113
4.20	Zoomed into initial response of Figure 4.18. . . . .	114
4.21	Zoomed into initial response of Figure 4.19. . . . .	115
4.22	Response for the base attitude angles $\theta_1, \theta_2, \theta_3$ at the desired configuration. The sharper oscillations are due to the response of the bars that sit atop the base. . . . .	116
4.23	Response for the bar orientation angles $\alpha_{1,2,3}$ and $\delta_{1,2,3}$ at the desired configuration. Note that the bars oscillate along with the oscillating base. . . . .	117
4.24	Nonlinear response for the base attitude angles $\theta_1, \theta_2, \theta_3$ due to the perturbed bars under the LQR control law. . . . .	118



4.25	Nonlinear response for the bar orientation angles $\alpha_{1,2,3}$ and $\delta_{1,2,3}$ perturbed from the desired configuration by $\{0.1, 0.2, 0.3\}^\circ$ for the first, second, and third bar angles, respectively. Note that the bars oscillate along with the oscillating base. . . . .	119
4.26	A slightly more complex tensegrity structure is one with 6 bars and 12 elastic tendons, where one of the ends of the lower bars are constrained to the base, and one of the ends of the upper bars are constrained to some massless plate. Both the bottom and top connection points form an equilateral triangle of the same size. . . . .	132
4.27	Position vectors to the center of mass of a bar not constrained to the base. The position of the bar relative to the base center of mass is given by the vector $[x_i, y_i, z_i]^t$ that defines the location of one end of the bar. The orientation of the bar is given by the angles $\alpha_i$ and $\delta_i$ measured from the axes of the $\{\mathbf{b}\}$ frame. . . . .	133

# List of Tables

4.1	Parameter values for simulation. . . . .	92
-----	--	----

# List of Symbols

$\phi$	latitudinal angle
$\Psi$	gravitational potential
$\alpha$	angle of bar measured from $\mathbf{b}_1$
$\delta$	angle of bar measured from $\mathbf{b}_3$
$\lambda$	longitudinal angle
$\mu$	Earth gravitational parameter
$\boldsymbol{\omega}_i$	angular velocity of $i$ th body
$\theta_1$	third rotation angle from $\{\mathbf{o}\}$ to $\{\mathbf{b}\}$
$\theta_2$	second rotation angle from $\{\mathbf{o}\}$ to $\{\mathbf{b}\}$
$\theta_3$	first rotation angle from $\{\mathbf{o}\}$ to $\{\mathbf{b}\}$
$\mathbf{A}(\mathbf{q})$	Jacobian of tendon lengths with respect to $\mathbf{q}$
$\overline{\mathbf{A}_i\mathbf{C}_i}$	position vector from point $A$ to point $c$
$\{\mathbf{b}\}$	base-centered body frame
$\overline{\mathbf{B}\mathbf{A}_i}$	position vector from point $b$ to point $A$
$\overline{\mathbf{B}\mathbf{C}_i}$	position vector from point $b$ to point $c$

$\{\mathbf{c}\}$	bar-centered body frame
$D_i$	$i$ th dimension of base
$\mathbf{F}$	vector of tendon forces
$\mathbf{F}_g$	force due to gravity
$\mathbf{F}_t$	force due to thruster controls
$G$	universal gravitational constant
$h$	altitude of spacecraft above Earth's surface
$\{\mathbf{i}\}$	Earth-centered inertial frame
$\mathbf{J}_i$	inertia matrix of $i$ th body
$\mathbf{k}_j$	stiffness of $j$ th tendon
$L$	length of bar
$\mathbf{M}_b$	mass matrix of bar
$m_b$	mass of bar
$M_\oplus$	Earth mass
$\mathbf{M}_g$	moment due to gravity
$\mathbf{M}_i$	mass matrix of bar
$m_i$	mass of bar
$\mathbf{M}_t$	moment due to thruster controls
$n$	orbital rate
$\{\mathbf{o}\}$	base-centered orbital frame
$[\mathbf{P}_i(\mathbf{q})]$	Jacobian matrix of $\mathbf{r}_i$ with respect to $\mathbf{q}$

$\mathbf{Q}$	vector of generalized forces
$\mathbf{q}$	vector of generalized coordinates
$\mathbf{q}_d$	generalized coordinates for desired configuration
$\mathbf{Q}_g$	gravitational generalized forces
$\mathbf{Q}_t$	generalized forces due to thruster controls
$\mathbf{r}_0$	position vector of base w.r.t. Earth origin
$R$	radius of orbit
$R_\oplus$	radius of Earth
$\mathbf{r}_i$	position vector of $i$ th bar w.r.t. base
$\dot{\mathbf{r}}_i$	translational velocity of $i$ th bar
$r_j$	rest length of $j$ th tendon
$[\mathbf{S}_i(\mathbf{q})]$	Jacobian matrix of $\boldsymbol{\omega}_i$ with respect to $\dot{\mathbf{q}}$
$T$	kinetic energy
$T_R$	rotational kinetic energy
$T_T$	translational kinetic energy
$\mathbf{u}_t$	vector of thruster controls
$V$	potential energy
$\nabla_{\mathbf{q}} V_e$	Jacobian of $V_e$ with respect to $\mathbf{q}$
$V_e$	elastic potential energy
$V_g$	gravitational potential energy

# Chapter 1

## Literature Review

*Tensegrity* is the union of the words *tensile* and *integrity*, used to describe a relatively new engineering principle that consists of a group of compressive and tensile elements joined together in such a way as to make a self-standing structure. The origins of tensegrity date back to 1948, when the artist Kenneth Snelson began creating sculptural forms made up of interconnected bars and cables. The term itself was coined by Buckminster Fuller when he began using the principle towards architectural structures, such as the geodesic dome.[9] Anthony Pugh[10] later defined tensegrity as “a set of discontinuous compressive components [that] interacts with a set of continuous tensile components to define a stable volume in space.”

Since then, the concept has evolved into a variety of fields.[11] For example, an offshoot of tensegrity in the biological sciences, called biotensegrity, has been used by Donald Ingber

to explain the “cell shape, movement, and cytoskeletal mechanics,”[12] a model that has been refined as advances in the understanding of the structure of cells have been made.[13] A larger scale example is the human skeleton itself, which is made up of a network of rigid bones and tendons that is very similar to the elements of tensegrity.



Figure 1.1: The Needle Tower at Hirshhorn Museum and Sculpture Garden in Washington D.C., created by Kenneth Snelson in 1968 using aluminum and stainless steel. The structure itself stands at 60 feet in height.[1]

The applications of tensegrity continue to be strong in both the arts and engineering. One of the earliest large scale tensegrity sculptures, *Needle Tower*, was created by Kenneth Snelson in 1968 and now sits in the Hirshhorn Museum and Sculpture Garden in Washington, D.C.[1] Also in Washington, D.C., at the National Building Museum, is a proposal by WilkinsonEyre in collaboration with Cecil Balmond to construct a tensegrity bridge linking high level gal-

leries, and is meant to be an exhibit itself.[14] In 2014, architecture students from Ball State University in Muncie, Indiana created a tensegrity pavilion made up of bars, cables, and elastic membranes.[15] There are additionally countless small-scale projects made by individual artists interested in the complex geometric patterns that make up a tensegrity structure.

The principals of tensegrity have also been applied to the field of civil engineering, particularly in the design of bridges and domes. One such bridge is the Kurilpa Bridge in Brisbane, Queensland, Australia, a pedestrian bridge designed by Cox Rayner Architects with Arup in 2009 to cross the Brisbane River. Closer to home, the Georgia Dome in Atlanta, Georgia was finished in 1992 as the centerpiece of the 1996 Olympic Games. Referred to by the design engineers as the first “hyper-tensegrity dome”, the dome itself was constructed by a pattern of posts held in place by pre-stressed cables and a teflon-coated fabric roof.[2] Other structures include the London 2012 Olympic Stadium designed by Buro Happold and the UCI World Cycling Centre Velodrome in Aigle, Switzerland.[16, 17]

The concepts of tensegrity has seen use and applications in robotics. The most notable project is the SuperBall Bot Tensegrity Planetary Lander, a tensegrity robot out of the National Aeronautics and Space Administration (NASA) that is being developed for possible use as a planetary lander. The benefit of such a structure is its flexibility, and thus has the capability to absorb the strong shocks upon impact. Furthermore, the bot can be artificially deformed in such a way as to cause it to roll across an uneven surface in a controlled manner, in ways that wheels might not allow.[18] Regarding this project, NASA has worked closely with the Berkeley Emergent Space Tensegrities Lab at UC Berkeley, run by Alice Agogino.[19]



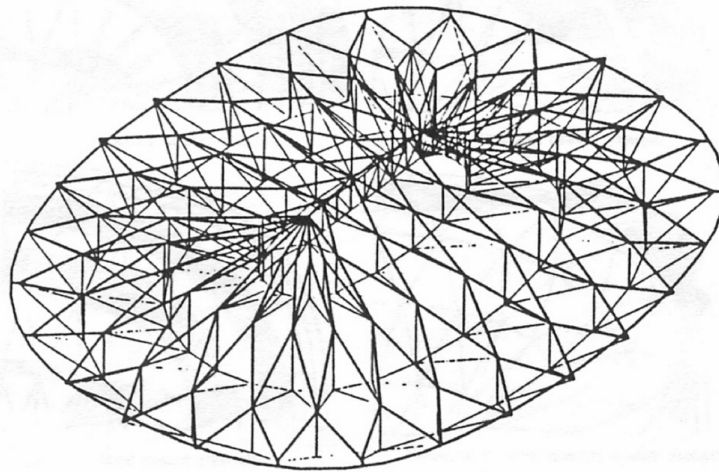


Figure 1.2: Sketch of the structure of the Georgia Dome in Atlanta, GA. The dome spans a length of nearly 800 feet and consists of interconnected cables and beams in a triangular truss pattern. It is built to withstand environmental loads such as snow, wind, and temperature.[2]

As of 2017, a prototype of the SUPERball tensegrity robot had been constructed, and preliminary analysis of its locomotion has been performed.[20]

The field toward which this paper is geared is that of aerospace engineering, particular the applications of tensegrity in a space environment. Because of their flexibility, and their potentially lightweight characteristics, tensegrity structures have been studied for use in antennas, larger space telescopes, and space station modules.

Experts in the field of tensegrity such as Cornel Sultan, Robert Skelton, and Martin Corless have investigated the dynamics and response of such structures.[21, 11] One of the main constraints of tensegrity is that all the tendons that connect the rigid bars must remain in

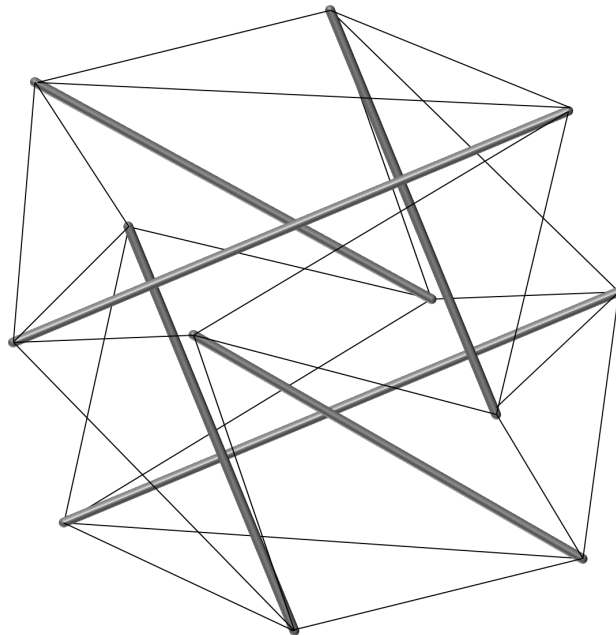


Figure 1.3: A generic simple tensegrity structure. Tensegrity consists of a collection of rigid bars (the thicker elements in the diagram) connected by a web of tendons (the thinner elements). The motion of one element of the system impacts the motion and forces on the others.

a state of stress, otherwise the structure may become unstable and collapse on itself. The previously mentioned authors introduced the term prestressability as a static equilibrium state chosen for the tensegrity structure that meets these constraints. They detail the process for choosing the orientation angles of the rigid bars such that this state of prestressability is met.[22] Another paper by Drs. Sultan and Skelton looks at strategies for the deployment of tensegrity structures. The lengths of the tendons can be adjusted in a way that collapses the tensegrity structure to a small volume, a configuration that would be useful, for example, if one desired to fit a large structure inside a launch vehicle. Once in space, the structure would

be deployed to fill a volume much larger than its original collapsed configuration.[4] Gunnar Tibert has researched the capability of tensegrity systems for large deployable satellites or space station modules.[23]

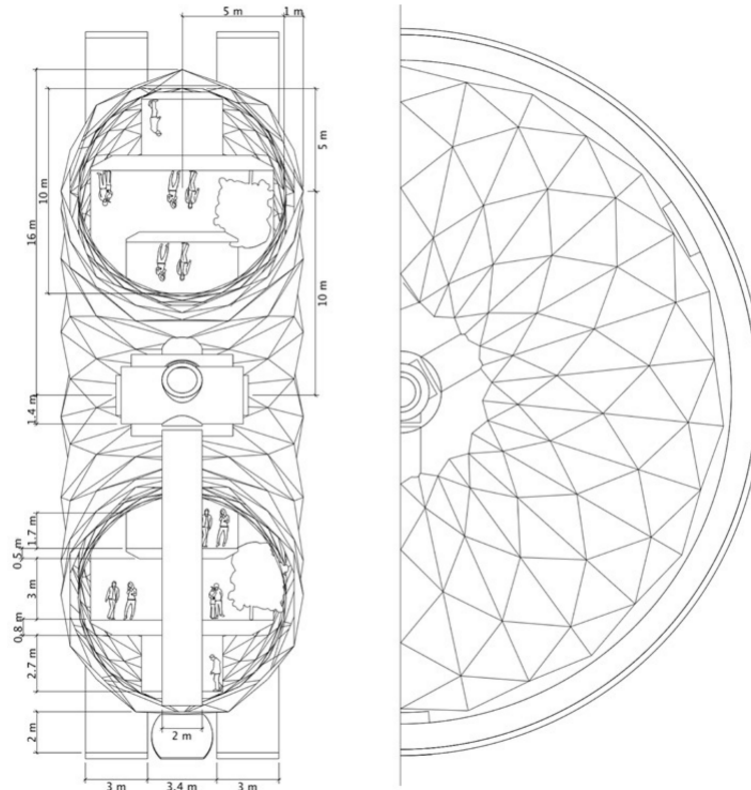


Figure 1.4: Tensegrity 1g habitation module proposed by Dr. Skelton and Dr. Longman. This research was rewarded a NASA NIAC 2013 Phase 1 grant to investigate the feasibility of such a structure.[3]

The applications of such a capability could be used in the deployment of habitation modules, where the module is folded up inside the launch vehicle and then expanded into a large volume. The tensegrity structure would serve as the skeleton of the module, over which some protective material would be stretched. This application is still in its early stages; a

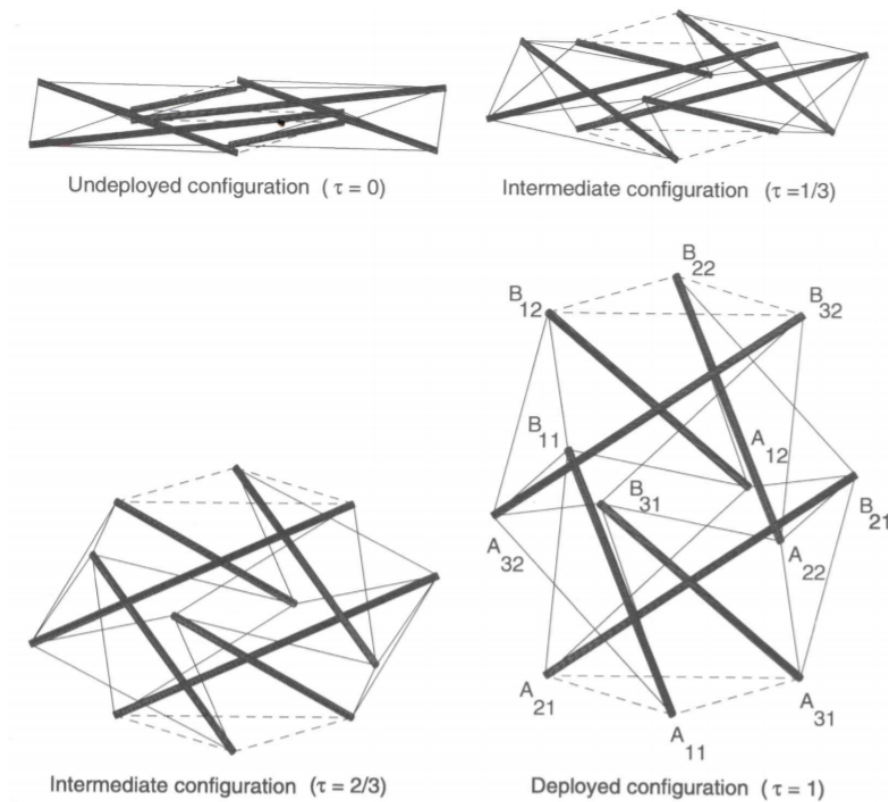


Figure 1.5: A deployable tensegrity system, in both the collapsed and expanded configurations.[4] The shape of the tensegrity structure is changed by modifying the lengths of the tendons, which can be done, for example, by means of actuators or piezo-electric materials.

proposal has been submitted by Dr. Skelton and Dr. Anthony Longman to NASA that puts forth the idea of a large spinning tensegrity-based habitat that could serve as an outpost to the long voyage to Mars.[24, 25] Another potential use would be in space telescopes. A long cylindrical-shaped tensegrity structure could serve as the structure connecting the primary and secondary mirrors of the telescope.[26] In the case of a composite primary mirror, where the large mirror is broken up into adjustable segments, the segments themselves could be

supported by a quasi-tensegrity network. Again, this would allow increasingly long telescopes and large mirrors to be folded up inside a launch vehicle, and allow for adjustments to the mirror while in space to counteract distortions due to external forces such as gravity, temperature fluctuations, drag, and solar pressure. At Virginia Polytechnic Institute and State University, Dr. Sultan has explored the design of adaptive space telescopes whose mirrors and instrumentation may be supported by a tensegrity system.

Finally, an application that has already seen substantial use is that for space antennas. Harris Corporation is a leading producer of mesh antennas, whose structure is held up by complicated tensegrity systems.[27] One of their simpler designs is their rigid-rib antenna, where the only hinge points are at the base and the antenna is folded out like an umbrella. This design was used for the NASA Galileo mission to Jupiter.[28] A more advanced concept is their hinge-ribbed antenna, which consists of long ribs over which a mesh is stretched. The ribs have hinged joints along their length, which allow them to fold into a stowable configuration.[23] Another product of Harris is their hoop/column antenna, where a string-loaded tensegrity-mesh structure is connected to a central column. When the column is deployed from its stowed position, the antenna springs out into its preloaded shape.[29]

All of these large designs are possible because of the structure's flexibility, and thus its ability to collapse and fit into the limited volume available in launch vehicles today. However, a downside of this flexibility characteristic in large tensegrity systems is that the structure is susceptible to undesirable deformations due to gravity. To date, studies and applications of tensegrity in space have focused on zero-g environments such as that available in deep space,

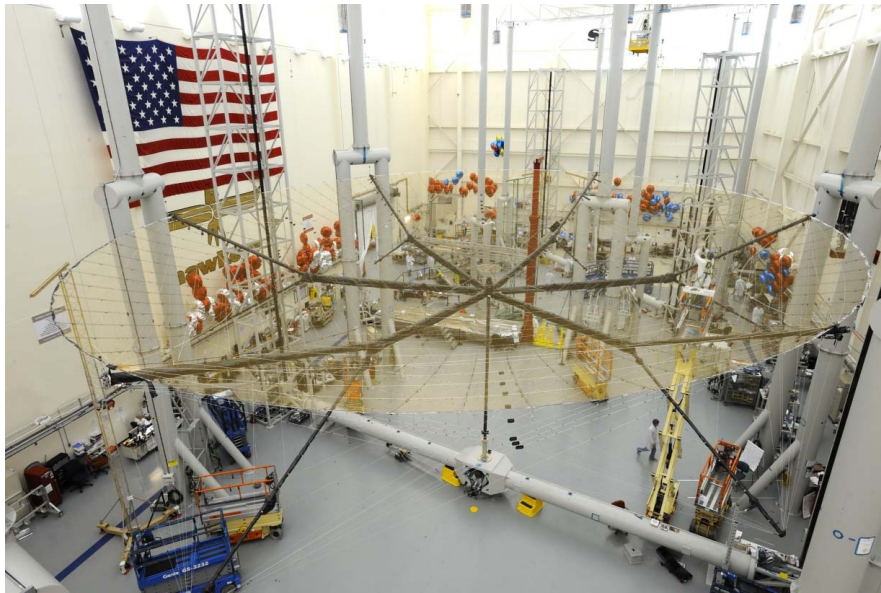


Figure 1.6: Harris Corporation deployable 18-meter antenna. This specific antenna was used for S-band communications on the TerreStar-1 satellite, launched in 2009.[5]

or shorter structures that would not be as affected by potential gravity gradients. However, the most-used real estate in space is low-Earth orbit (LEO), an area that ranges from an altitude of 2,000 km to just 160 km above the Earth's surface, where the effects of gravity are still very much present.

This thesis is the first to investigate and develop accurate models and methods of control for tensegrity systems in a LEO environment whose individual elements are subject to gravity gradients. It first aims to derive the dynamics of a general tensegrity system, regardless of the tensegrity geometry chosen, and can serve as a guideline for increasingly complex structures. The equations of motion of such a structure are dependent upon the internal kinetic energy

of the system and the potential energy present in the web of tendons. This paper also introduces gravity gradients as it applies to large tensegrity structures - for increasingly long bars, the gravity force along the length of the bar varies enough as to induce moments on the bars, thus distorting the entire system. Methods of controlling and diminishing the deformations caused by these gravity gradients on the different elements of the system are discussed. Finally, several examples of simple tensegrity systems and their derived dynamics are provided. It is the goal of the author to provide a road map to future researchers that show interest in the possibilities of large tensegrity structures in a non-zero-g orbital environment.

# Chapter 2

## General Dynamics

Begin by deriving the dynamics of a generic tensegrity spacecraft.

The Earth is assumed to be a spherical body of uniform mass that is fixed in inertial space, at whose center of mass is defined an inertial frame  $\{\mathbf{i}\}$ . The spacecraft in Figure 2.1 orbits the Earth at some radius  $R$  from the Earth center of mass, which is equivalent to the summation of the radius of the Earth  $R_{\oplus}$  and the altitude  $h$  of the spacecraft above the Earth's surface:

$$R = R_{\oplus} + h. \tag{2.1}$$

Its position in the inertial frame is defined in terms of what will be referred to here as the longitudinal angle  $\lambda$  and the latitudinal angle  $\phi$ . The angle  $\lambda$  is measured from the  $\mathbf{i}_1$  axis clockwise about the  $\mathbf{i}_3$  axis, and the angle  $\phi$  is measured from the  $\mathbf{i}_3$  axis counterclockwise



about the  $\mathbf{i}_2$  axis. Using these parameters, the position vector  $\mathbf{r}_0$  is given as

$$\mathbf{r}_0 = R \begin{bmatrix} \cos \lambda \sin \phi \\ \sin \lambda \sin \phi \\ \cos \phi \end{bmatrix}. \quad (2.2)$$

Next is to define the rigid base of the spacecraft upon which the tensegrity structure will be attached. There are two reference frames whose origins coincide with the center of mass of the base: an orbital frame  $\{\mathbf{o}\}$  and a body frame  $\{\mathbf{b}\}$ . These two frames are depicted in Figure 2.2.

The orbital frame  $\{\mathbf{o}\}$  is a rotating frame, whose axes are  $\{\mathbf{o}_\phi, \mathbf{o}_\lambda, \mathbf{o}_r\}$  and correspond to the  $\{1, 2, 3\}$  axes of the  $\{\mathbf{o}\}$  frame. The  $\{\mathbf{o}\}$  frame is related to the inertial frame  $\{\mathbf{i}\}$  by means of a 3-2 rotation sequence through the longitudinal and latitudinal angles  $\lambda$  and  $\phi$ , given by

$$\mathbf{R}^{oi} = \mathbf{R}_2(\phi)\mathbf{R}_3(\lambda), \quad (2.3)$$

where

$$\mathbf{R}_2(\phi) = \begin{bmatrix} \cos \phi & 0 & -\sin \phi \\ 0 & 1 & 0 \\ \sin \phi & 0 & \cos \phi \end{bmatrix} \quad (2.4)$$

$$\mathbf{R}_3(\lambda) = \begin{bmatrix} \cos \lambda & \sin \lambda & 0 \\ -\sin \lambda & \cos \lambda & 0 \\ 0 & 0 & 1 \end{bmatrix}. \quad (2.5)$$

The position vector  $\mathbf{r}_0$  can thus be rotated into the orbital frame, yielding the simpler vector

$${}^o\mathbf{r}_0 = \mathbf{R}^{oi}\mathbf{r}_0 = [0 \ 0 \ R]^T. \quad (2.6)$$

Similar to the orbital frame, the body frame  $\{\mathbf{b}\}$  is also centered at the mass center of the base; however, its axes are aligned with the principal axes of the base. The orbital frame is rotated into the base body frame by means of a 3-2-1 rotation sequence through the Euler angles  $\theta_3$ ,  $\theta_2$ , and  $\theta_1$  (kept in that order for notation simplicity later on). The resulting transformation is

$$\mathbf{R}^{bo} = \mathbf{R}_1(\theta_1)\mathbf{R}_2(\theta_2)\mathbf{R}_3(\theta_3), \quad (2.7)$$

where

$$\mathbf{R}_1(\theta_1) = \begin{bmatrix} 1 & 0 & 0 \\ 0 & \cos \theta_1 & \sin \theta_1 \\ 0 & -\sin \theta_1 & \cos \theta_1 \end{bmatrix} \quad (2.8)$$

$$\mathbf{R}_2(\theta_2) = \begin{bmatrix} \cos \theta_2 & 0 & -\sin \theta_2 \\ 0 & 1 & 0 \\ \sin \theta_2 & 0 & \cos \theta_2 \end{bmatrix} \quad (2.9)$$

$$\mathbf{R}_3(\theta_3) = \begin{bmatrix} \cos \theta_3 & \sin \theta_3 & 0 \\ -\sin \theta_3 & \cos \theta_3 & 0 \\ 0 & 0 & 1 \end{bmatrix}. \quad (2.10)$$

Finally, the last component of the spacecraft is the tensegrity system that sits upon the base, which consists of  $R$  bars and  $E$  tendons. To simplify the derivation of the dynamics of the

system, the bars are assumed to have negligible thickness and the tendons to be massless and linear elastic.

Consider the  $i$ th bar depicted in Fig. 2.3. A coordinate frame  $\{\mathbf{c}\}$  is defined at the center of mass of the bar, where the  $\mathbf{c}_3$  axis is coincident with the length of the bar. The bar has a length of  $L_i$ , and an ascension angle  $\alpha_i$  and declination angle  $\delta_i$ , angles which are measured from the base frame  $\{\mathbf{b}\}$  of the base. The ascension angle is measured about the 3 axis  $\mathbf{b}_3$  and the declination angle about the second axis  $\mathbf{b}_1$ ; from this, the 3-2 rotation from the  $\{\mathbf{b}\}$  frame to the  $\{\mathbf{c}\}$  frame can therefore be expressed as

$$\mathbf{R}^{cb} = \mathbf{R}_2(\delta_i)\mathbf{R}_3(\alpha_i), \quad (2.11)$$

where

$$\mathbf{R}_2(\delta_i) = \begin{bmatrix} \cos \delta_i & 0 & -\sin \delta_i \\ 0 & 1 & 0 \\ \sin \delta_i & 0 & \cos \delta_i \end{bmatrix} \quad (2.12)$$

$$\mathbf{R}_3(\alpha_i) = \begin{bmatrix} \cos \alpha_i & \sin \alpha_i & 0 \\ -\sin \alpha_i & \cos \alpha_i & 0 \\ 0 & 0 & 1 \end{bmatrix}. \quad (2.13)$$

Finally, the position vector of the center of mass of this bar from the center of mass of the base can be written in the  $\{\mathbf{b}\}$  frame as

$$\mathbf{r}_i^b = [x_i \quad y_i \quad z_i]^T + \overline{\mathbf{A}_i \mathbf{C}_i}, \quad (2.14)$$

where

$$\overline{\mathbf{A}_i \mathbf{C}_i}^b = \frac{L_i}{2} \begin{bmatrix} \cos \alpha_i \sin \delta_i \\ \sin \alpha_i \sin \delta_i \\ \cos \delta_i \end{bmatrix}. \quad (2.15)$$

A set of independent generalized coordinates are extracted from the above analysis for the dynamics of the interconnected base and bars, and consolidated into the vector

$$\mathbf{q} = [R \ \lambda \ \phi \ \theta_1 \ \theta_2 \ \theta_3 \ x_i \ y_i \ z_i \ \alpha_i \ \delta_i]^T, \quad (2.16)$$

where the index  $i$  varies from 1 to the number of bars.

The dynamics of the spacecraft can be derived using Lagrange's equation, expressed here as

$$\frac{d}{dt}(\nabla_{\dot{\mathbf{q}}} L) - \nabla_{\mathbf{q}} L = \mathbf{Q}, \quad (2.17)$$

where the term  $\nabla_{\mathbf{q}} f$  represents the gradient of a function  $f$  with respect to the generalized coordinates  $\mathbf{q}$  such that

$$\nabla_{\mathbf{q}} f = \left[ \frac{\partial f}{\partial q_1} \ \frac{\partial f}{\partial q_2} \ \cdots \ \frac{\partial f}{\partial q_N} \right]^T, \quad (2.18)$$

where  $N$  is the number of elements in  $\mathbf{q}$ .  $\mathbf{Q}$  is the vector of generalized forces and the Lagrangian  $L$  is equal to the difference between the kinetic and potential energy of the system, i.e.  $L = T - V$ . Thus Lagrange's equations become

$$\frac{d}{dt}(\nabla_{\dot{\mathbf{q}}}(T - V)) - \nabla_{\mathbf{q}}(T - V) = \mathbf{Q}. \quad (2.19)$$

Rearranging terms, and recognizing that the potential energy in this system has no dependence on the time derivatives of the generalized coordinates, yields

$$\frac{d}{dt}(\nabla_{\dot{\mathbf{q}}} T) - \nabla_{\mathbf{q}} T = -\nabla_{\mathbf{q}} V + \mathbf{Q}. \quad (2.20)$$

There are four components considered in this paper that contribute to the elements of the above dynamical system. The first, of course, is the kinetic energy  $T$  of the system, which is derived in Section 2.1. The next are the gravitational forces on all the massive members of the system. There are two approaches one can take in deriving the gravitational effects: an energy approach, which would factor into the potential energy  $V$  term of the dynamical system, or a force approach, which would factor into the generalized force term  $\mathbf{Q}$ . Both approaches are considered in Section 2.2. The third component, derived in Section 2.3, is the potential energy  $V_e$  due to the elastic tendons that make up the tensegrity system, which contributes to the  $V$  term. Finally are the generalized thruster forces  $\mathbf{Q}_t$  on the base of the spacecraft that work to maintain the attitude and trajectory of the spacecraft, and are derived in Section 2.4.

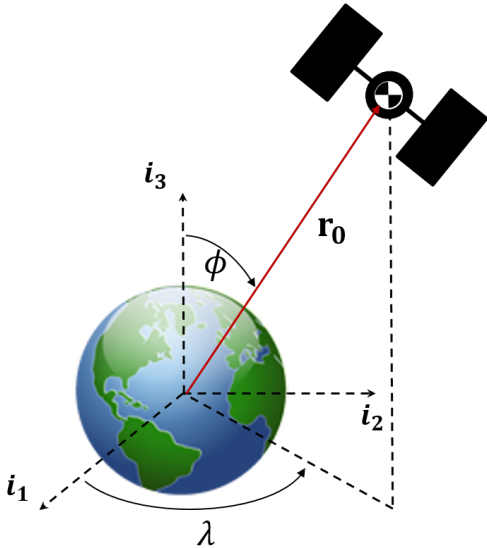


Figure 2.1: Earth-centered inertial frame  $\{\mathbf{i}\}$  and spacecraft position. The position vector  $\mathbf{r}_0$  of the spacecraft relative to the center of the Earth is a function of the orbit radius  $R$  and the latitude and longitude angles  $\phi$  and  $\delta$ .

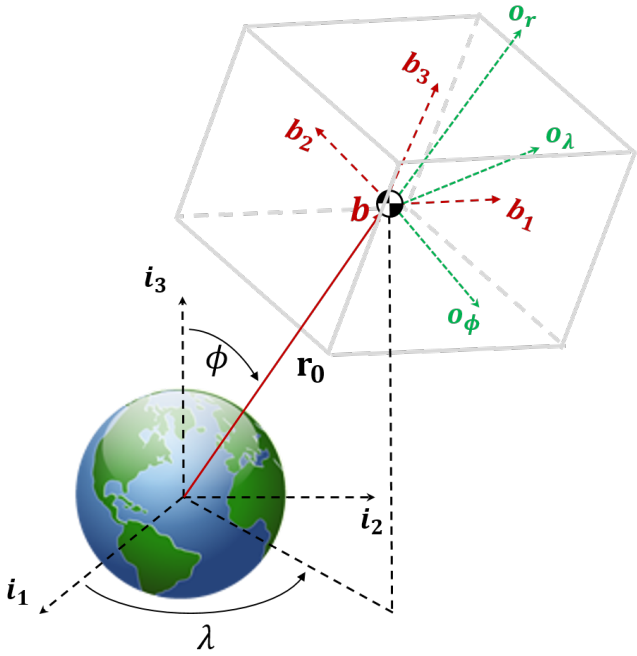


Figure 2.2: Base-centered orbital frame  $\{o\}$  and body frame  $\{b\}$ . The  $\{o_\phi, o_\lambda, o_r\}$  axes are the  $\{1, 2, 3\}$  axes of the orbital frame. The axes of the body frame lie along the principal axes of the base.

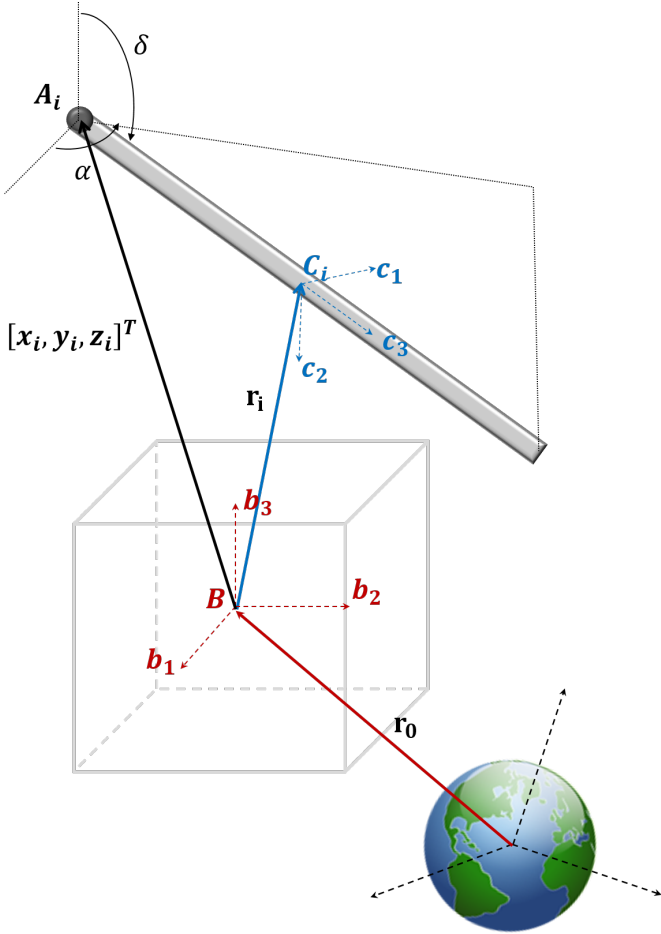


Figure 2.3: The bar-centered body frame for the  $i$ th bar is defined at the center of mass of the bar. Each bar is oriented an angle  $\alpha$  and  $\delta$  (referred to as the ascension and declination angles) from the base body frame  $\{\mathbf{b}\}$ . An endpoint of the bar (point  $A_i$ ) is located at a distance  $[x_i, y_i, z_i]^t$  from the center of mass of the base.



## 2.1 Kinetic Energy

The total kinetic energy  $T$  is the summation of the translational ( $T_T$ ) and rotational ( $T_R$ ) components of the kinetic energy for all massive bodies of the system:

$$T = \sum_{i=0}^{\mathcal{B}} \{T_T + T_R\}_i \quad (2.21)$$

for a system made up of  $\mathcal{B}$  massive bodies. In this thesis,  $i = 0$  will correspond to the rigid base of the spacecraft system, and  $i = 1, 2, \dots, R$  to the rigid bars that make up the tensegrity structure.

In the following sections, the translational and rotational components for a generic system are derived.

### 2.1.1 Translational Kinetic Energy

The general expression for the translational kinetic energy of the  $i$ th body, expressed in vector format, is

$$T_{T_i} = \frac{1}{2} \dot{\mathbf{r}}_i^T \mathbf{M}_i \dot{\mathbf{r}}_i \quad (2.22)$$

where  $\dot{\mathbf{r}}_i$  is the translational velocity of the center of mass of the body, and  $\mathbf{M}_i$  is the mass matrix of that body. The goal is to write the velocity vector in terms of the time derivative of the generalized coordinates. Begin by manipulating the velocity vector as follows:

$$\dot{\mathbf{r}}_i = \frac{d\mathbf{r}_i}{dt} = \frac{\partial \mathbf{r}_i}{\partial \mathbf{q}} \frac{d\mathbf{q}}{dt} = \frac{\partial \mathbf{r}_i}{\partial \mathbf{q}} \dot{\mathbf{q}}. \quad (2.23)$$

This yields an expression for the velocity vector that consists of a Jacobian derivative matrix and the time derivative of the vector of generalized coordinates. A matrix  $[\mathbf{P}_i(\mathbf{q})]$ , that is a function of the generalized coordinates, is assigned to the Jacobian matrix:

$$[\mathbf{P}_i(\mathbf{q})] = \frac{\partial \mathbf{r}_i}{\partial \mathbf{q}}. \quad (2.24)$$

Thus the velocity vector becomes

$$\dot{\mathbf{r}}_i = [\mathbf{P}_i(\mathbf{q})]\dot{\mathbf{q}}. \quad (2.25)$$

This form for the velocity vector is then substituted into the expression for the translational kinetic energy, yielding

$$T_{T_i} = \frac{1}{2} \dot{\mathbf{q}}^T [\mathbf{P}_i(\mathbf{q})]^T \mathbf{M}_i [\mathbf{P}_i(\mathbf{q})] \dot{\mathbf{q}} \quad (2.26)$$

### 2.1.2 Rotational Kinetic Energy

The rotational energy is given by the general expression

$$T_{R_i} = \frac{1}{2} \boldsymbol{\omega}_i^T \mathbf{J}_i \boldsymbol{\omega}_i \quad (2.27)$$

where  $\boldsymbol{\omega}_i$  is the angular velocity of the body and  $\mathbf{J}_i$  is its inertia matrix. It is desirable to choose the inertia matrix to be about the principal axes of the body, so that  $\mathbf{J}_i$  becomes a diagonal matrix. This, however, necessitates that the components of the angular velocity all be rotated into the frame that is coincident with the body's principal axes. This process will be discussed in more detail in the sections deriving the dynamics of the actual spacecraft system.

Theoretically, one could follow a process similar to that detailed in the derivation of the translational energy, where the angular velocity can be separated into a Jacobian derivative matrix of the angular position and the time derivative of the vector of generalized coordinates:

$$\boldsymbol{\omega}_i = \dot{\boldsymbol{\theta}}_i = \frac{d\boldsymbol{\theta}_i}{dt} = \frac{\partial\boldsymbol{\theta}_i}{\partial\mathbf{q}} \frac{d\mathbf{q}}{dt} = \frac{\partial\boldsymbol{\theta}_i}{\partial\mathbf{q}} \dot{\mathbf{q}}. \quad (2.28)$$

From this, the Jacobian matrix would be given as

$$[\mathbf{S}_i(\mathbf{q})] = \frac{\partial\boldsymbol{\theta}_i}{\partial\mathbf{q}}. \quad (2.29)$$

However, the author found it simpler to work with angular velocities instead of angular positions. The exact process followed is detailed in the example tensegrity structure in Section 4.2.1, but the end result is the same: the angular velocity can be written as a Jacobian matrix times the time derivative of the independent generalized coordinates, as such:

$$\boldsymbol{\omega}_i = [\mathbf{S}_i(\mathbf{q})]\dot{\mathbf{q}}, \quad (2.30)$$

where the Jacobian which is then substituted into the rotational kinetic energy equation, yielding

$$T_{R_i} = \frac{1}{2} \dot{\mathbf{q}}^T [\mathbf{S}_i(\mathbf{q})]^T \mathbf{J}_i [\mathbf{S}_i(\mathbf{q})] \dot{\mathbf{q}} \quad (2.31)$$

### 2.1.3 Total Kinetic Energy

Now that the expressions for the translational and rotational kinetic energy have been derived, these are substituted into Equation (2.21), which recall from Equation (2.21) was

$$T = \sum_{i=0}^{\mathcal{B}} \{T_T + T_R\}_i \quad (2.32)$$

The equation for the total kinetic energy of the system thus becomes

$$T = \sum_{i=0}^{\mathcal{B}} \left\{ \frac{1}{2} \dot{\mathbf{q}}^T [\mathbf{P}_i(\mathbf{q})]^T \mathbf{M}_i [\mathbf{P}_i(\mathbf{q})] \dot{\mathbf{q}} + \frac{1}{2} \dot{\mathbf{q}}^T [\mathbf{S}_i(\mathbf{q})]^T \mathbf{J}_i [\mathbf{S}_i(\mathbf{q})] \dot{\mathbf{q}} \right\} \quad (2.33)$$

$$= \frac{1}{2} \dot{\mathbf{q}}^T \sum_{i=0}^{\mathcal{B}} \{ [\mathbf{P}_i(\mathbf{q})]^T \mathbf{M}_i [\mathbf{P}_i(\mathbf{q})] + [\mathbf{S}_i(\mathbf{q})]^T \mathbf{J}_i [\mathbf{S}_i(\mathbf{q})] \} \dot{\mathbf{q}} \quad (2.34)$$

$$= \frac{1}{2} \dot{\mathbf{q}}^T \mathbf{M}(\mathbf{q}) \dot{\mathbf{q}}. \quad (2.35)$$

## 2.2 Gravitational Effects

The gravitational effects of the Earth on the individual rigid elements of the tensegrity spacecraft are due to the interaction between the Earth and the mass elements of tensegrity.

As discussed previously, the tendons are assumed massless; thus, the only contributions to the gravitational effects of the system are those due to the rigid base and the bars that make up the tensegrity system.

For the following discussion, recall the Lagrangian derivation of the equations of motion mentioned earlier:

$$\frac{d}{dt}(\nabla_{\dot{\mathbf{q}}} T) - \nabla_{\mathbf{q}} T = -\nabla_{\mathbf{q}} V + \mathbf{Q}. \quad (2.36)$$

There are two ways to approach the derivation of these gravitational effects that are discussed in this thesis. The first is through an energy approach, where gravity is treated as a component of the potential energy of the system. Each of the massive rigid elements of the system have some contribution to the total potential energy, which shows up in the potential energy term  $\nabla_{\mathbf{q}}V$  of the above equation.

The second method is by treating the gravity as a force. Each massive element of the system has its own gravitational force, which are all then included in the vector of generalized forces  $\mathbf{Q}$ .

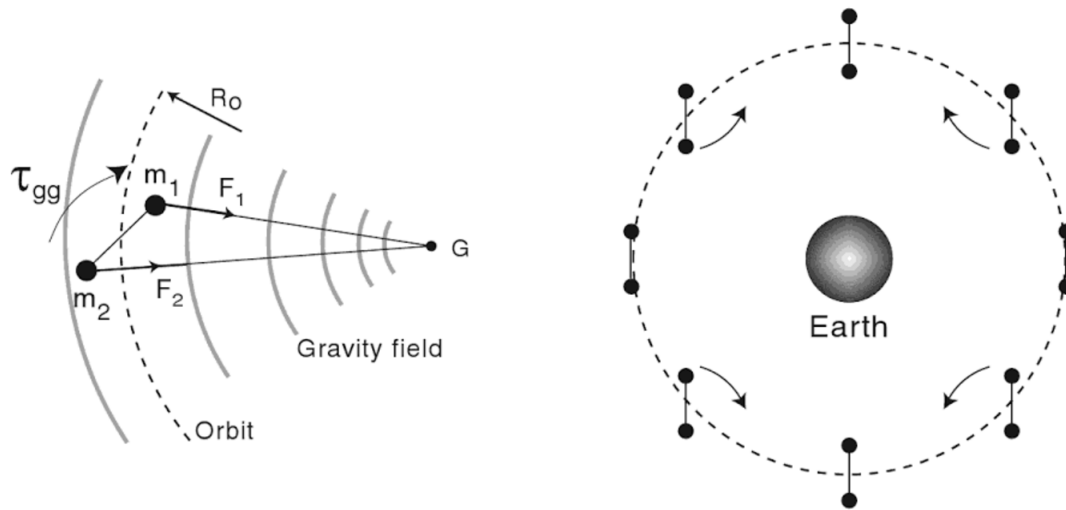


Figure 2.4: The concept of gravity gradient, as illustrated by Pierre Bely.[6]

This diagram shows the gravity forces on two point masses connected via a massless rod, where the force on  $m_1$  will be greater than that on  $m_2$  and will thus induce a moment. The analysis in this thesis spreads these point masses out to a long rigid body; in the case of a tensegrity structure, the long bars. The gravity force along the length of the bar will vary, and will similarly induce a moment on the bar.

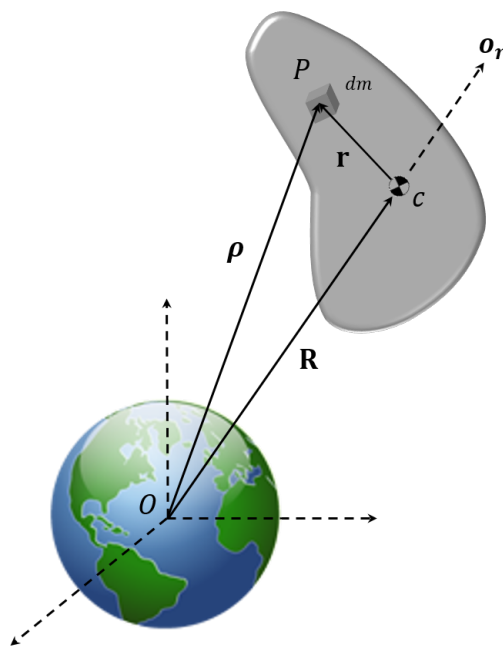


Figure 2.5: Parameters defining orbiting rigid body. The vector  $\mathbf{R}$  is the position of the center of mass of the body relative to the Earth center, whereas  $\mathbf{r}$  is the vector from the mass center of the body to a differential mass  $dm$  in the body.  $\mathbf{R}$  lies along the orbit radius direction  $\mathbf{o}_r$ . The Earth-centered frame pictured is an inertial frame.

### 2.2.1 Gravity Potential Energy

Begin with the energy approach for deriving the gravitational effects on the system. The gravitational potential energy of a generic rigid body orbiting the Earth is

$$V_g = M_{\oplus} \Psi$$

$V_g$  where  $M_{\oplus}$  is the mass of a central massive spherical Earth and the gravitational potential  $\Psi$  is

$$\Psi = -G \int_{\mathcal{B}} \frac{dm}{\|\boldsymbol{\rho}\|} \quad (2.37)$$

where  $G$  is the universal gravitational constant and  $\boldsymbol{\rho}$  can be expressed as the summation

$$\boldsymbol{\rho} = \mathbf{R} + \mathbf{r}$$

where  $\mathbf{R}$  is the vector from the Earth mass center to the mass center of the orbiting rigid body and  $\mathbf{r}$  is the vector from the mass center of the orbiting rigid body to a differential mass  $dm$ .

The gravitational potential thus becomes

$$\Psi = -G \int_{\mathcal{B}} \frac{dm}{\|\mathbf{R} + \mathbf{r}\|} \quad (2.38)$$

where the denominator can be manipulated to allow for closed integration:

$$\begin{aligned} \|\mathbf{R} + \mathbf{r}\| &= R \sqrt{1 + \frac{2\mathbf{R} \cdot \mathbf{r}}{R^2} + \frac{r^2}{R^2}} \\ &= R \sqrt{1 + \frac{2r \cos \Theta}{R} + \frac{r^2}{R^2}} \end{aligned}$$



where  $R = \|\mathbf{R}\|$ ,  $r = \|\mathbf{r}\|$ , and  $\Theta$  is the angle between the two position vectors such that

$$\cos \Theta = \frac{\mathbf{R} \cdot \mathbf{r}}{Rr}.$$

The gravitational potential equation becomes

$$\Psi = -\frac{G}{R} \int_{\mathcal{B}} \frac{1}{\sqrt{1 + 2u \cos \Theta + u^2}} dm \quad (2.39)$$

where  $u = r/R$ . This is in the form of the binomial theorem, which states

$$\frac{1}{\sqrt{1 - 2ux + u^2}} = \sum_{n=0}^{\infty} P_n(x)u^n \quad (2.40)$$

where  $P_n$  is a Legendre polynomial of the  $n$ th degree in  $x$ . [30] Letting  $x = -\cos \Theta$ , the potential becomes

$$\Psi = -\frac{G}{R} \int_{\mathcal{B}} \sum_{n=0}^{\infty} P_n(-\cos \Theta) \left(\frac{r}{R}\right)^n dm \quad (2.41)$$

The Legendre polynomials are found using the Rodrigues Formula: [31]

$$P_n(x) = \frac{1}{2^n n!} \frac{d^n}{dx^n} [(x^2 - 1)^n].$$

Substituting in  $(-\cos \Theta)$  for  $x$  yields the following Legendre polynomials

$$P_0(-\cos \Theta) = 1$$

$$P_1(-\cos \Theta) = -\cos \Theta$$

$$P_2(-\cos \Theta) = \frac{3 \cos^2 \Theta - 1}{2}$$

where polynomials of degree higher than  $n = 2$  are higher order terms that are assumed negligible. The resulting gravitational potential function becomes

$$\Psi = -\frac{G}{R} \int_{\mathcal{B}} dm + \frac{G}{R^2} \int_{\mathcal{B}} r \cos \Theta dm - \frac{G}{2R^3} \int_{\mathcal{B}} r^2 (3 \cos^2 \Theta - 1) dm.$$

Using the identity  $\cos^2 \Theta + \sin^2 \Theta = 1$ , the potential becomes

$$\Psi = -\frac{G}{R} \int_{\mathcal{B}} dm + \frac{G}{R^2} \int_{\mathcal{B}} r \cos \Theta dm - \frac{G}{R^3} \int_{\mathcal{B}} r^2 dm + \frac{3G}{2R^2} \int_{\mathcal{B}} r^2 \sin^2 \Theta dm.$$

The first term is the potential of a point mass. The second term,  $\int_{\mathcal{B}} r \cos \Theta dm$ , is zero since the origin  $O$  of the rigid body is chosen to be the center of mass, causing any results within this integral to cancel out. The third term can be manipulated thusly:

$$\begin{aligned} -\frac{G}{R^3} \int_{\mathcal{B}} r^2 dm &= -\frac{G}{R^3} \int_{\mathcal{B}} (x^2 + y^2 + z^2) dm \\ &= -\frac{G}{2R^3} (J_1 + J_2 + J_3) \end{aligned}$$

where  $J_1$ ,  $J_2$ , and  $J_3$  are the principal moments of inertia of the rigid body about  $O$ , defined as:

$$\begin{aligned} J_1 &= \int_{\mathcal{B}} (y^2 + z^2) dm \\ J_2 &= \int_{\mathcal{B}} (x^2 + z^2) dm \\ J_3 &= \int_{\mathcal{B}} (x^2 + y^2) dm \end{aligned}$$

In fourth term  $\int_{\mathcal{B}} r^2 \sin^2 \Theta dm$ ,  $r \sin \Theta$  projects  $\mathbf{r}$  onto a plane that is perpendicular to the axis coincident with the vector  $\mathbf{R}$ . It is the moment of inertia of the body about this axis, and is written as  $I$ . Combining terms, the potential becomes

$$\Psi = -\frac{Gm}{R} - \frac{G}{2R^3} (J_1 + J_2 + J_3 - 3I) \quad (2.42)$$

which is known as MacCullagh's formula.[32, 33]

To arrive at the gravitational potential energy, multiply the gravitational potential by the

mass of the Earth:

$$V_g = -\frac{GM_{\oplus}m}{R} - \frac{GM_{\oplus}}{2R^3}(J_1 + J_2 + J_3 - 3I) \quad (2.43)$$

Taking the Jacobian of the above expression,  $\nabla_{\mathbf{q}}V_g$ , yields the contribution of the rigid body to the total gravitational potential energy of the system.

### 2.2.2 Gravity Generalized Forces

The effect of the gravitational forces on the elements of the system are reflected in this analysis in the generalized forces. The formula for the vector of generalized forces due to gravity on the system is

$$\mathbf{Q}_g = \sum_{i=0}^{\mathcal{B}} \left[ \left( \frac{\partial \dot{\mathbf{r}}_i}{\partial \dot{\mathbf{q}}} \right)^T \mathbf{F}_{g_i} \right] + \sum_{i=0}^{\mathcal{B}} \left[ \left( \frac{\partial \dot{\boldsymbol{\omega}}_i}{\partial \dot{\mathbf{q}}} \right)^T \mathbf{M}_{g_i} \right] \quad (2.44)$$

where  $\dot{\mathbf{r}}_i$  and  $\dot{\boldsymbol{\omega}}_i$  are the translational and angular velocities of the  $i$ th rigid body, respectively, where  $\mathcal{B}$  refers to the total number of rigid bodies that make up the system.

#### Derivation of Gravitational Force

Consider the Earth-orbiting generic rigid body of mass  $m$  depicted in Fig. 2.5. The Earth is assumed to be a central massive spherical body of mass  $M_{\oplus}$  whose mass center is located at the origin  $O$  of an inertial frame. The vector  $\mathbf{R}$  defines the position of the center of mass  $c$  of the rigid body with respect to  $O$ , and  $\mathbf{r}$  is the position vector from  $c$  to some differential mass  $dm$  along the body located at point  $P$ . Finally,  $\boldsymbol{\rho}$  is the combination of the two vectors.

In order to determine the gravitational force on the tensegrity elements, a general expression is derived for the force exerted by the Earth on an arbitrary 3-D rigid body, shown in Fig. 2.5. The derivation follows a process outlined in a publication by Kane,[34] and is included here in sufficient detail to provide completeness and clarity to this paper. The resulting force formula can then be specialized for bars, plates, or other potential rigid components of a tensegrity structure.

Begin with the definition of the gravitational force,

$$\mathbf{F}_g = -\mu \int_{\mathcal{B}} \frac{\boldsymbol{\rho}}{\|\boldsymbol{\rho}\|^3} dm. \quad (2.45)$$

Recalling that  $\boldsymbol{\rho} = \mathbf{R} + \mathbf{r}$ , the expression for the gravity force becomes

$$\mathbf{F}_g = -\mu \int_{\mathcal{B}} \frac{\mathbf{R} + \mathbf{r}}{\|\mathbf{R} + \mathbf{r}\|^3} dm. \quad (2.46)$$

The Earth's gravitational parameter  $\mu$  is defined as the product between the universal gravitational constant  $G$  and the mass of the Earth  $M_{\oplus}$ , i.e.  $\mu = GM_{\oplus}$ , and is a constant.

The denominator of this expression can be manipulated as follows:

$$\begin{aligned} \|\mathbf{R} + \mathbf{r}\|^3 &= [(\mathbf{R} + \mathbf{r}) \cdot (\mathbf{R} + \mathbf{r})]^{3/2} \\ &= [\mathbf{R} \cdot \mathbf{R} + 2\mathbf{R} \cdot \mathbf{r} + \mathbf{r} \cdot \mathbf{r}]^{3/2} \\ &= \left[ \frac{R^2}{R^2} (\mathbf{R}^T \mathbf{R} + 2\mathbf{R}^T \mathbf{r} + \mathbf{r}^T \mathbf{r}) \right]^{3/2} \\ &= R^3 \left[ 1 + \frac{2\mathbf{R}^T \mathbf{r}}{R^2} + \frac{\mathbf{r}^T \mathbf{r}}{R^2} \right]^{3/2} \end{aligned}$$

Substituting this expression into the gravity force equation yields

$$\mathbf{F}_g = -\frac{\mu}{R^2} \int_{\mathcal{B}} \frac{(\mathbf{R} + \mathbf{r})}{R} \left[ 1 + \frac{2\mathbf{R}^T \mathbf{r}}{R^2} + \frac{\mathbf{r}^T \mathbf{r}}{R^2} \right]^{-3/2} dm, \quad (2.47)$$

where  $R$  is the magnitude of the vector  $\mathbf{R}$ . In order to simplify the remaining derivation, define a unit vector  $\mathbf{o}_r = \mathbf{R}/R$  and a vector  $\mathbf{q} = \mathbf{r}/R$ . The gravity force can then be written as

$$\mathbf{F}_g = -\frac{\mu}{R^2} \int_{\mathcal{B}} (\mathbf{o}_r + \mathbf{q}) [1 + 2\mathbf{o}_r^T \mathbf{q} + \mathbf{q}^T \mathbf{q}]^{-3/2} dm. \quad (2.48)$$

To obtain an expression that can be integrated, a series expansion is used. The general formula for a binomial series expansion is

$$(1 + x)^a = 1 + ax + \frac{a(a-1)x^2}{2!} + \frac{a(a-1)(a-2)x^3}{3!} + \dots \quad (2.49)$$

where a condition for convergence is  $\|x\| < 1$ . This formula is applied to the expression  $[1 + 2\mathbf{o}_r^T \mathbf{q} + \mathbf{q}^T \mathbf{q}]^{-3/2}$ , where  $a = -3/2$  and  $x = 2\mathbf{o}_r^T \mathbf{q} + \mathbf{q}^T \mathbf{q}$ . Note that this choice of  $x$  satisfies the convergence condition, since  $\mathbf{o}_r$  is a unit vector and  $\|\mathbf{q}\| \ll 1$ . The resultant expansion is

$$\begin{aligned} [1 + 2\mathbf{o}_r^T \mathbf{q} + \mathbf{q}^T \mathbf{q}]^{-3/2} &= 1 - \frac{3}{2}(2\mathbf{o}_r^T \mathbf{q} + \mathbf{q}^T \mathbf{q}) + \frac{15}{8}(2\mathbf{o}_r^T \mathbf{q} + \mathbf{q}^T \mathbf{q})^2 + \dots \\ &= 1 - 3\mathbf{o}_r^T \mathbf{q} - \frac{3}{2}\mathbf{q}^T \mathbf{q} + \frac{15}{8}(4\mathbf{o}_r^T \mathbf{q} \mathbf{o}_r^T \mathbf{q} + 4\mathbf{o}_r^T \mathbf{q} \mathbf{q}^T \mathbf{q} + \mathbf{q}^T \mathbf{q} \mathbf{q}^T \mathbf{q}) + \dots \\ &\approx 1 - 3\mathbf{o}_r^T \mathbf{q} - \frac{3}{2}\mathbf{q}^T \mathbf{q} + \frac{15}{2}\mathbf{o}_r^T \mathbf{q} \mathbf{o}_r^T \mathbf{q} \end{aligned}$$

where terms of degree three and higher in  $\|\mathbf{q}\|$  are assumed small for our purposes and eliminated. Neglecting these higher order terms, the gravity force is written as

$$\mathbf{F}_g = -\frac{\mu}{R^2} \int_{\mathcal{B}} (\mathbf{o}_r + \mathbf{q}) \left[ 1 - 3\mathbf{o}_r^T \mathbf{q} - \frac{3}{2}\mathbf{q}^T \mathbf{q} + \frac{15}{2}\mathbf{o}_r^T \mathbf{q} \mathbf{o}_r^T \mathbf{q} \right] dm, \quad (2.50)$$

which, again ignoring terms of degree three and higher in  $\|\mathbf{q}\|$ , becomes

$$\mathbf{F}_g = -\frac{\mu}{R^2} \int_{\mathcal{B}} \left[ \mathbf{o}_r - 3\mathbf{o}_r \mathbf{o}_r^T \mathbf{q} - \frac{3}{2}\mathbf{o}_r \mathbf{q}^T \mathbf{q} + \frac{15}{2}\mathbf{o}_r \mathbf{o}_r^T \mathbf{q} \mathbf{o}_r^T \mathbf{q} + \mathbf{q} - 3\mathbf{q} \mathbf{o}_r^T \mathbf{q} \right] dm. \quad (2.51)$$

Recall the integral is being taken about the mass center of the body, which means that

$\int \mathbf{q} dm = 0$ . This further simplifies the force equation to

$$\mathbf{F}_g = -\frac{\mu}{R^2} \int_{\mathcal{B}} \left[ \mathbf{o}_r - \frac{3}{2} \mathbf{o}_r \mathbf{q}^T \mathbf{q} + \frac{15}{2} \mathbf{o}_r \mathbf{o}_r^T \mathbf{q} \mathbf{o}_r^T \mathbf{q} - 3 \mathbf{q} \mathbf{o}_r^T \mathbf{q} \right] dm, \quad (2.52)$$

whose terms can be expanded and rearranged to yield

$$\mathbf{F}_g = -\frac{\mu}{R^2} \int_{\mathcal{B}} \left[ \mathbf{o}_r - \frac{3}{2} \mathbf{o}_r \mathbf{q}^T \mathbf{q} + \frac{15}{2} \mathbf{o}_r \mathbf{o}_r^T \mathbf{q} \mathbf{q}^T \mathbf{o}_r - 3 \mathbf{q} \mathbf{q}^T \mathbf{o}_r \right] dm. \quad (2.53)$$

Recalling that  $\mathbf{q} = \mathbf{r}/R$ , and noting that  $\mathbf{o}_r$  is constant over the volume of integration, the gravitational force equation becomes

$$\mathbf{F}_g = -\frac{\mu m}{R^2} \mathbf{o}_r + \frac{3\mu}{2R^4} \left[ \mathbf{o}_r \int_{\mathcal{B}} \mathbf{r}^T \mathbf{r} dm - 5 \mathbf{o}_r \mathbf{o}_r^T \int_{\mathcal{B}} \mathbf{r} \mathbf{r}^T dm \mathbf{o}_r + 2 \int_{\mathcal{B}} \mathbf{r} \mathbf{r}^T dm \mathbf{o}_r \right]. \quad (2.54)$$

The remaining integrals can be solved by using the definition of the moment of inertia of a rigid body

$$\mathbf{J} = \int_{\mathcal{B}} (\mathbf{r}^T \mathbf{r} \mathbb{I} - \mathbf{r} \mathbf{r}^T) dm, \quad (2.55)$$

where  $\mathbb{I}$  is a  $3 \times 3$  identity matrix. The trace of the inertia matrix is the sum of its diagonal elements, and can be manipulated as such:

$$\begin{aligned} \text{tr}(\mathbf{J}) &= \mathbf{n}_1^T \mathbf{J} \mathbf{n}_1 + \mathbf{n}_2^T \mathbf{J} \mathbf{n}_2 + \mathbf{n}_3^T \mathbf{J} \mathbf{n}_3 \\ &= \mathbf{n}_1^T \int_{\mathcal{B}} (\mathbf{r}^T \mathbf{r} \mathbb{I} - \mathbf{r} \mathbf{r}^T) dm \mathbf{n}_1 + \mathbf{n}_2^T \int_{\mathcal{B}} (\mathbf{r}^T \mathbf{r} \mathbb{I} - \mathbf{r} \mathbf{r}^T) dm \mathbf{n}_2 + \mathbf{n}_3^T \int_{\mathcal{B}} (\mathbf{r}^T \mathbf{r} \mathbb{I} - \mathbf{r} \mathbf{r}^T) dm \mathbf{n}_3 \\ &= \int_{\mathcal{B}} (\mathbf{r}^T \mathbf{r} - \mathbf{n}_1^T \mathbf{r} \mathbf{r}^T \mathbf{n}_1 + \mathbf{r}^T \mathbf{r} - \mathbf{n}_2^T \mathbf{r} \mathbf{r}^T \mathbf{n}_2 + \mathbf{r}^T \mathbf{r} - \mathbf{n}_3^T \mathbf{r} \mathbf{r}^T \mathbf{n}_3) dm \\ &= \int_{\mathcal{B}} (3 \mathbf{r}^T \mathbf{r} - \mathbf{r}^T \mathbf{r}) dm \\ \text{tr}(\mathbf{J}) &= 2 \int_{\mathcal{B}} \mathbf{r}^T \mathbf{r} dm \end{aligned} \quad (2.56)$$

Furthermore, the integral definition of the inertia can be rearranged as

$$\begin{aligned} \int_{\mathcal{B}} \mathbf{r}\mathbf{r}^T dm &= \mathbb{I} \int_{\mathcal{B}} \mathbf{r}^T \mathbf{r} dm - \mathbf{J} \\ &= \mathbb{I} \frac{1}{2} \text{tr}(\mathbf{J}) - \mathbf{J} \end{aligned} \quad (2.57)$$

Substituting these relations into the force equation, one arrives to

$$\mathbf{F}_g = -\frac{\mu m}{R^2} \mathbf{o}_r - \frac{3\mu}{2R^4} \left[ -\frac{1}{2} \text{tr}(\mathbf{J}) + 5(\mathbf{o}_r^T (\mathbb{I} \frac{1}{2} \text{tr}(\mathbf{J}) - \mathbf{J}) \mathbf{o}_r) \right] \mathbf{o}_r - \frac{3\mu}{R^4} (\mathbb{I} \frac{1}{2} \text{tr}(\mathbf{J}) - \mathbf{J}) \mathbf{o}_r \quad (2.58)$$

Collecting terms and simplifying yields the final equation for the gravitational force expressed in the trajectory frame  $\{\mathbf{o}\}$ ,

$$\mathbf{F}_g = -\frac{\mu m}{R^2} \mathbf{o}_r - \frac{3\mu}{2R^4} [\text{tr}(\mathbf{J}) - 5\mathbf{o}_r^T \mathbf{J} \mathbf{o}_r] \mathbf{o}_r - \frac{3\mu}{R^4} \mathbf{J} \mathbf{o}_r. \quad (2.59)$$

This can also be written as

$$\mathbf{F}_g = -\frac{\mu m}{R^2} \mathbf{o}_r + \mathbf{f}. \quad (2.60)$$

This is the resulting approximated form of the gravitational force exerted by the Earth on a general 3-D rigid body, where  $\mathbf{f}$  represents the gravitational perturbative forces. This form is particularly useful because it separates out the perturbative gravitational forces acting on the rigid bodies. Specifically, the perturbative force considering an orbiting spacecraft as a rigid body instead of a simple point mass is

$$\mathbf{f} = -\frac{3\mu}{2R^4} [\text{tr}(\mathbf{J}) - 5\mathbf{o}_r^T \mathbf{J} \mathbf{o}_r] \mathbf{o}_r - \frac{3\mu}{R^4} \mathbf{J} \mathbf{o}_r. \quad (2.61)$$

Eq. (2.59) provides a straightforward formula for determining the effects of gravitational forces on the base and bars that make up a tensegrity spacecraft. The resulting gravity force

formulas for each rigid member can be directly used in Equation (4.48) for the approximate generalized forces due to gravity.

### Derivation of Gravitational Moment

The moment due to the gravitational force acting on a generic 3-D rigid massive body is defined as

$$\mathbf{M}_g = \int_B \mathbf{r}^\times d\mathbf{F}_g, \quad (2.62)$$

where the skew symmetric matrix  $\mathbf{r}^\times$  of a vector  $\mathbf{r} = [r_1 \ r_2 \ r_3]^\text{T}$  is defined as

$$\mathbf{r}^\times = \begin{bmatrix} 0 & -r_3 & r_2 \\ r_3 & 0 & -r_1 \\ -r_2 & r_1 & 0 \end{bmatrix}.$$

Using the relation  $\boldsymbol{\rho} = \mathbf{r} + \mathbf{R}$ , the moment can be written as

$$\begin{aligned} \mathbf{M}_g &= \int_B (\boldsymbol{\rho} - \mathbf{R})^\times d\mathbf{F}_g \\ &= \int_B \boldsymbol{\rho}^\times d\mathbf{F}_g - \int_B \mathbf{R}^\times d\mathbf{F}_g \\ &= \int_B \boldsymbol{\rho}^\times d\mathbf{F}_g - \mathbf{R}^\times \mathbf{F}_g \end{aligned} \quad (2.63)$$

However, because  $d\mathbf{F}_g$  is parallel to  $\boldsymbol{\rho}$ , this means that  $\boldsymbol{\rho}^\times d\mathbf{F}_g = 0$ . Thus,

$$\mathbf{M}_g = -\mathbf{R}^\times \mathbf{F}_g. \quad (2.64)$$

This equation can be further manipulated by substituting in the expression for  $\mathbf{F}_g$  and letting  $\mathbf{R} = R\mathbf{o}_r$ , which yields

$$\mathbf{M}_g = -R\mathbf{o}_r^\times \left[ -\frac{\mu m}{R^2} \mathbf{o}_r - \frac{3\mu}{2R^4} [\text{tr}(\mathbf{J}) - 5\mathbf{o}_r^\text{T} \mathbf{J} \mathbf{o}_r] \mathbf{o}_r - \frac{3\mu}{R^4} \mathbf{J} \mathbf{o}_r \right] \quad (2.65)$$



Recognizing that  $\mathbf{o}_r^\times \mathbf{o}_r = 0$ , the gravitational moment on the rigid body expressed in the  $\{\mathbf{o}\}$  frame becomes

$$\mathbf{M}_g = \frac{3\mu}{R^3} \mathbf{o}_r^\times \mathbf{J} \mathbf{o}_r. \quad (2.66)$$

## 2.3 Elastic Potential Energy

The tendon elastic effects on the system are derived in a previous paper by the author[8, 35], and are included here. Recall that the tendons are assumed to be massless and linear elastic. For a tendon  $j$  experiencing a tensile load of  $F_j$  and an elongation of  $\varepsilon_j$ , the potential energy of this tendon is

$$V_{e_j} = \int_0^{\varepsilon_j'} F_j d\varepsilon_j. \quad (2.67)$$

The elongation is defined as the difference between the rest length  $r_j$  of the tendon and its stretched length due to the load  $F_j$ . Thus the elongation is  $\varepsilon = l_j - r_j$  and, given that the rest length is a constant, the elongation differential  $d\varepsilon_j$  can alternatively be written as

$$d\varepsilon_j = dl_j = \sum_{k=1}^N \frac{\partial l_j}{\partial q_k} dq_k, \quad (2.68)$$

where  $N$  is the number of generalized coordinates. Using this alternate expression for the differential, the elastic potential energy of the  $j$ th tendon becomes

$$V_{e_j} = \int_{q_0}^q F_j \sum_{k=1}^N \frac{\partial l_j}{\partial q_k} dq_k, \quad (2.69)$$

where  $q_0$  and  $q$  are the rest (unstressed) and elongated tendon configurations, respectively.

The impact of all the tendons on the tensegrity structure is simply a summation of all of

their individual potential energies, namely:

$$V_e = \sum_{j=1}^E V_{e_j}, \quad (2.70)$$

where  $E$  are the total number of tendons that make up the tensegrity structure.

It is desirable to write this in a form that is easily substituted into the equations of motion from Equation (2.20) - that is, as a gradient of the elastic potential energy with respect to the generalized coordinates. Thus the expression for  $V_e$  can be arranged as follows

$$\nabla_{\mathbf{q}} V_e = \mathbf{A}(\mathbf{q}) \mathbf{F}. \quad (2.71)$$

where the elements of the matrix  $\mathbf{A}(\mathbf{q})$  are[22]

$$A_{kj} = \frac{\partial l_j}{\partial q_k}, \quad k = 1, \dots, N, j = 1, \dots, E, \quad (2.72)$$

and  $\mathbf{F}$  is the vector of tendon elastic forces, whose elements are given by

$$F_j = \frac{k_j}{r_j} (l_j - r_j) \quad (2.73)$$

where  $k_j$  is the stiffness of the  $j$ th tendon.

## 2.4 Thruster Generalized Forces

To maintain the spacecraft's desired orbit and attitude, a set of six thrusters are mounted on the base of the spacecraft. Three of those thrusters are chosen to generate forces along the three principle axes, and the three generate perfect moments about those three axes.

Expressed in the body frame  $\{\mathbf{b}\}$  of the base, those forces and moments are

$$\begin{aligned} \mathbf{F}_{t_1} &= [u_1 \ 0 \ 0]^T & \mathbf{F}_{t_2} &= [0 \ u_2 \ 0]^T & \mathbf{F}_{t_3} &= [0 \ 0 \ u_3]^T \\ \mathbf{M}_{t_1} &= [u_4 \ 0 \ 0]^T & \mathbf{M}_{t_2} &= [0 \ u_5 \ 0]^T & \mathbf{M}_{t_3} &= [0 \ 0 \ u_6]^T \end{aligned} \quad (2.74)$$

where  $u_i$  is the magnitude of the control force or moment. These controls can be written in a matrix format as a function of the thruster control vector  $\mathbf{u}_t = [u_1 \ u_2 \ u_3 \ u_4 \ u_5 \ u_6]^T$  by summing the controls:

$$\sum_{i=1}^3 \mathbf{F}_{t_i} = \begin{bmatrix} u_1 \\ u_2 \\ u_3 \end{bmatrix} = [\mathbb{I}_{3 \times 3} \ \mathbf{0}_{3 \times 3}] \mathbf{u}_t = \bar{\mathbf{F}}_t \mathbf{u}_t \quad (2.75)$$

and

$$\sum_{i=1}^3 \mathbf{M}_{t_i} = \begin{bmatrix} u_4 \\ u_5 \\ u_6 \end{bmatrix} = [\mathbf{0}_{3 \times 3} \ \mathbb{I}_{3 \times 3}] \mathbf{u}_t = \bar{\mathbf{M}}_t \mathbf{u}_t \quad (2.76)$$

Now that the force and moments due to the thrusters are known, a vector of generalized forces can be created. The formula for the generalized forces due to the thruster controls is

$$\mathbf{Q}_t = \sum_{i=1}^3 \left[ \left( \frac{\partial \dot{\mathbf{r}}_0}{\partial \dot{\mathbf{q}}} \right)^T \mathbf{F}_{t_i} \right] + \sum_{i=1}^3 \left[ \left( \frac{\partial \boldsymbol{\omega}_0}{\partial \dot{\mathbf{q}}} \right)^T \mathbf{M}_{t_i} \right], \quad (2.77)$$

where  $\mathbf{F}_{t_i}$  and  $\mathbf{M}_{t_i}$  are those forces and moments due to the  $i$ th control that were just derived, and  $\dot{\mathbf{r}}_0$  and  $\boldsymbol{\omega}_0$  represent the translational and angular velocities of the base, the partial derivatives of which are given in Equation (2.24) and (2.29). Thus the generalized forces become

$$\mathbf{Q}_t = [\mathbf{P}_0(\mathbf{q})]^T \sum_{i=1}^3 \mathbf{F}_{t_i} + [\mathbf{S}_0(\mathbf{q})]^T \sum_{i=1}^3 \mathbf{M}_{t_i}. \quad (2.78)$$

Substituting in the summation of the force and moment controls, the resulting vector of generalized thruster forces is

$$\mathbf{Q}_t = [\mathbf{P}_0(\mathbf{q})]^T \bar{\mathbf{F}}_t \mathbf{u}_t + [\mathbf{S}_0(\mathbf{q})]^T \bar{\mathbf{M}}_t \mathbf{u}_t = \begin{bmatrix} \bar{\mathbf{Q}}_t \\ \mathbf{0}_{6 \times 6} \end{bmatrix} \mathbf{u}_t \quad (2.79)$$

## 2.5 General Equations of Motion

The previous sections derived all components of the dynamics of the system that are being considered, including the total kinetic energy, the gravitational effects on all massive elements, the elastic potential energy in the tendons that make up the tensegrity structure, and the thruster control forces on the spacecraft base. Now these components are incorporated into Equation (2.20), which recall was:

$$\frac{d}{dt}(\nabla_{\dot{\mathbf{q}}} T) - \nabla_{\mathbf{q}} T = -\nabla_{\mathbf{q}} V + \mathbf{Q}. \quad (2.80)$$

Substituting in the derived components, the resulting equations of motion of the system are:

$$\mathbf{M}(\mathbf{q})\ddot{\mathbf{q}} + \mathbf{C}(\mathbf{q}, \dot{\mathbf{q}})\dot{\mathbf{q}} = -\nabla_{\mathbf{q}} V_e + \mathbf{Q}_g + \mathbf{Q}_t, \quad (2.81)$$

where the elements of  $\mathbf{C}(\mathbf{q}, \dot{\mathbf{q}})$  are found using the mass matrix:[21]

$$C_{ij} = \frac{1}{2} \sum_{k=1}^{12} \left( \frac{\partial M_{ij}}{\partial q_k} + \frac{\partial M_{ik}}{\partial q_j} + \frac{\partial M_{jk}}{\partial q_i} \right) \dot{q}_k. \quad (2.82)$$

These are the general equations of motion that will be used to analyze the dynamics of the 3-bar and 6-bar tensegrity spacecraft that are to be discussed in Chapter 4.

# Chapter 3

## General Control

The equations of motion that were derived for the tensegrity spacecraft are second order nonlinear equations. This chapter details the process for using a linear quadratic regulator (LQR) to control the orientation of the spacecraft and the shape of the tensegrity structure. The equations of motion describe a nonlinear second order system; thus, the first step is to linearize the system about some desired equilibrium configuration, performed in Section 3.1. Following this, a linear quadratic regulator can be applied to the new first-order system, a process that is described in Section 3.2. Finally, the process for applying this linear control to the derived nonlinear system is discussed.

### 3.1 Linearization

Consider the generic second order system

$$F(\mathbf{q}, \dot{\mathbf{q}}, \ddot{\mathbf{q}}, \mathbf{u}) = \mathbf{M}(\mathbf{q})\ddot{\mathbf{q}} + \mathbf{C}(\mathbf{q}, \dot{\mathbf{q}})\dot{\mathbf{q}} + f(\mathbf{q}, \mathbf{u}) = 0 \quad (3.1)$$

where

$$\mathbf{M}(\mathbf{q}) = \begin{bmatrix} m_{11} & \dots & m_{1n} \\ \vdots & \ddots & \vdots \\ m_{n1} & \dots & m_{nn} \end{bmatrix} = [\mathbf{m}_1 \quad \dots \quad \mathbf{m}_n] \quad (3.2)$$

$$\mathbf{C}(\mathbf{q}, \dot{\mathbf{q}}) = \begin{bmatrix} c_{11} & \dots & c_{1n} \\ \vdots & \ddots & \vdots \\ c_{n1} & \dots & c_{nn} \end{bmatrix} = [\mathbf{c}_1 \quad \dots \quad \mathbf{c}_n] \quad (3.3)$$

$$\mathbf{f}(\mathbf{q}, \mathbf{u}) = \begin{bmatrix} f_1 \\ \vdots \\ f_n \end{bmatrix} \quad (3.4)$$

and generalized coordinates  $\mathbf{q}$  and controls  $\mathbf{u}$  vectors

$$\mathbf{q} = [q_1 \quad \dots \quad q_n]^T \quad \mathbf{u} = [u_1 \quad \dots \quad u_m]^T \quad (3.5)$$

The system can be linearized using a Taylor series expansion:

$$F(\mathbf{x}) \triangleq F(\mathbf{x}_d) + \sum_{k=1}^4 \frac{\partial F(\mathbf{x})}{\partial x_k} \delta x_k + h.o.t \quad (3.6)$$

where  $\mathbf{x} = [\mathbf{q} \quad \dot{\mathbf{q}} \quad \ddot{\mathbf{q}} \quad \mathbf{u}]^T$  and  $\mathbf{x}_d$  are these variables evaluated at some desired equilibrium condition. Thus the linearized system is

$$\tilde{F}(\mathbf{x}) \approx F(\mathbf{x}) - F(\mathbf{x}_d) = \left. \frac{\partial F}{\partial \mathbf{q}} \right|_d \delta \mathbf{q} + \left. \frac{\partial F}{\partial \dot{\mathbf{q}}} \right|_d \delta \dot{\mathbf{q}} + \left. \frac{\partial F}{\partial \ddot{\mathbf{q}}} \right|_d \delta \ddot{\mathbf{q}} + \left. \frac{\partial F}{\partial \mathbf{u}} \right|_d \delta \mathbf{u} \quad (3.7)$$

which is evaluated at the desired configuration  $\mathbf{x}_d$ .

Begin with the first term of Eq. (3.7):

$$\frac{\partial F}{\partial \mathbf{q}} = \frac{\partial \mathbf{M}(\mathbf{q})\ddot{\mathbf{q}}}{\partial \mathbf{q}} + \frac{\partial \mathbf{C}(\mathbf{q}, \dot{\mathbf{q}})\dot{\mathbf{q}}}{\partial \mathbf{q}} + \frac{\partial f(\mathbf{q}, \mathbf{u})}{\partial \mathbf{q}} \quad (3.8)$$

$$= \frac{\partial \mathbf{M}(\mathbf{q})}{\partial \mathbf{q}} \ddot{\mathbf{q}} + \frac{\partial \mathbf{C}(\mathbf{q}, \dot{\mathbf{q}})}{\partial \mathbf{q}} \dot{\mathbf{q}} + \frac{\partial f(\mathbf{q}, \mathbf{u})}{\partial \mathbf{q}} \quad (3.9)$$

where each of the parts are derived as follows:

$$\frac{\partial \mathbf{M}(\mathbf{q})}{\partial \mathbf{q}} \ddot{\mathbf{q}} = \begin{bmatrix} \frac{\partial m_{11}}{\partial \mathbf{q}} & \cdots & \frac{\partial m_{1n}}{\partial \mathbf{q}} \\ \vdots & \ddots & \vdots \\ \frac{\partial m_{n1}}{\partial \mathbf{q}} & \cdots & \frac{\partial m_{nn}}{\partial \mathbf{q}} \end{bmatrix} \begin{bmatrix} \ddot{q}_1 \\ \vdots \\ \ddot{q}_n \end{bmatrix} \quad (3.10)$$

$$= \begin{bmatrix} \left[ \frac{\partial m_{11}}{\partial \mathbf{q}_1} & \cdots & \frac{\partial m_{11}}{\partial \mathbf{q}_n} \right] \ddot{q}_1 + \cdots + \left[ \frac{\partial m_{1n}}{\partial \mathbf{q}_1} & \cdots & \frac{\partial m_{1n}}{\partial \mathbf{q}_n} \right] \ddot{q}_n \\ \vdots \\ \left[ \frac{\partial m_{n1}}{\partial \mathbf{q}_1} & \cdots & \frac{\partial m_{n1}}{\partial \mathbf{q}_n} \right] \ddot{q}_1 + \cdots + \left[ \frac{\partial m_{nn}}{\partial \mathbf{q}_1} & \cdots & \frac{\partial m_{nn}}{\partial \mathbf{q}_n} \right] \ddot{q}_n \end{bmatrix} \quad (3.11)$$

$$= \begin{bmatrix} \frac{\partial m_{11}}{\partial \mathbf{q}_1} \ddot{q}_1 + \cdots + \frac{\partial m_{1n}}{\partial \mathbf{q}_1} \ddot{q}_n & \cdots & \frac{\partial m_{11}}{\partial \mathbf{q}_n} \ddot{q}_1 + \cdots + \frac{\partial m_{1n}}{\partial \mathbf{q}_n} \ddot{q}_n \\ \vdots & \ddots & \vdots \\ \frac{\partial m_{n1}}{\partial \mathbf{q}_1} \ddot{q}_1 + \cdots + \frac{\partial m_{nn}}{\partial \mathbf{q}_1} \ddot{q}_n & \cdots & \frac{\partial m_{n1}}{\partial \mathbf{q}_n} \ddot{q}_1 + \cdots + \frac{\partial m_{nn}}{\partial \mathbf{q}_n} \ddot{q}_n \end{bmatrix} \quad (3.12)$$

$$= \begin{bmatrix} \frac{\partial m_{11}}{\partial \mathbf{q}_1} \ddot{q}_1 & \cdots & \frac{\partial m_{11}}{\partial \mathbf{q}_n} \ddot{q}_1 \\ \vdots & \ddots & \vdots \\ \frac{\partial m_{n1}}{\partial \mathbf{q}_1} \ddot{q}_1 & \cdots & \frac{\partial m_{n1}}{\partial \mathbf{q}_n} \ddot{q}_1 \end{bmatrix} + \begin{bmatrix} \frac{\partial m_{1n}}{\partial \mathbf{q}_1} \ddot{q}_n & \cdots & \frac{\partial m_{1n}}{\partial \mathbf{q}_n} \ddot{q}_n \\ \vdots & \ddots & \vdots \\ \frac{\partial m_{nn}}{\partial \mathbf{q}_1} \ddot{q}_n & \cdots & \frac{\partial m_{nn}}{\partial \mathbf{q}_n} \ddot{q}_n \end{bmatrix} \quad (3.13)$$

$$= \frac{\partial \mathbf{m}_1}{\partial \mathbf{q}} \ddot{q}_1 + \cdots + \frac{\partial \mathbf{m}_n}{\partial \mathbf{q}} \ddot{q}_n \quad (3.14)$$

$$= \sum_{k=1}^n \frac{\partial \mathbf{m}_k}{\partial \mathbf{q}} \ddot{q}_k \quad (3.15)$$



$$\frac{\partial \mathbf{C}(\mathbf{q}, \dot{\mathbf{q}})}{\partial \mathbf{q}} \dot{\mathbf{q}} = \begin{bmatrix} \frac{\partial c_{11}}{\partial \mathbf{q}} & \cdots & \frac{\partial c_{1n}}{\partial \mathbf{q}} \\ \vdots & \ddots & \vdots \\ \frac{\partial c_{n1}}{\partial \mathbf{q}} & \cdots & \frac{\partial c_{nn}}{\partial \mathbf{q}} \end{bmatrix} \begin{bmatrix} \dot{q}_1 \\ \vdots \\ \dot{q}_n \end{bmatrix} \quad (3.16)$$

$$= \begin{bmatrix} \left[ \frac{\partial c_{11}}{\partial \mathbf{q}_1} & \cdots & \frac{\partial c_{11}}{\partial \mathbf{q}_n} \right] \dot{q}_1 + \cdots + \left[ \frac{\partial c_{1n}}{\partial \mathbf{q}_1} & \cdots & \frac{\partial c_{1n}}{\partial \mathbf{q}_n} \right] \dot{q}_n \\ \vdots \\ \left[ \frac{\partial c_{n1}}{\partial \mathbf{q}_1} & \cdots & \frac{\partial c_{n1}}{\partial \mathbf{q}_n} \right] \dot{q}_1 + \cdots + \left[ \frac{\partial c_{nn}}{\partial \mathbf{q}_1} & \cdots & \frac{\partial c_{nn}}{\partial \mathbf{q}_n} \right] \dot{q}_n \end{bmatrix} \quad (3.17)$$

$$= \begin{bmatrix} \frac{\partial c_{11}}{\partial \mathbf{q}_1} \dot{q}_1 + \cdots + \frac{\partial c_{1n}}{\partial \mathbf{q}_1} \dot{q}_n & \cdots & \frac{\partial c_{11}}{\partial \mathbf{q}_n} \dot{q}_1 + \cdots + \frac{\partial c_{1n}}{\partial \mathbf{q}_n} \dot{q}_n \\ \vdots & \ddots & \vdots \\ \frac{\partial c_{n1}}{\partial \mathbf{q}_1} \dot{q}_1 + \cdots + \frac{\partial c_{nn}}{\partial \mathbf{q}_1} \dot{q}_n & \cdots & \frac{\partial c_{n1}}{\partial \mathbf{q}_n} \dot{q}_1 + \cdots + \frac{\partial c_{nn}}{\partial \mathbf{q}_n} \dot{q}_n \end{bmatrix} \quad (3.18)$$

$$= \begin{bmatrix} \frac{\partial c_{11}}{\partial \mathbf{q}_1} \dot{q}_1 & \cdots & \frac{\partial c_{11}}{\partial \mathbf{q}_n} \dot{q}_1 \\ \vdots & \ddots & \vdots \\ \frac{\partial c_{n1}}{\partial \mathbf{q}_1} \dot{q}_1 & \cdots & \frac{\partial c_{n1}}{\partial \mathbf{q}_n} \dot{q}_1 \end{bmatrix} + \begin{bmatrix} \frac{\partial c_{1n}}{\partial \mathbf{q}_1} \dot{q}_n & \cdots & \frac{\partial c_{1n}}{\partial \mathbf{q}_n} \dot{q}_n \\ \vdots & \ddots & \vdots \\ \frac{\partial c_{nn}}{\partial \mathbf{q}_1} \dot{q}_n & \cdots & \frac{\partial c_{nn}}{\partial \mathbf{q}_n} \dot{q}_n \end{bmatrix} \quad (3.19)$$

$$= \frac{\partial \mathbf{c}_1}{\partial \mathbf{q}} \dot{q}_1 + \cdots + \frac{\partial \mathbf{c}_n}{\partial \mathbf{q}} \dot{q}_n \quad (3.20)$$

$$= \sum_{k=1}^n \frac{\partial \mathbf{c}_k}{\partial \mathbf{q}} \dot{q}_k \quad (3.21)$$

$$\frac{\partial f(\mathbf{q}, \mathbf{u})}{\partial \mathbf{q}} = \begin{bmatrix} \frac{\partial f_1}{\partial \mathbf{q}} \\ \vdots \\ \frac{\partial f_n}{\partial \mathbf{q}} \end{bmatrix} = \begin{bmatrix} \frac{\partial f_1}{\partial q_1} & \cdots & \frac{\partial f_1}{\partial q_n} \\ \vdots & \ddots & \vdots \\ \frac{\partial f_n}{\partial q_1} & \cdots & \frac{\partial f_n}{\partial q_n} \end{bmatrix} \quad (3.22)$$

Evaluating at  $\mathbf{x}_d$ , the first term of Eq. (3.7) becomes

$$\left. \frac{\partial F}{\partial \mathbf{q}} \right|_d = \sum_{k=1}^n \left. \frac{\partial \mathbf{m}_k}{\partial \mathbf{q}} \right|_d \ddot{q}_{d_k} + \sum_{k=1}^n \left. \frac{\partial \mathbf{c}_k}{\partial \mathbf{q}} \right|_d \dot{q}_{d_k} + \left. \frac{\partial f(\mathbf{q}, \mathbf{u})}{\partial \mathbf{q}} \right|_d \quad (3.23)$$

Moving on to the second term of Eq. (3.7), the resulting expression becomes

$$\frac{\partial F}{\partial \dot{\mathbf{q}}} = \frac{\partial \mathbf{M}(\mathbf{q}) \ddot{\mathbf{q}}}{\partial \dot{\mathbf{q}}} + \frac{\partial \mathbf{C}(\mathbf{q}, \dot{\mathbf{q}}) \dot{\mathbf{q}}}{\partial \dot{\mathbf{q}}} + \frac{\partial f(\mathbf{q}, \mathbf{u})}{\partial \dot{\mathbf{q}}} \quad (3.24)$$

$$= \mathbf{C}(\mathbf{q}, \dot{\mathbf{q}}) + \frac{\partial \mathbf{C}(\mathbf{q}, \dot{\mathbf{q}})}{\partial \dot{\mathbf{q}}} \dot{\mathbf{q}} \quad (3.25)$$

where

$$\frac{\partial \mathbf{C}(\mathbf{q}, \dot{\mathbf{q}})}{\partial \dot{\mathbf{q}}} \dot{\mathbf{q}} = \begin{bmatrix} \frac{\partial c_{11}}{\partial \dot{\mathbf{q}}} & \cdots & \frac{\partial c_{1n}}{\partial \dot{\mathbf{q}}} \\ \vdots & \ddots & \vdots \\ \frac{\partial c_{n1}}{\partial \dot{\mathbf{q}}} & \cdots & \frac{\partial c_{nn}}{\partial \dot{\mathbf{q}}} \end{bmatrix} \begin{bmatrix} \dot{q}_1 \\ \vdots \\ \dot{q}_n \end{bmatrix} \quad (3.26)$$

$$= \begin{bmatrix} \left[ \frac{\partial c_{11}}{\partial \dot{\mathbf{q}}} & \cdots & \frac{\partial c_{11}}{\partial \dot{\mathbf{q}}_n} \right] \dot{q}_1 + \cdots + \left[ \frac{\partial c_{1n}}{\partial \dot{\mathbf{q}}} & \cdots & \frac{\partial c_{1n}}{\partial \dot{\mathbf{q}}_n} \right] \dot{q}_n \\ \vdots \\ \left[ \frac{\partial c_{n1}}{\partial \dot{\mathbf{q}}} & \cdots & \frac{\partial c_{n1}}{\partial \dot{\mathbf{q}}_n} \right] \dot{q}_1 + \cdots + \left[ \frac{\partial c_{nn}}{\partial \dot{\mathbf{q}}} & \cdots & \frac{\partial c_{nn}}{\partial \dot{\mathbf{q}}_n} \right] \dot{q}_n \end{bmatrix} \quad (3.27)$$

$$= \begin{bmatrix} \frac{\partial c_{11}}{\partial \dot{\mathbf{q}}_1} \dot{q}_1 + \cdots + \frac{\partial c_{1n}}{\partial \dot{\mathbf{q}}_1} \dot{q}_n & \cdots & \frac{\partial c_{11}}{\partial \dot{\mathbf{q}}_n} \dot{q}_1 + \cdots + \frac{\partial c_{1n}}{\partial \dot{\mathbf{q}}_n} \dot{q}_n \\ \vdots & \ddots & \vdots \\ \frac{\partial c_{n1}}{\partial \dot{\mathbf{q}}_1} \dot{q}_1 + \cdots + \frac{\partial c_{nn}}{\partial \dot{\mathbf{q}}_1} \dot{q}_n & \cdots & \frac{\partial c_{n1}}{\partial \dot{\mathbf{q}}_n} \dot{q}_1 + \cdots + \frac{\partial c_{nn}}{\partial \dot{\mathbf{q}}_n} \dot{q}_n \end{bmatrix} \quad (3.28)$$

$$= \begin{bmatrix} \frac{\partial c_{11}}{\partial \dot{\mathbf{q}}_1} \dot{q}_1 & \cdots & \frac{\partial c_{11}}{\partial \dot{\mathbf{q}}_n} \dot{q}_1 \\ \vdots & \ddots & \vdots \\ \frac{\partial c_{n1}}{\partial \dot{\mathbf{q}}_1} \dot{q}_1 & \cdots & \frac{\partial c_{n1}}{\partial \dot{\mathbf{q}}_n} \dot{q}_1 \end{bmatrix} + \begin{bmatrix} \frac{\partial c_{1n}}{\partial \dot{\mathbf{q}}_1} \dot{q}_n & \cdots & \frac{\partial c_{1n}}{\partial \dot{\mathbf{q}}_n} \dot{q}_n \\ \vdots & \ddots & \vdots \\ \frac{\partial c_{nn}}{\partial \dot{\mathbf{q}}_1} \dot{q}_n & \cdots & \frac{\partial c_{nn}}{\partial \dot{\mathbf{q}}_n} \dot{q}_n \end{bmatrix} \quad (3.29)$$

$$= \frac{\partial \mathbf{c}_1}{\partial \dot{\mathbf{q}}} \dot{q}_1 + \cdots + \frac{\partial \mathbf{c}_n}{\partial \dot{\mathbf{q}}} \dot{q}_n \quad (3.30)$$

$$= \sum_{k=1}^n \frac{\partial \mathbf{c}_k}{\partial \dot{\mathbf{q}}} \dot{q}_k \quad (3.31)$$

Evaluating at  $\mathbf{x}_d$ , the second term of Eq. (3.7) becomes

$$\left. \frac{\partial F}{\partial \dot{\mathbf{q}}} \right|_d = \mathbf{C}(\mathbf{q}_d, \dot{\mathbf{q}}_d) + \sum_{k=1}^n \left. \frac{\partial \mathbf{c}_k}{\partial \dot{\mathbf{q}}} \right|_d \dot{q}_{d_k} \quad (3.32)$$

The third term of Eq. (3.7) is simply

$$\frac{\partial F}{\partial \ddot{\mathbf{q}}} = \frac{\partial \mathbf{M}(\mathbf{q}) \ddot{\mathbf{q}}}{\partial \ddot{\mathbf{q}}} + \frac{\partial \mathbf{C}(\mathbf{q}, \dot{\mathbf{q}}) \dot{\mathbf{q}}}{\partial \ddot{\mathbf{q}}} + \frac{\partial f(\mathbf{q}, \mathbf{u})}{\partial \ddot{\mathbf{q}}} \quad (3.33)$$

$$\left. \frac{\partial F}{\partial \ddot{\mathbf{q}}} \right|_d = \mathbf{M}(\mathbf{q}_d) \quad (3.34)$$

Finally, the fourth term of Eq. (3.7) is

$$\frac{\partial F}{\partial \mathbf{u}} = \frac{\partial \mathbf{M}(\mathbf{q})\ddot{\mathbf{q}}}{\partial \mathbf{u}} + \frac{\partial \mathbf{C}(\mathbf{q}, \dot{\mathbf{q}})\dot{\mathbf{q}}}{\partial \mathbf{u}} + \frac{\partial f(\mathbf{q}, \mathbf{u})}{\partial \mathbf{u}} \quad (3.35)$$

$$\left. \frac{\partial F}{\partial \mathbf{u}} \right|_d = \left. \frac{\partial f(\mathbf{q}, \mathbf{u})}{\partial \mathbf{u}} \right|_d \quad (3.36)$$

where

$$\frac{\partial f(\mathbf{q}, \mathbf{u})}{\partial \mathbf{u}} = \begin{bmatrix} \frac{\partial f_1}{\partial \mathbf{u}} \\ \vdots \\ \frac{\partial f_n}{\partial \mathbf{u}} \end{bmatrix} = \begin{bmatrix} \frac{\partial f_1}{\partial u_1} & \cdots & \frac{\partial f_1}{\partial u_m} \\ \vdots & \ddots & \vdots \\ \frac{\partial f_n}{\partial u_1} & \cdots & \frac{\partial f_n}{\partial u_m} \end{bmatrix} \quad (3.37)$$

Thus, Eq. (3.7) can be written as the linearized EOM

$$\tilde{\mathbf{K}}\delta\mathbf{q} + \tilde{\mathbf{C}}\delta\dot{\mathbf{q}} + \tilde{\mathbf{M}}\delta\ddot{\mathbf{q}} + \tilde{\mathbf{B}}\delta\mathbf{u} = 0 \quad (3.38)$$

where each of the terms derived are summarized below

$$\tilde{\mathbf{K}} = \sum_{k=1}^n \frac{\partial \mathbf{m}_k}{\partial \mathbf{q}} \Big|_d \ddot{q}_{d_k} + \sum_{k=1}^n \frac{\partial \mathbf{c}_k}{\partial \mathbf{q}} \Big|_d \dot{q}_{d_k} + \left. \frac{\partial f(\mathbf{q}, \mathbf{u})}{\partial \mathbf{q}} \right|_d \quad (3.39)$$

$$\tilde{\mathbf{C}} = \mathbf{C}(\mathbf{q}_d, \dot{\mathbf{q}}_d) + \sum_{k=1}^n \frac{\partial \mathbf{c}_k}{\partial \dot{\mathbf{q}}} \Big|_d \dot{q}_{d_k} \quad (3.40)$$

$$\tilde{\mathbf{M}} = \mathbf{M}(\mathbf{q}_d) \quad (3.41)$$

$$\tilde{\mathbf{B}} = \left. \frac{\partial f(\mathbf{q}, \mathbf{u})}{\partial \mathbf{u}} \right|_d \quad (3.42)$$

## 3.2 LQR Control

The equations of motion for the tensegrity system can be arranged as such:

$$\mathbf{M}(\mathbf{q})\ddot{\mathbf{q}} + \mathbf{C}(\mathbf{q}, \dot{\mathbf{q}})\dot{\mathbf{q}} + (\nabla_{\mathbf{q}}V_e(\mathbf{q}, \mathbf{u}) - \mathbf{Q}_g(\mathbf{q}) - \mathbf{Q}_t(\mathbf{q}, \mathbf{u})) = \mathbf{0}, \quad (3.43)$$

where  $\mathbf{q}$  are the generalized coordinates and  $\mathbf{u}$  the controls, which include the thruster controls and the tendon length controls. Linearizing about some desired configuration yields the linearized second order system

$$\tilde{\mathbf{M}}\delta\ddot{\mathbf{q}} + \tilde{\mathbf{C}}\delta\dot{\mathbf{q}} + \tilde{\mathbf{K}}\delta\mathbf{q} + \tilde{\mathbf{B}}\delta\mathbf{u} = \mathbf{0}. \quad (3.44)$$

This system can be converted into the first order system

$$\dot{\mathbf{x}} = \tilde{\mathbf{A}}\mathbf{x} + \tilde{\mathbf{B}}\mathbf{u}, \quad \mathbf{x}(0) = \mathbf{x}_d, \quad (3.45)$$

where  $\mathbf{x} = [\delta\mathbf{q} \quad \delta\dot{\mathbf{q}}]^T = [(\mathbf{q} - \mathbf{q}_d) \quad (\dot{\mathbf{q}} - \dot{\mathbf{q}}_d)]^T$  and  $\mathbf{u} = \delta\mathbf{u} = (\mathbf{u} - \mathbf{u}_d)$ , and where

$$\tilde{\mathbf{A}} = \begin{bmatrix} \mathbf{0} & \mathbb{I} \\ -\tilde{\mathbf{M}}^{-1}\tilde{\mathbf{K}} & -\tilde{\mathbf{M}}^{-1}\tilde{\mathbf{C}} \end{bmatrix} \quad (3.46)$$

$$\tilde{\mathbf{B}} = \begin{bmatrix} \mathbf{0} \\ -\tilde{\mathbf{M}}^{-1}\tilde{\mathbf{B}} \end{bmatrix}. \quad (3.47)$$

Let  $\mathbf{C}$  be a matrix that satisfies  $\mathbf{Q} = \mathbf{C}^T\mathbf{C}$ . If the system  $(\mathbf{A}, \mathbf{B})$  is stabilizable and  $(\mathbf{A}, \mathbf{C})$  is detectable, then a linear quadratic regulator (LQR) can be developed such that the optimal state feedback control law

$$\mathbf{u} = -\mathbf{K}\mathbf{x} \quad (3.48)$$

minimizes the cost function

$$V = \int_0^\infty (\mathbf{x}^T\mathbf{Q}\mathbf{x} + \mathbf{u}^T\mathbf{R}\mathbf{u}) dt, \quad (3.49)$$

where  $\mathbf{Q}$  is positive semidefinite and  $\mathbf{R}$  is positive definite:

$$\mathbf{Q} = \mathbf{Q}^T \geq 0 \quad \text{and} \quad \mathbf{R} = \mathbf{R}^T > 0. \quad (3.50)$$

The choice of  $\mathbf{Q}$  and  $\mathbf{R}$  largely depend on the system and the response desired. Selecting a large  $\mathbf{Q}$  relative to  $\mathbf{R}$  will put greater weight on the state  $\mathbf{x}$ , thus requiring smaller state to keep the cost function  $V$  small. Similarly, a larger  $\mathbf{R}$  will result in a smaller control input  $\mathbf{u}$ .

Substituting in the control law  $\mathbf{u}$  yields a closed loop cost of

$$V = \int_0^{\infty} (\mathbf{x}^T \mathbf{Q} \mathbf{x} + \mathbf{x}^T \mathbf{K}^T \mathbf{R} \mathbf{K} \mathbf{x}) dt \quad (3.51)$$

$$= \int_0^{\infty} \mathbf{x}^T (\mathbf{Q} + \mathbf{K}^T \mathbf{R} \mathbf{K}) \mathbf{x} dt \quad (3.52)$$

which is minimized by selecting

$$\mathbf{K} = \mathbf{R}^{-1} \tilde{\mathbf{B}}^T \mathbf{P}, \quad (3.53)$$

where  $\mathbf{P}$  is the positive definite matrix solution to the continuous algebraic Riccati equation (ARE),

$$\tilde{\mathbf{A}}^T \mathbf{P} + \mathbf{P} \tilde{\mathbf{A}} - \mathbf{P} \tilde{\mathbf{B}} \mathbf{R}^{-1} \tilde{\mathbf{B}}^T \mathbf{P} + \mathbf{Q} = \mathbf{0}. \quad (3.54)$$

The resultant closed-loop system

$$\dot{\mathbf{x}} = (\tilde{\mathbf{A}} - \tilde{\mathbf{B}} \mathbf{K}) \mathbf{x} = (\tilde{\mathbf{A}} - \tilde{\mathbf{B}} \mathbf{R}^{-1} \tilde{\mathbf{B}}^T \mathbf{P}) \mathbf{x} \quad (3.55)$$

will be exponentially stable.

Following this, the control law developed for the linearized system can then be applied to the nonlinear system, though it is important to recognize that this control law will work only for small disturbances of the nonlinear system from its equilibrium. The control law derived for the linear system was

$$\mathbf{u} = -\mathbf{K} \mathbf{x} \quad (3.56)$$

which is equivalent to

$$(\mathbf{u} - \mathbf{u}_d) = -\mathbf{K} [(\mathbf{q} - \mathbf{q}_d) \quad (\dot{\mathbf{q}} - \dot{\mathbf{q}}_d)]^T. \quad (3.57)$$

The resulting controls  $\mathbf{u}$  can be incorporated into the nonlinear system, to account for small disturbances from equilibrium.

# Chapter 4

## Application to Simple Tensegrity

### Spacecraft

#### 4.1 Spacecraft Base

Consider first the dynamics of the base of the spacecraft. For this analysis, the base is chosen to be a rectangular prism of mass  $m_0$  and dimensions along the first, second, and third axis are  $D_1$ ,  $D_2$ , and  $D_3$ , respectively, as shown in Figure 4.1.



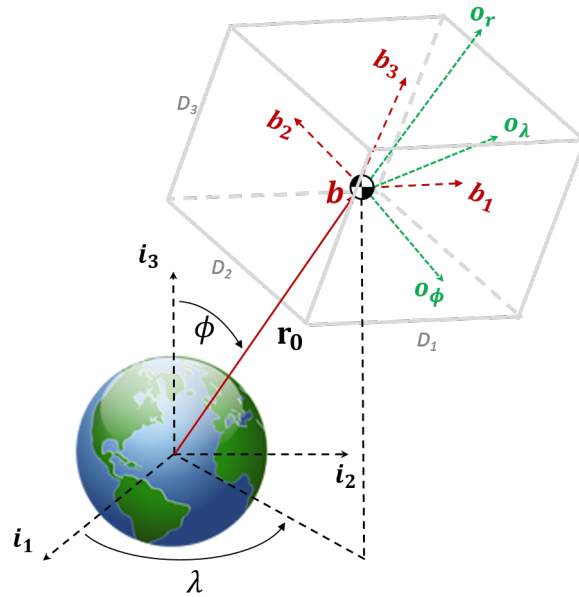


Figure 4.1: Position vectors and dimensions of rectangular-prism spacecraft base. The base has dimensions along its  $\{1, 2, 3\}$  principal axes of  $D_1$ ,  $D_2$ , and  $D_3$ , respectively. As the base is considered a rigid body, these dimensions are remain static.

### 4.1.1 Base Kinetic Energy

This section derives the kinetic energy of the base, which will consist of the summation of its total translational and rotational energy:

$$T = \{T_T + T_R\} \tag{4.1}$$

## Translational Energy

The translational component of the energy of the base is

$$T_T = \frac{1}{2} \dot{\mathbf{r}}_0^T \mathbf{M}_0 \dot{\mathbf{r}}_0, \quad (4.2)$$

where  $\mathbf{r}_0$  is the translational velocity of the center of mass of the base and  $\mathbf{M}_0 = m_0 \mathbb{I}_{3 \times 3}$  is the mass matrix of the base,  $m_0$  being the base mass. The velocity vector is written as

$$\dot{\mathbf{r}}_0 = \frac{\partial \mathbf{r}_0}{\partial \mathbf{q}} \dot{\mathbf{q}} = [\mathbf{P}_0(\mathbf{q})] \dot{\mathbf{q}} \quad (4.3)$$

where the matrix  $[\mathbf{P}_0(\mathbf{q})]$  is defined here as the derivative of the position vector with respect to the vector of generalized coordinates. Recalling that the position vector expressed in the inertial frame is

$$\mathbf{r}_0 = R \begin{bmatrix} \cos \lambda \sin \phi \\ \sin \lambda \sin \phi \\ \cos \phi \end{bmatrix}, \quad (4.4)$$

the velocity in the inertial frame is

$$\dot{\mathbf{r}}_0 = \frac{\partial \mathbf{r}_0}{\partial \mathbf{q}} \dot{\mathbf{q}} = [\mathbf{P}_0(\mathbf{q})] \dot{\mathbf{q}} \quad (4.5)$$

where

$$[\mathbf{P}_0(\mathbf{q})] = \begin{bmatrix} R \cos \lambda \cos \phi & -R \sin \lambda \sin \phi & \cos \lambda \sin \phi & \\ R \sin \lambda \cos \phi & R \cos \lambda \sin \phi & \sin \lambda \sin \phi & \mathbf{0}_{3 \times N-3} \\ -R \sin \phi & 0 & \cos \phi & \end{bmatrix} \quad (4.6)$$

where  $N$  is the total number of generalized coordinates, which varies depending on the number of bars and tiers that make up the tensegrity system.

Thus the translational kinetic energy of the base is

$$T_T = \frac{1}{2} \dot{\mathbf{q}}^T [\mathbf{P}_0(\mathbf{q})]^T \mathbf{M}_0 [\mathbf{P}_0(\mathbf{q})] \dot{\mathbf{q}}. \quad (4.7)$$

Performing the calculation for the sake of verification, one arrives at

$$T_T = \frac{1}{2} m_0 (R^2 \dot{\phi}^2 + R^2 \sin^2 \phi \dot{\lambda} + \dot{R}^2). \quad (4.8)$$

**Note** Another method for finding the translational kinetic energy of the base involves the use of the equation

$$T_T = \frac{1}{2} m_0 \mathbf{v} \cdot \mathbf{v} = \frac{1}{2} m_0 v^2 \quad (4.9)$$

where  $\mathbf{v}$  is the velocity vector of the base center of mass in the inertial frame. To add validity to previous derivations, begin instead in the orbital frame. Recall the position vector expressed in the orbital frame is

$${}^o \mathbf{r}_0 = [0 \quad 0 \quad R]^T, \quad (4.10)$$

of which the time derivative is

$${}^o \dot{\mathbf{r}}_0 = [0 \quad 0 \quad \dot{R}]^T. \quad (4.11)$$

To find the velocity vector in the inertial frame, the following equation is used:

$$\mathbf{v} = {}^o \dot{\mathbf{r}}_0 + {}^o \boldsymbol{\omega}^{o/i} \times {}^o \mathbf{r}_0, \quad (4.12)$$

where the cross term accounts for the rotating nature of the orbital frame. The angular velocity  ${}^o \boldsymbol{\omega}^{o/i}$  of the orbital frame with respect to the inertial frame is derived in the subsequent section. Once again performing the calculation, the translational kinetic energy becomes

$$T_T = \frac{1}{2} m_0 (R^2 \dot{\phi}^2 + R^2 \sin^2 \phi \dot{\lambda} + \dot{R}^2), \quad (4.13)$$

which matches previously derived result for the translational kinetic energy.

## Rotational Energy

The rotational kinetic energy of the base is expressed as

$$T_R = \frac{1}{2} \boldsymbol{\omega}_0^T \mathbf{J}_0 \boldsymbol{\omega}_0 \quad (4.14)$$

where  $\boldsymbol{\omega}_0$  is the angular velocity of the base and  $\mathbf{J}_0$  is the inertia matrix of the base.

It is desirable to choose the inertia matrix to be about the principal axes of the base (i.e. the  $\{\mathbf{b}\}$  frame), so that  $\mathbf{J}_0 = \frac{m_0}{12} \text{diag}[D_2^2 + D_3^2, D_1^2 + D_3^2, D_1^2 + D_2^2]$ . Therefore, the total angular velocity of the base about the inertial frame, expressed in the  $\{\mathbf{b}\}$  frame, is found by summing the angular velocities of  $\{\mathbf{b}\}$  with respect to  $\{\mathbf{o}\}$  and  $\{\mathbf{o}\}$  with respect to  $\{\mathbf{i}\}$ :

$$\boldsymbol{\omega}_0 = {}^b\boldsymbol{\omega}^{b/i} = {}^b\boldsymbol{\omega}^{b/o} + {}^b\boldsymbol{\omega}^{o/i} \quad (4.15)$$

Begin with  ${}^b\boldsymbol{\omega}^{b/o}$ . Recall that  $\{\mathbf{o}\}$  rotates into  $\{\mathbf{b}\}$  through a 3-2-1 rotation sequence, so the angular velocity can be written as the summation of the angular velocities through each rotation,

$${}^b\boldsymbol{\omega}^{b/o} = {}^b\boldsymbol{\omega}^{b/o''} + {}^b\boldsymbol{\omega}^{o''/o'} + {}^b\boldsymbol{\omega}^{o'/o}. \quad (4.16)$$

The resultant angular velocity is expressed in the  $\{\mathbf{b}\}$  frame as

$${}^b\boldsymbol{\omega}^{b/o} = \mathbb{I}[\dot{\theta}_1 \quad 0 \quad 0]^T + \mathbf{R}_1(\theta_1)[0 \quad \dot{\theta}_2 \quad 0]^T + \mathbf{R}_1(\theta_1)\mathbf{R}_2(\theta_2)[0 \quad 0 \quad \dot{\theta}_3]^T, \quad (4.17)$$

which becomes

$${}^b\boldsymbol{\omega}^{b/o} = \begin{bmatrix} 1 & 0 & -\sin \theta_2 \\ 0 & \cos \theta_1 & \sin \theta_1 \cos \theta_2 \\ 0 & -\sin \theta_1 & \cos \theta_1 \cos \theta_2 \end{bmatrix} \begin{bmatrix} \dot{\theta}_1 \\ \dot{\theta}_2 \\ \dot{\theta}_3 \end{bmatrix}. \quad (4.18)$$

The second component of the total angular velocity is expressed in the body frame as  ${}^b\boldsymbol{\omega}^{o/i}$ .

First, this angular velocity must be found in the orbital frame as

$${}^o\boldsymbol{\omega}^{o/i} = {}^o\boldsymbol{\omega}^{o/i'} + {}^o\boldsymbol{\omega}^{i'/i} \quad (4.19)$$

where each term represents the angular velocity through each rotation. Recalling that  $\{\mathbf{i}\}$  rotates into  $\{\mathbf{o}\}$  through a 3-2 sequence, the resultant angular velocity between the two frames becomes

$${}^o\boldsymbol{\omega}^{o/i} = \mathbb{I}[0 \ \dot{\phi} \ 0]^T + \mathbf{R}_2(\phi)[0 \ 0 \ \dot{\lambda}]^T \quad (4.20)$$

which is equivalent to

$${}^o\boldsymbol{\omega}^{o/i} = \begin{bmatrix} 0 & -\sin \phi & 0 \\ 0 & 0 & 1 \\ 0 & \cos \phi & 0 \end{bmatrix} \begin{bmatrix} \dot{R} \\ \dot{\lambda} \\ \dot{\phi} \end{bmatrix}. \quad (4.21)$$

This must be rotated into the body frame:

$${}^b\boldsymbol{\omega}^{o/i} = \mathbf{R}^{bo} {}^o\boldsymbol{\omega}^{o/i} = \mathbf{R}_1(\theta_1)\mathbf{R}_2(\theta_2)\mathbf{R}_3(\theta_3){}^o\boldsymbol{\omega}^{o/i}. \quad (4.22)$$

The total angular velocity of the base is found by substituting in the above terms into

Eq. (4.15), yielding

$$\begin{aligned} \boldsymbol{\omega}_0 = & \begin{bmatrix} 1 & 0 & -\sin \theta_2 \\ 0 & \cos \theta_1 & \sin \theta_1 \cos \theta_2 \\ 0 & -\sin \theta_1 & \cos \theta_1 \cos \theta_2 \end{bmatrix} \begin{bmatrix} \dot{\theta}_1 \\ \dot{\theta}_2 \\ \dot{\theta}_3 \end{bmatrix} \\ & + \mathbf{R}_1(\theta_1)\mathbf{R}_2(\theta_2)\mathbf{R}_3(\theta_3) \begin{bmatrix} 0 & -\sin \phi & 0 \\ 0 & 0 & 1 \\ 0 & \cos \phi & 0 \end{bmatrix} \begin{bmatrix} \dot{R} \\ \dot{\lambda} \\ \dot{\phi} \end{bmatrix} \end{aligned} \quad (4.23)$$

or, in simpler notation,

$$\boldsymbol{\omega}_0 = \mathbf{s}_2 \dot{\mathbf{q}}_{4 \rightarrow 6} + \mathbf{s}_1 \dot{\mathbf{q}}_{1 \rightarrow 3}. \quad (4.24)$$

The terms can be combined to yield

$$\boldsymbol{\omega}_0 = [\mathbf{S}_0(\mathbf{q})] \dot{\mathbf{q}} \quad (4.25)$$

where

$$[\mathbf{S}_0(\mathbf{q})] = [\mathbf{s}_1 \quad \mathbf{s}_2 \quad \mathbf{0}_{3 \times N-6}]. \quad (4.26)$$

Substituting the expression for the angular velocity into the kinetic rotational energy equation,

$$T_R = \frac{1}{2} \dot{\mathbf{q}}^T [\mathbf{S}_0(\mathbf{q})]^T \mathbf{J}_0 [\mathbf{S}_0(\mathbf{q})] \dot{\mathbf{q}} \quad (4.27)$$

**Note** For verification purposes, suppose we work in the inertial frame instead. The angular velocity of the base as expressed in the inertial frame is

$$\boldsymbol{\omega}_0 = {}^i \boldsymbol{\omega}^{i/b} = {}^i \boldsymbol{\omega}^{i/o} + {}^i \boldsymbol{\omega}^{o/b}. \quad (4.28)$$

This treats the angular velocity of the base as the rotation of the inertial and orbital frames with respect to the base, instead of the more conventional method of treating the base as rotating within the two frames.

Begin with  ${}^i\boldsymbol{\omega}^{o/b}$ , which is the summation of the angular velocities through all three rotations from  $\{\mathbf{b}\}$  to  $\{\mathbf{o}\}$ , expressed in the  $\{\mathbf{b}\}$  frame as:

$${}^b\boldsymbol{\omega}^{o/b} = {}^b\boldsymbol{\omega}^{o/b''} + {}^b\boldsymbol{\omega}^{b''/b'} + {}^b\boldsymbol{\omega}^{b'/b}. \quad (4.29)$$

The resultant angular velocity is

$${}^b\boldsymbol{\omega}^{o/b} = \mathbb{I}[0 \ 0 \ \dot{\theta}_3]^T + \mathbf{R}_3^T(\theta_3)[0 \ \dot{\theta}_2 \ 0]^T + \mathbf{R}_3^T(\theta_3)\mathbf{R}_2^T(\theta_2)[\dot{\theta}_1 \ 0 \ 0]^T, \quad (4.30)$$

which becomes

$${}^b\boldsymbol{\omega}^{o/b} = \begin{bmatrix} \cos \theta_3 \cos \theta_2 & -\sin \theta_3 & 0 \\ \sin \theta_3 \cos \theta_2 & \cos \theta_3 & 0 \\ -\sin \theta_2 & 0 & 1 \end{bmatrix} \begin{bmatrix} \dot{\theta}_1 \\ \dot{\theta}_2 \\ \dot{\theta}_3 \end{bmatrix}. \quad (4.31)$$

This must be rotated into the inertial frame:

$${}^i\boldsymbol{\omega}^{o/b} = \mathbf{R}^{ob} {}^b\boldsymbol{\omega}^{o/b} = \mathbf{R}_3^T(\theta_3)\mathbf{R}_2^T(\theta_2)\mathbf{R}_1^T(\theta_1){}^b\boldsymbol{\omega}^{o/b}. \quad (4.32)$$

The second component of the total angular velocity is expressed in the inertial frame as  ${}^i\boldsymbol{\omega}^{i/o}$ , given as the summation

$${}^i\boldsymbol{\omega}^{i/o} = {}^i\boldsymbol{\omega}^{i/o'} + {}^i\boldsymbol{\omega}^{o'/o} \quad (4.33)$$

where each term represents the angular velocity through each rotation. The resultant angular velocity between the two frames becomes

$${}^i\boldsymbol{\omega}^{i/o} = \mathbb{I}[0 \ 0 \ \dot{\lambda}]^T + \mathbf{R}_3^T(\lambda)[0 \ \dot{\phi} \ 0]^T \quad (4.34)$$

which becomes

$${}^i\boldsymbol{\omega}^{i/o} = \begin{bmatrix} 0 & 0 & -\sin \lambda \\ 0 & 0 & \cos \lambda \\ 0 & 1 & 0 \end{bmatrix} \begin{bmatrix} \dot{R} \\ \dot{\lambda} \\ \dot{\phi} \end{bmatrix}. \quad (4.35)$$

The total angular velocity of the base in the inertial frame is found by summing both components, yielding

$$\boldsymbol{\omega}_0 = \begin{bmatrix} 0 & 0 & -\sin \lambda \\ 0 & 0 & \cos \lambda \\ 0 & 1 & 0 \end{bmatrix} \begin{bmatrix} \dot{R} \\ \dot{\lambda} \\ \dot{\phi} \end{bmatrix} + \mathbf{R}_3^T(\theta_3)\mathbf{R}_2^T(\theta_2)\mathbf{R}_1^T(\theta_1) \begin{bmatrix} \cos \theta_3 \cos \theta_2 & -\sin \theta_3 & 0 \\ \sin \theta_3 \cos \theta_2 & \cos \theta_3 & 0 \\ -\sin \theta_2 & 0 & 1 \end{bmatrix} \begin{bmatrix} \dot{\theta}_1 \\ \dot{\theta}_2 \\ \dot{\theta}_3 \end{bmatrix} \quad (4.36)$$

or, in simpler notation,

$$\boldsymbol{\omega}_0 = \mathbf{s}_1 \dot{\mathbf{q}}_{1 \rightarrow 3} + \mathbf{s}_2 \dot{\mathbf{q}}_{4 \rightarrow 6}. \quad (4.37)$$

The terms can be combined to yield

$$\boldsymbol{\omega}_0 = [\mathbf{S}_0(\mathbf{q})]\dot{\mathbf{q}} \quad (4.38)$$

where

$$[\mathbf{S}_0(\mathbf{q})] = [\mathbf{s}_1 \quad \mathbf{s}_2 \quad \mathbf{0}_{3 \times N-6}]. \quad (4.39)$$

Before substituting the expression for the angular velocity into the kinetic rotational energy equation, we must recognize that because we're working in the inertial frame, the base's inertia



matrix must be rotated into this frame. So,

$${}^i\mathbf{J}_0 = \mathbf{R}^{ib}\mathbf{J}_0\mathbf{R}^{bi}. \quad (4.40)$$

Thus the rotational energy is

$$T_R = \frac{1}{2}\dot{\mathbf{q}}^T[\mathbf{S}_0(\mathbf{q})]^T {}^i\mathbf{J}_0[\mathbf{S}_0(\mathbf{q})]\dot{\mathbf{q}} \quad (4.41)$$

### Total Kinetic Energy

The total kinetic energy of the base is the summation of the derived translational and rotational energies:

$$T = \{T_T + T_R\}_0 \quad (4.42)$$

$$= \frac{1}{2}\dot{\mathbf{q}}^T[\mathbf{P}_0(\mathbf{q})]^T\mathbf{M}_0[\mathbf{P}_0(\mathbf{q})]\dot{\mathbf{q}} + \frac{1}{2}\dot{\mathbf{q}}^T[\mathbf{S}_0(\mathbf{q})]^T\mathbf{J}_0[\mathbf{S}_0(\mathbf{q})]\dot{\mathbf{q}} \quad (4.43)$$

$$= \frac{1}{2}\dot{\mathbf{q}}^T\{[\mathbf{P}_0(\mathbf{q})]^T\mathbf{M}_0[\mathbf{P}_0(\mathbf{q})] + [\mathbf{S}_0(\mathbf{q})]^T\mathbf{J}_0[\mathbf{S}_0(\mathbf{q})]\}\dot{\mathbf{q}} \quad (4.44)$$

$$= \frac{1}{2}\dot{\mathbf{q}}^T\mathbf{M}(\mathbf{q})\dot{\mathbf{q}} \quad (4.45)$$

#### 4.1.2 Gravitational Effects

The gravitational effects on the base can be derived one of two ways. The first is through an energy approach, where the resultant gravitational potential energy contributes to the  $\nabla_{\mathbf{q}}V$  term of the equations of motion. The second method is to treat gravity as a force on

the system, thus contributing to the generalized force term  $\mathbf{Q}$ . Both methods are discussed below.

### Energy Approach

Recall the general formula for the gravitational potential energy derived in Section 2.2:

$$V_g = -\frac{GM_{\oplus}m_0}{R} - \frac{GM_{\oplus}}{2R^3}\text{tr}(\mathbf{J}_0) + \frac{3GM_{\oplus}}{2R^3}I. \quad (4.46)$$

This formula is applied to the base, whose moment of inertia matrix is  $\mathbf{J}_0 = \frac{m_0}{12}\text{diag}[D_2^2 + D_3^2, D_1^2 + D_3^2, D_1^2 + D_2^2]$  and  $I = {}^o\mathbf{J}_0(3, 3)$ , where

$${}^o\mathbf{J}_0 = \mathbf{R}^{ob}\mathbf{J}_0\mathbf{R}^{bo},$$

in which  ${}^o\mathbf{J}_0$  is the inertia matrix rotated into the orbital frame.

Taking the Jacobian of the above expression yields the contribution of the gravitational potential energy to the equations of motion of the base:

$$\nabla_{\mathbf{q}}V_g = GM_{\oplus}m_0 [g_R \ 0 \ 0 \ g_{\theta_1} \ g_{\theta_2} \ 0]^T, \quad (4.47)$$

where

$$\begin{aligned} g_R &= \frac{1}{8R^4} [8R^2 - D_1^2 - D_2^2 + 2D_3^2 + 3\sin^2\theta_1(D_2^2 - D_3^2) \\ &\quad + 3\sin^2\theta_2(D_1^2 - D_3^2) + 3\sin^2\theta_1\sin^2\theta_2(D_3^2 - D_2^2)] \\ g_{\theta_1} &= -\frac{1}{4R^3} [\cos(\theta_1)\sin(\theta_1)\cos^2(\theta_2)(D_2^2 - D_3^2)] \\ g_{\theta_2} &= \frac{1}{4R^3} [\cos\theta_2\sin\theta_2(D_2^2 - D_1^2) + \cos^2\theta_1\cos\theta_2\sin\theta_2(D_3^2 - D_2^2)]. \end{aligned}$$

Note that the elements that correspond to  $\lambda$ ,  $\phi$ , and  $\theta_3$  are zero - none of these variables impact the gravitational effects on the system.

### Force Approach

Start with a general expression for the generalized forces on the base:

$$\mathbf{Q}_g = \left[ \left( \frac{\partial \dot{\mathbf{r}}_0}{\partial \dot{\mathbf{q}}} \right)^T \mathbf{F}_{g_0} \right] + \left[ \left( \frac{\partial \boldsymbol{\omega}_0}{\partial \dot{\mathbf{q}}} \right)^T \mathbf{M}_{g_0} \right] \quad (4.48)$$

where  $\dot{\mathbf{r}}_0$  and  $\boldsymbol{\omega}_0$  are the translational and angular velocities of the base. The gravitational forces and moments,  $\mathbf{F}_{g_0}$  and  $\mathbf{M}_{g_0}$ , are found using a process by Kane,[34, 35] yielding

$$\mathbf{F}_{g_0} = -\frac{\mu m}{R^2} \mathbf{o}_r - \frac{3\mu}{2R^4} [\text{tr}(\mathbf{J}_0) - 5\mathbf{o}_r^T \mathbf{J}_0 \mathbf{o}_r] \mathbf{o}_r - \frac{3\mu}{R^4} \mathbf{J}_0 \mathbf{o}_r \quad (4.49)$$

$$\mathbf{M}_{g_0} = \frac{3\mu}{R^3} \mathbf{o}_r^\times \mathbf{J}_0 \mathbf{o}_r, \quad (4.50)$$

where  $\mathbf{o}_r$  is a unit vector that points along the direction of orbital radius vector  $\mathbf{r}_0$ , which also coincides with the third axis of the orbital frame  $\{\mathbf{o}\}$ .

The generalized velocities can be determined using the derivations for the kinetic energy.

Begin with the translational velocity of the base, which is alternatively written as

$$\dot{\mathbf{r}}_0 = \frac{d\mathbf{r}_0}{dt} = \frac{\partial \mathbf{r}_0}{\partial \mathbf{q}} \frac{d\mathbf{q}}{dt} = \frac{\partial \mathbf{r}_0}{\partial \mathbf{q}} \dot{\mathbf{q}}. \quad (4.51)$$

Taking the partial derivative of both sides of the equation, and rearranging terms, it is found that

$$\frac{\partial \dot{\mathbf{r}}_0}{\partial \dot{\mathbf{q}}} = \frac{\partial \mathbf{r}_0}{\partial \mathbf{q}}. \quad (4.52)$$

Combining the above two equations results in

$$\dot{\mathbf{r}}_0 = \frac{\partial \dot{\mathbf{r}}_0}{\partial \dot{\mathbf{q}}} \dot{\mathbf{q}}. \quad (4.53)$$

Now, recall from the derivations of the kinetic energy that the translational velocity of the base is

$$\dot{\mathbf{r}}_0 = [\mathbf{P}_0(\mathbf{q})] \dot{\mathbf{q}}. \quad (4.54)$$

Thus,

$$\frac{\partial \dot{\mathbf{r}}_0}{\partial \dot{\mathbf{q}}} = [\mathbf{P}_0(\mathbf{q})]. \quad (4.55)$$

A similar process is used to find that

$$\frac{\partial \boldsymbol{\omega}_0}{\partial \dot{\mathbf{q}}} = [\mathbf{S}_0(\mathbf{q})]. \quad (4.56)$$

Combining the above expressions, the generalized gravitational forces on the base become

$$\mathbf{Q}_g = [\mathbf{P}_0(\mathbf{q})]^T \mathbf{F}_{g_0} + [\mathbf{S}_0(\mathbf{q})]^T \mathbf{M}_{g_0}. \quad (4.57)$$

Choose to work in the  $\{\mathbf{b}\}$  frame, so that the moment of inertia in the  $\{\mathbf{b}\}$  frame (i.e.  $\mathbf{J}_0 = \frac{m_0}{12} \text{diag}[D_2^2 + D_3^2, D_1^2 + D_3^2, D_1^2 + D_2^2]$ ) can be used. The unit vector  $\mathbf{o}_r$  must also be expressed in the same frame. If  ${}^o\mathbf{o}_r$  in the  $\{\mathbf{o}\}$  frame is

$${}^o\mathbf{o}_r = [0 \ 0 \ 1]^T, \quad (4.58)$$

then, in the  $\{\mathbf{b}\}$  frame, it's

$${}^b\mathbf{o}_r = \mathbf{R}^{bo} {}^o\mathbf{o}_r = \mathbf{R}_1(\theta_1)\mathbf{R}_2(\theta_2)\mathbf{R}(\theta_3)[0 \ 0 \ 1]^T. \quad (4.59)$$

Thus, the gravitational force and moment in the  $\{\mathbf{b}\}$  frame is

$${}^b\mathbf{F}_{g_0} = -\frac{\mu m}{R^2} {}^b\mathbf{o}_r - \frac{3\mu}{2R^4} [\text{tr}(\mathbf{J}_0) - 5 {}^b\mathbf{o}_r^T \mathbf{J}_0 {}^b\mathbf{o}_r] {}^b\mathbf{o}_r - \frac{3\mu}{R^4} \mathbf{J}_0 {}^b\mathbf{o}_r \quad (4.60)$$

$${}^b\mathbf{M}_{g_0} = \frac{3\mu}{R^3} {}^b\mathbf{o}_r^\times \mathbf{J}_0 {}^b\mathbf{o}_r, \quad (4.61)$$

The generalized velocities  $[\mathbf{P}_0(\mathbf{q})]$  and  $[\mathbf{S}_0(\mathbf{q})]$  must also be in the chosen coordinate frame.

Consider first the generalized translational velocity. In the body frame, it is found to be

$$[\mathbf{P}_0(\mathbf{q})] = \frac{\partial {}^b\mathbf{r}_0}{\partial \mathbf{q}}, \quad (4.62)$$

where

$${}^b\mathbf{r}_0 = \mathbf{R}^{bi} \mathbf{r}_0 \quad (4.63)$$

and

$$\mathbf{r}_0 = R \begin{bmatrix} \cos \lambda \sin \phi \\ \sin \lambda \sin \phi \\ \cos \phi \end{bmatrix}. \quad (4.64)$$

For the generalized rotational velocity, consider the fact that we're trying to find the contribution of the gravitational moment about the base body frame  $\{\mathbf{b}\}$ . Since the gravitational moment itself is expressed in the body frame, the generalized rotational velocity is

$$[\mathbf{S}_0(\mathbf{q})] = \frac{\partial {}^b\boldsymbol{\omega}_0^{b/b}}{\partial \dot{\mathbf{q}}} \quad (4.65)$$

where  ${}^b\boldsymbol{\omega}_0^{b/b}$  is the angular velocity of the  $\{\mathbf{b}\}$  frame about itself. Naturally, this is zero:

$${}^b\boldsymbol{\omega}_0^{b/b} = [0 \ 0 \ 0]^T. \quad (4.66)$$

Thus, the generalized rotational velocity becomes

$$[\mathbf{S}_0(\mathbf{q})] = [\mathbf{0}_{3 \times 6}], \quad (4.67)$$

meaning that there will be no contribution from the gravitational moment.

And so, the generalized gravitational forces are

$$\mathbf{Q}_g = [\mathbf{P}_0(\mathbf{q})]^T {}^b \mathbf{F}_{g_0} \quad (4.68)$$

which becomes

$$\mathbf{Q}_g = -GM_E m_0 [g_R \ 0 \ 0 \ g_{\theta_1} \ g_{\theta_2} \ 0]^T, \quad (4.69)$$

where

$$\begin{aligned} g_R &= \frac{1}{8R^4} [8R^2 - D_1^2 - D_2^2 + 2D_3^2 + 3 \sin^2 \theta_1 (D_2^2 - D_3^2) \\ &\quad + 3 \sin^2 \theta_2 (D_1^2 - D_3^2) + 3 \sin^2 \theta_1 \sin^2 \theta_2 (D_3^2 - D_2^2)] \\ g_{\theta_1} &= -\frac{1}{4R^3} [\cos(\theta_1) \sin(\theta_1) \cos^2(\theta_2) (D_2^2 - D_3^2)] \\ g_{\theta_2} &= \frac{1}{4R^3} [\cos \theta_2 \sin \theta_2 (D_2^2 - D_1^2) + \cos^2 \theta_1 \cos \theta_2 \sin \theta_2 (D_3^2 - D_2^2)]. \end{aligned}$$

This exactly matches the gravitational effects derived using the energy approach.

**Note** To verify the results of the generalized forces, choose another coordinate frame to work in - for example, the inertial frame. The force and moment expressed in this frame becomes

$${}^i \mathbf{F}_{g_0} = -\frac{\mu m}{R^2} {}^i \mathbf{o}_r - \frac{3\mu}{2R^4} [tr({}^i \mathbf{J}_0) - 5 {}^i \mathbf{o}_r^T {}^i \mathbf{J}_0 {}^i \mathbf{o}_r] {}^i \mathbf{o}_r - \frac{3\mu}{R^4} {}^i \mathbf{J}_0 {}^i \mathbf{o}_r \quad (4.70)$$

$${}^i \mathbf{M}_{g_0} = \frac{3\mu}{R^3} {}^i \mathbf{o}_r^\times {}^i \mathbf{J}_0 {}^i \mathbf{o}_r, \quad (4.71)$$

where

$${}^i\mathbf{o}_r = \mathbf{R}^{io} \mathbf{o}_r = \mathbf{R}_3^T(\lambda) \mathbf{R}_2^T(\phi) [0 \ 0 \ 1]^T \quad (4.72)$$

and

$${}^i\mathbf{J}_0 = \mathbf{R}^{ib} \mathbf{J}_0 \mathbf{R}^{bi}. \quad (4.73)$$

The generalized translational velocity is

$$[\mathbf{P}_0(\mathbf{q})] = \frac{\partial \mathbf{r}_0}{\partial \dot{\mathbf{q}}}, \quad (4.74)$$

where

$$\mathbf{r}_0 = R \begin{bmatrix} \cos \lambda \sin \phi \\ \sin \lambda \sin \phi \\ \cos \phi \end{bmatrix}. \quad (4.75)$$

The generalized rotational velocity (expressed in the  $\{\mathbf{i}\}$  frame) about the body frame  $\{\mathbf{b}\}$  is

$$[\mathbf{S}_0(\mathbf{q})] = \frac{\partial {}^i\boldsymbol{\omega}_0^{i/b}}{\partial \dot{\mathbf{q}}}, \quad (4.76)$$

where  ${}^i\boldsymbol{\omega}^{i/b}$  was found in the kinetic energy section to be

$${}^i\boldsymbol{\omega}_0^{i/b} = {}^i\boldsymbol{\omega}_0^{i/o} + {}^i\boldsymbol{\omega}_0^{o/b} \quad (4.77)$$

$$= \begin{bmatrix} 0 & 0 & -\sin \lambda \\ 0 & 0 & \cos \lambda \\ 0 & 1 & 0 \end{bmatrix} \begin{bmatrix} \dot{R} \\ \dot{\lambda} \\ \dot{\phi} \end{bmatrix} + \mathbf{R}_3^T(\theta_3)\mathbf{R}_2^T(\theta_2)\mathbf{R}_1^T(\theta_1) \begin{bmatrix} \cos \theta_3 \cos \theta_2 & -\sin \theta_3 & 0 \\ \sin \theta_3 \cos \theta_2 & \cos \theta_3 & 0 \\ -\sin \theta_2 & 0 & 1 \end{bmatrix} \begin{bmatrix} \dot{\theta}_1 \\ \dot{\theta}_2 \\ \dot{\theta}_3 \end{bmatrix} \quad (4.78)$$

$$= \mathbf{s}_1\dot{\mathbf{q}}_{1 \rightarrow 3} + \mathbf{s}_2\dot{\mathbf{q}}_{4 \rightarrow 6} \quad (4.79)$$

$$= [\mathbf{S}_0(\mathbf{q})]\dot{\mathbf{q}}. \quad (4.80)$$

Substituting into the expression for the generalized forces yields

$$\mathbf{Q}_g = [\mathbf{P}_0(\mathbf{q})]^T {}^i\mathbf{F}_{g_0} + [\mathbf{S}_0(\mathbf{q})]^T {}^i\mathbf{M}_{g_0}, \quad (4.81)$$

which ends up being equivalent to the  $\mathbf{Q}_g$  vector found in the  $\{\mathbf{b}\}$  frame.

### 4.1.3 Methods of Passive Control

Spacecraft whose attitude is maintained solely by gravity gradient methods are stable only under certain conditions. Though the thrusters attached to the base of the spacecraft discussed in this paper serve to control its attitude, it is useful to add some form of passive control as well by means of gravity gradient. What follows is a discussion of the parameters required for gravity gradient stabilization.[7]



Consider a base with moment of inertia  $\mathbf{J} = \text{diag}[J_1, J_2, J_3]$  in a circular orbit. Kane's equation states that the rotational dynamics of a system can be described by

$$\mathbf{M}_g - (\mathbf{J}\dot{\boldsymbol{\omega}} - \boldsymbol{\omega}^\times \mathbf{J}\boldsymbol{\omega}) = \mathbf{0} \quad (4.82)$$

where  $\mathbf{M}_g$  is the gravitational moment derived in Section 2.2,

$$\mathbf{M}_g = \frac{3\mu}{R^3} \mathbf{o}_r^\times \mathbf{J} \mathbf{o}_r. \quad (4.83)$$

Thus, the rotational dynamics of a single rigid body are

$$\mathbf{J}\dot{\boldsymbol{\omega}} - \boldsymbol{\omega}^\times \mathbf{J}\boldsymbol{\omega} = 3n^2 \mathbf{o}_r^\times \mathbf{J} \mathbf{o}_r. \quad (4.84)$$

where  $n = \sqrt{\mu/R^3}$  is the orbital rate and  $\boldsymbol{\omega}$  represents the total angular velocity of the base which, recall from before, is

$$\begin{aligned} \boldsymbol{\omega} = \boldsymbol{\omega}_0 = & \begin{bmatrix} 1 & 0 & -\sin \theta_2 \\ 0 & \cos \theta_1 & \sin \theta_1 \cos \theta_2 \\ 0 & -\sin \theta_1 & \cos \theta_1 \cos \theta_2 \end{bmatrix} \begin{bmatrix} \dot{\theta}_1 \\ \dot{\theta}_2 \\ \dot{\theta}_3 \end{bmatrix} \\ & + \mathbf{R}_1(\theta_1) \mathbf{R}_2(\theta_2) \mathbf{R}_3(\theta_3) \begin{bmatrix} 0 & -\sin \phi & 0 \\ 0 & 0 & 1 \\ 0 & \cos \phi & 0 \end{bmatrix} \begin{bmatrix} \dot{R} \\ \dot{\lambda} \\ \dot{\phi} \end{bmatrix}. \end{aligned} \quad (4.85)$$

Since the goal is to align the body with the orbital frame, with minimal deviations from that orientation, a small angle assumption can be used, so that  $\cos \theta_i \approx 1$  and  $\sin \theta_i \approx \theta_i$ . Also, for simplicity's sake in this example, let the orbit be equatorial, so that  $\phi = \pi/2$ , thus allowing  $\dot{\lambda} = n$ . This simplifying assumption makes sense for a circular orbit around a spherically

uniform Earth: at any non-zero orbital inclination, the behavior of the rigid body will be the same as for an orbit with zero inclination (equatorial). The angular velocity under these assumptions becomes

$$\boldsymbol{\omega} = \begin{bmatrix} \dot{\theta}_1 - n\theta_2 \\ \dot{\theta}_2 + n\theta_1 \\ \dot{\theta}_3 \end{bmatrix}$$

The angular acceleration can be easily found by taking the time derivative of the above, yielding

$$\dot{\boldsymbol{\omega}} = \begin{bmatrix} \ddot{\theta}_1 - n\dot{\theta}_2 \\ \ddot{\theta}_2 + n\dot{\theta}_1 \\ \ddot{\theta}_3 \end{bmatrix}$$

Substituting the angular velocity and acceleration into Eq. (4.84) yields the following equations of motion:

$$J_1\ddot{\theta}_1 - n(J_1 + J_2 - J_3)\dot{\theta}_2 + n^2(J_3 - J_2)\theta_1 = 0 \quad (4.86)$$

$$J_2\ddot{\theta}_2 + n(J_1 + J_2 - J_3)\dot{\theta}_1 + 4n^2(J_3 - J_1)\theta_2 = 0 \quad (4.87)$$

$$J_3\ddot{\theta}_3 + 3n^2(J_2 - J_1)\theta_3 = 0 \quad (4.88)$$

where the 1-, 2-, and 3-axis are referred to as the yaw, roll, and pitch axes, respectively. These equations of motion match those found in the literature,[7] taking into account that the above equations were derived using an alternate coordinate frame.

Note that the pitch is decoupled from the yaw and roll, and so the characteristic equation

of the pitch axis is

$$\lambda^2 + 3n^2 \left( \frac{J_2 - J_1}{J_3} \right) = 0 \quad (4.89)$$

whose roots are pure imaginary numbers if  $J_2 > J_1$ , meaning the equation is Lyapunov, or neutrally, stable. Otherwise this motion is unstable.

Consider now the yaw and roll axis equations. These can be written in matrix form as

$$\mathbf{M}\ddot{\mathbf{x}} + \mathbf{G}\dot{\mathbf{x}} + \mathbf{K}\mathbf{x} = 0 \quad (4.90)$$

where  $x = [\theta_1 \ \theta_2]^T$  and  $\mathbf{M}$ ,  $\mathbf{G}$ , and  $\mathbf{K}$  are the mass, damping, and stiffness matrices, defined as

$$\mathbf{M} = \begin{bmatrix} J_1 & 0 \\ 0 & J_2 \end{bmatrix}, \quad \mathbf{G} = n(J_1 + J_2 - J_3) \begin{bmatrix} 0 & -1 \\ 1 & 0 \end{bmatrix}, \quad \mathbf{K} = n^2 \begin{bmatrix} (J_3 - J_2) & 0 \\ 0 & 4(J_3 - J_1) \end{bmatrix}$$

Multiplying this matrix equation by  $\mathbf{M}^{-1}$  yields

$$\mathbb{I}\ddot{\mathbf{x}} + \mathbf{M}^{-1}\mathbf{G}\dot{\mathbf{x}} + \mathbf{M}^{-1}\mathbf{K}\mathbf{x} = 0 \quad (4.91)$$

where

$$\mathbf{M}^{-1}\mathbf{G} = n \begin{bmatrix} 0 & k_1 - 1 \\ 1 - k_2 & 0 \end{bmatrix}, \quad \mathbf{M}^{-1}\mathbf{K} = n^2 \begin{bmatrix} k_1 & 0 \\ 0 & 4k_2 \end{bmatrix}$$

and

$$k_1 = \frac{J_3 - J_2}{J_1}, \quad k_2 = \frac{J_3 - J_1}{J_2} \quad (4.92)$$

Consider an exponential solution to Eq. (4.91), specifically of the form  $\mathbf{x} = e^{\lambda t}c$ . The first and second derivatives of this solution become, respectively,  $\dot{\mathbf{x}} = \lambda e^{\lambda t}c = \lambda\mathbf{x}$  and

$\ddot{\mathbf{x}} = \lambda^2 e^{\lambda t} \mathbf{c} = \lambda^2 \mathbf{x}$ . Substituting these solutions into Eq. (4.91) yields

$$[\mathbb{I}\lambda^2 + \mathbf{M}^{-1}\mathbf{G}\lambda + \mathbf{M}^{-1}\mathbf{K}]e^{\lambda t} \mathbf{c} = \mathbf{A}e^{\lambda t} \mathbf{c} = 0 \quad (4.93)$$

Since  $e^{\lambda t} \neq 0$ , this equation can have non-trivial solutions, where  $\mathbf{c} \neq 0$ , only if  $\mathbf{A}$  is singular.

For a matrix to be singular, its determinant must equal zero. Therefore, substituting in the values from Eq. (4.1.3) into  $\mathbf{A}$ , this condition for singularity is expressed as

$$\begin{vmatrix} \lambda^2 + n^2 k_1 & \lambda n(k_1 - 1) \\ \lambda n(1 - k_2) & \lambda^2 + 4n^2 k_2 \end{vmatrix} = 0$$

which, taking the determinant, results in

$$\frac{\lambda^4}{n^4} + (1 + 3k_2 + k_1 k_2) \frac{\lambda^2}{n^2} + 4k_1 k_2 = 0 \quad (4.94)$$

This characteristic equation is in the form  $as + bs + c = 0$  (where  $s = \lambda^2/n^2$  and  $a$ ,  $b$ , and  $c$  are constants) and can be solved using the quadratic equation:

$$s_{1,2} = \frac{-b \pm \sqrt{b^2 - 4ac}}{2a} \quad (4.95)$$

In order to ensure stability, the eigenvalues  $\lambda$  of the system must be purely imaginary, implying that the values of  $s$  must be real and negative. For this to be true, the following conditions can be determined from the quadratic equation:

$$b > 0, \quad c > 0, \quad b^2 - 4ac > 0 \quad (4.96)$$

Finally from the analysis of pitch stability, it was determined that  $J_2 > J_1$ , which is equivalent

to saying  $k_2 > k_1$ . Thus, in summary, the conditions for stability are

$$\begin{aligned}
 k_2 &> k_1 \\
 k_1 k_2 &> 0 \\
 1 + 3k_2 + k_1 k_2 &> 0 \\
 (1 + 3k_2 + k_1 k_2)^2 - 16k_1 k_2 &> 0
 \end{aligned} \tag{4.97}$$

Additionally, from the properties of moment of inertia (i.e. the sum of any two principal moments of inertia must be greater than the third), it can be shown that

$$\|k_1\| < 1 \quad \text{and} \quad \|k_2\| < 1 \tag{4.98}$$

These conditions are visually depicted in Fig. 4.3. Regions *I*, *II*, *III*, and *IV* correspond to the stability conditions listed in Eq. (4.97), in that order. The unshaded regions are those ranges of  $k_1$  and  $k_2$  that are stable.

The dynamic response of the system is shown for both the stable case (Figure 4.5) and an unstable one (Figure 4.4). The unstable response is due to the first condition in Eq. (4.97) not being met, where a small initial disturbance in the  $\theta_i$  angles grows exponentially. The stable response depicts a case where all the stability conditions are met, and although the dynamics of the system are oscillatory, they are bounded by an upper and lower limit.

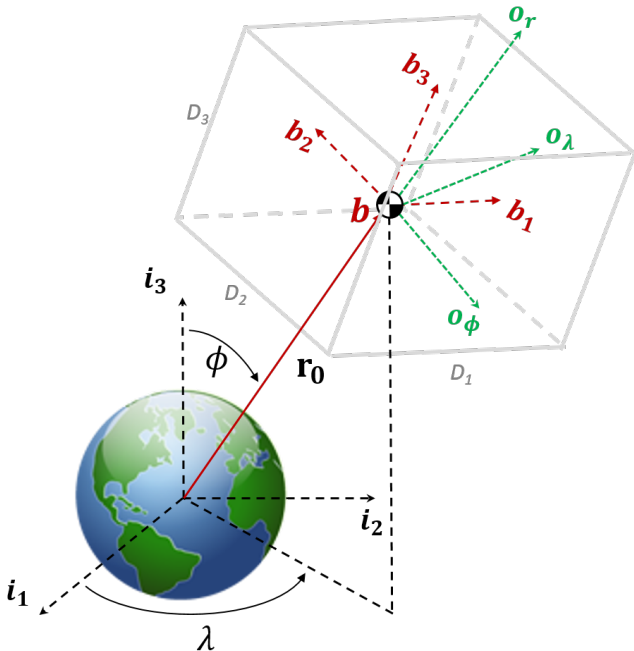


Figure 4.2: Dimensions of a rectangular prism base,  $\{D_1, D_2, D_3\}$ .

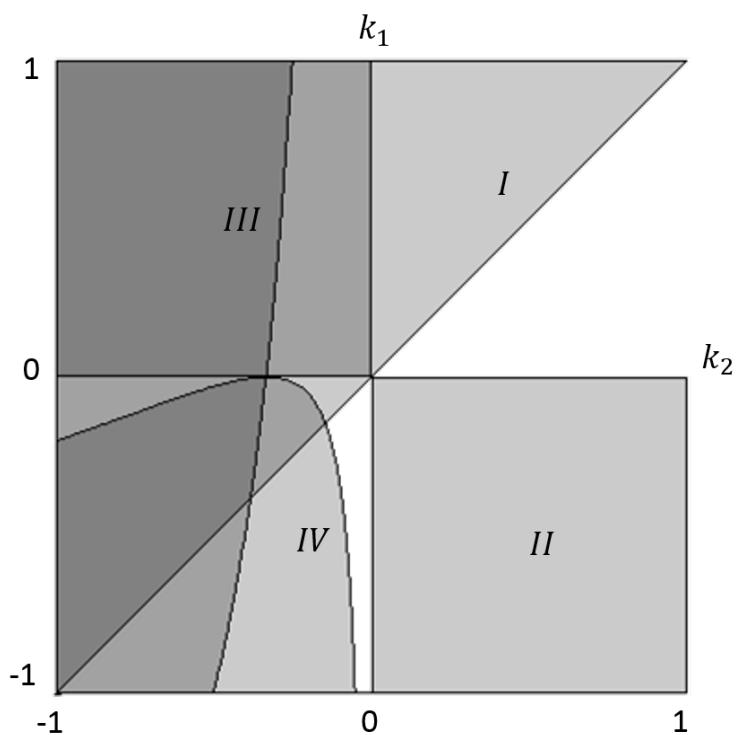


Figure 4.3: Stability regions for a rigid body in a circular orbit, where the unshaded regions denote Lyapunov (neutral) stability. It is beneficial to design the rigid body such that its principal moments of inertial lead to Lyapunov stability. The shaded region above the diagonal denotes a body with unstable pitch ( $\theta_3$ ) authority, whereas shaded regions below the diagonal denote unstable roll or yaw ( $\theta_1, \theta_2$ ) authority.[7]

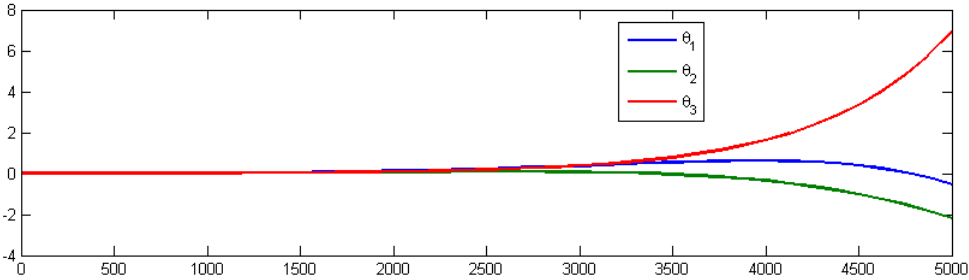


Figure 4.4: Unstable dynamics of an orbiting rigid body where all the conditions for neutral stability are not met; specifically in this case ( $k_2 \not> k_1$ ). The attitude of the rigid body slowly diverges from the desired orientation.

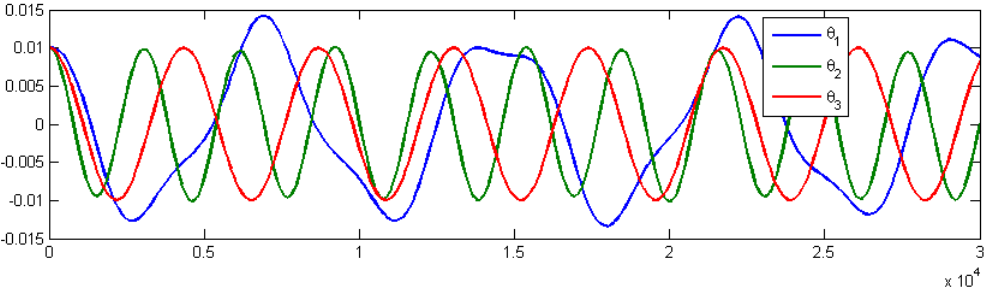


Figure 4.5: Dynamics of an orbiting rigid body where all the conditions for neutral stability are met. This system is neutrally stable since it never converges to an equilibrium, but rather fluctuates around the equilibrium.



## 4.2 3-Bar Tensegrity Structure

This section derives the dynamics of the 3-bar tensegrity spacecraft depicted in Figure 4.6.

Begin by considering a single bar, as shown in Figure 4.7. The position vector of the center

of mass of the  $i$ th bar is given by the summation of the position vectors  $\overline{\mathbf{BC}}_i = \overline{\mathbf{BA}}_i + \overline{\mathbf{A}_i\mathbf{C}_i}$ ,

where  $\overline{\mathbf{BA}}_i$  is the vector from the base mass center to the connection point of each bar to

the surface of the base, and  $\overline{\mathbf{A}_i\mathbf{C}_i}$  is the vector from the connection point to the bar center

of mass. Expressed in the  $\{\mathbf{b}\}$  frame, the values for these vectors are:

$$\overline{\mathbf{BA}}_1^b = \frac{1}{2} \begin{bmatrix} -D_1 \\ -D_2 \\ D_3 \end{bmatrix} \quad \overline{\mathbf{BA}}_2^b = \frac{1}{2} \begin{bmatrix} 0 \\ D_2 \\ D_3 \end{bmatrix} \quad \overline{\mathbf{BA}}_3^b = \frac{1}{2} \begin{bmatrix} D_1 \\ -D_2 \\ D_3 \end{bmatrix} \quad (4.99)$$

and

$$\overline{\mathbf{A}_i\mathbf{C}_i}^b = \frac{L_i}{2} \begin{bmatrix} \cos \alpha_i \sin \delta_i \\ \sin \alpha_i \sin \delta_i \\ \cos \delta_i \end{bmatrix} \quad (4.100)$$

where  $D_1$ ,  $D_2$ , and  $D_3$  are the dimensions of the rectangular prism base, and  $L_i$  is the length

of the bar; these dimensions are assumed constant over time.

Recalling the independent generalized coordinates from Equation (2.16), and recognizing that

the current system is a single-tier tensegrity structure, the vector of independent generalized

coordinates is

$$\mathbf{q} = [R \ \lambda \ \phi \ \theta_1 \ \theta_2 \ \theta_3 \ \alpha_1 \ \delta_1 \ \alpha_2 \ \delta_2 \ \alpha_3 \ \delta_3]^T. \quad (4.101)$$

Choosing to use the force-based approach to determining the gravitational effects on the

system, the dynamics equations of a 3-bar system are

$$\frac{d}{dt}(\nabla_{\dot{\mathbf{q}}}T) - \nabla_{\mathbf{q}}T = -\nabla_{\mathbf{q}}V_e + \mathbf{Q}_g + \mathbf{Q}_t. \quad (4.102)$$

The following sections derive the kinetic energy  $T$ , the gravitational generalized forces  $\mathbf{Q}_g$ , and the elastic potential energy  $V_e$  of this system. The thruster generalized forces were found in Section 4.1.

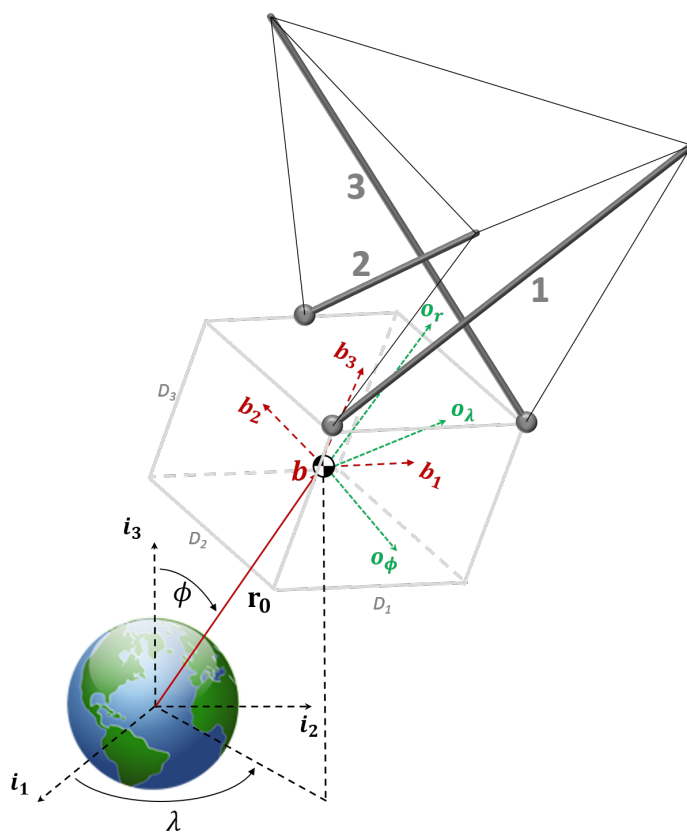


Figure 4.6: A simple 3-bar tensegrity structure mounted to an orbiting rectangular prism base. The moments of inertia of the base are chosen to induce some amount of passive stability (see previous section about Lyapunov stability). The bars are attached to the base at one end; the other ends are constrained by the web of 6 elastic tendons.

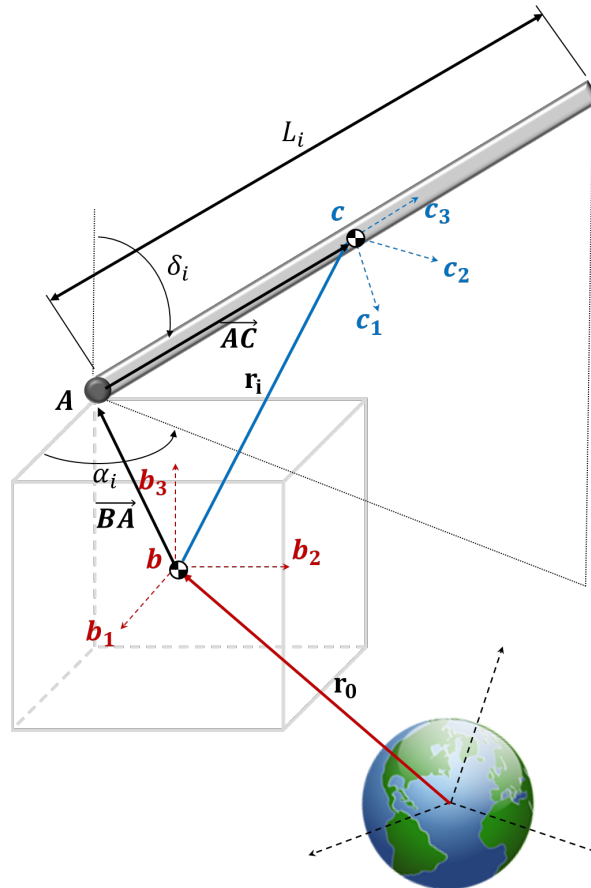


Figure 4.7: The position vector of the center of mass of the bar with respect to the inertial frame  $\{i\}$  is found by summing the position vector to the base  $\mathbf{r}_0$  and the position vector from the base to the  $i$ th bar center  $\mathbf{r}_i$ . This vector can be further split into a static vector  $\mathbf{BA}$  (which defines the position of the bar connection points) and the vector  $\mathbf{AC}$  (whose magnitude remains static, but whose direction is defined by the angles  $\alpha_i$  and  $\delta_i$

### 4.2.1 Kinetic Energy

Recall from Equation (2.21) the expression for the total kinetic energy of a general system.

For a system consisting of a base and three bars, the total kinetic energy becomes

$$T = \sum_{i=0}^3 \{T_T + T_R\}_i \quad (4.103)$$

where  $i = 0$  corresponds to the base and  $i = 1, 2, 3$  to the three bars that make up the tensegrity structure. The kinetic energy for the base was already derived in Section 4.1; the following sections derive the kinetic energy for the three bars.

#### Translational Kinetic Energy

Begin with the translational kinetic energy of the bars:

$$T_T = \sum_{i=1}^3 \frac{1}{2} \dot{\mathbf{r}}_i^T \mathbf{M}_i \dot{\mathbf{r}}_i, \quad (4.104)$$

where  $\mathbf{M}_i = m_i \mathbb{I}_{3 \times 3}$  is the mass matrix,  $m_i$  being the mass of the  $i$ th bar. The vector  $\dot{\mathbf{r}}_i$  of the bar is the translational velocity of the center of mass of the  $i$ th bar with respect to the origin of the Earth inertial frame, and is equal to

$$\dot{\mathbf{r}}_i = \dot{\mathbf{r}}_0 + \overline{\mathbf{BC}}_i = \dot{\mathbf{r}}_0 + \overline{\mathbf{BA}}_i + \overline{\mathbf{A}_i\mathbf{C}_i}. \quad (4.105)$$

$\overline{\mathbf{BA}}_i$  and  $\overline{\mathbf{A}_i\mathbf{C}_i}$  are given in Equation (4.233) and (4.100), respectively, in the body frame and must be rotated into the inertial reference frame using the rotation matrix

$$\mathbf{R}^{ib} = \mathbf{R}^{io} \mathbf{R}^{ob} = \mathbf{R}_3^T(\lambda) \mathbf{R}_2^T(\pi/2 - \phi) \mathbf{R}_3(\theta_3) \mathbf{R}_2(\theta_2) \mathbf{R}_1(\theta_1). \quad (4.106)$$

So  $\dot{\mathbf{r}}_i$  can be expanded into

$$\dot{\mathbf{r}}_i = \dot{\mathbf{r}}_0 + \frac{d}{dt}(\mathbf{R}^{ib})\overline{\mathbf{B}\mathbf{A}_i}^b + \frac{d}{dt}(\mathbf{R}^{ib})\overline{\mathbf{A}_i\mathbf{C}_i}^b + \mathbf{R}^{ib} \frac{d}{dt}(\overline{\mathbf{A}_i\mathbf{C}_i}^b). \quad (4.107)$$

$\dot{\mathbf{r}}_0$  is the translational velocity of the base center of mass and was derived in the previous section, but for the purposes of the following derivation  $\dot{\mathbf{R}}$  is written as

$$\dot{\mathbf{r}}_0 = \dot{R}\mathbf{r}_{0R} + \dot{\lambda}\mathbf{r}_{0\lambda} + \dot{\phi}\mathbf{r}_{0\phi} \quad (4.108)$$

where  $\mathbf{r}_{0R}$ ,  $\mathbf{r}_{0\lambda}$ , and  $\mathbf{r}_{0\phi}$  are the partial derivatives of the vector  $\dot{\mathbf{r}}_0$  with respect to  $R$ ,  $\lambda$ , and  $\phi$ , in that order. The time derivative of the rotation matrix  $\mathbf{R}^{ib}$  can be expanded into

$$\frac{d}{dt}\mathbf{R}^{ib} = \dot{\lambda}\mathbf{R}_\lambda^{ib} + \dot{\phi}\mathbf{R}_\phi^{ib} + \dot{\theta}_1\mathbf{R}_{\theta_1}^{ib} + \dot{\theta}_2\mathbf{R}_{\theta_2}^{ib} + \dot{\theta}_3\mathbf{R}_{\theta_3}^{ib} \quad (4.109)$$

where  $\mathbf{R}_*^{ib}$  is the partial derivative of the rotation matrix  $\mathbf{R}^{ib}$  with respect to the variable (\*). The time derivative of  $\overline{\mathbf{A}_i\mathbf{C}_i}^b$  can be expanded to yield

$$\frac{d}{dt}(\overline{\mathbf{A}_i\mathbf{C}_i}^b) = \dot{\alpha}_i\overline{\mathbf{A}_i\mathbf{C}_i}_{\alpha_i}^b + \dot{\delta}_i\overline{\mathbf{A}_i\mathbf{C}_i}_{\delta_i}^b \quad (4.110)$$

where  $\overline{\mathbf{A}_i\mathbf{C}_i}_{\alpha_i}^b$  and  $\overline{\mathbf{A}_i\mathbf{C}_i}_{\delta_i}^b$  are the partial derivatives of  $\overline{\mathbf{A}_i\mathbf{C}_i}^b$  with respect to  $\alpha_i$  and  $\delta_i$ .

Equation (4.108), (4.109), and (4.110) are substituted into Equation (4.107), and terms are collected and generalized coordinates extracted to yield

$$\dot{\mathbf{r}}_i = [\mathbf{r}_{0R} \quad \mathbf{r}_{0\lambda} + \mathbf{R}_\lambda^{ib}\overline{\mathbf{B}\mathbf{C}_i}^b \quad \mathbf{r}_{0\phi} + \mathbf{R}_\phi^{ib}\overline{\mathbf{B}\mathbf{C}_i}^b \quad \mathbf{R}_{\theta_1}^{ib}\overline{\mathbf{B}\mathbf{C}_i}^b \quad \mathbf{R}_{\theta_2}^{ib}\overline{\mathbf{B}\mathbf{C}_i}^b \quad \mathbf{R}_{\theta_3}^{ib}\overline{\mathbf{B}\mathbf{C}_i}^b \quad [\mathbf{W}]_i] \dot{\mathbf{q}} \quad (4.111)$$

where

$$\begin{aligned} [\mathbf{W}]_1 &= [\mathbf{R}^{ib}\overline{\mathbf{A}_1\mathbf{C}_1}_{\alpha_1}^b \quad \mathbf{R}^{ib}\overline{\mathbf{A}_1\mathbf{C}_1}_{\delta_1}^b \quad \mathbf{0}_{3 \times 2} \quad \mathbf{0}_{3 \times 2}] \\ [\mathbf{W}]_2 &= [\mathbf{0}_{3 \times 2} \quad \mathbf{R}^{ib}\overline{\mathbf{A}_2\mathbf{C}_2}_{\alpha_2}^b \quad \mathbf{R}^{ib}\overline{\mathbf{A}_2\mathbf{C}_2}_{\delta_2}^b \quad \mathbf{0}_{3 \times 2}] \end{aligned} \quad (4.112)$$

$$[\mathbf{W}]_3 = [\mathbf{0}_{3 \times 2} \quad \mathbf{0}_{3 \times 2} \quad \mathbf{R}^{ib} \overline{\mathbf{A}_3 \mathbf{C}_{3\alpha_3}^{-b}} \quad \mathbf{R}^{ib} \overline{\mathbf{A}_3 \mathbf{C}_{3\delta_3}^{-b}}]$$

For notation purposes,  $\dot{\mathbf{r}}_i$  is written as

$$\dot{\mathbf{r}}_i = [\mathbf{P}_i(\mathbf{q})] \dot{\mathbf{q}} \quad (4.113)$$

which is substituted into Equation (4.104) to yield the total translational kinetic energy

$$\begin{aligned} T_T &= \frac{1}{2} \dot{\mathbf{q}}^T [\mathbf{P}_1(\mathbf{q})]^T \mathbf{M}_1 [\mathbf{P}_1(\mathbf{q})] \dot{\mathbf{q}} + \frac{1}{2} \dot{\mathbf{q}}^T [\mathbf{P}_2(\mathbf{q})]^T \mathbf{M}_2 [\mathbf{P}_2(\mathbf{q})] \dot{\mathbf{q}} + \frac{1}{2} \dot{\mathbf{q}}^T [\mathbf{P}_3(\mathbf{q})]^T \mathbf{M}_3 [\mathbf{P}_3(\mathbf{q})] \dot{\mathbf{q}} \\ &= \frac{1}{2} \dot{\mathbf{q}}^T \{ [\mathbf{P}_1(\mathbf{q})]^T \mathbf{M}_1 [\mathbf{P}_1(\mathbf{q})] + [\mathbf{P}_2(\mathbf{q})]^T \mathbf{M}_2 [\mathbf{P}_2(\mathbf{q})] + [\mathbf{P}_3(\mathbf{q})]^T \mathbf{M}_3 [\mathbf{P}_3(\mathbf{q})] \} \dot{\mathbf{q}} \\ &= \frac{1}{2} \dot{\mathbf{q}}^T \left\{ \sum_{i=1}^3 [\mathbf{P}_i(\mathbf{q})]^T \mathbf{M}_i [\mathbf{P}_i(\mathbf{q})] \right\} \dot{\mathbf{q}} \end{aligned} \quad (4.114)$$

### Rotational Kinetic Energy

The total rotational energy of the bars is expressed as

$$T_R = \sum_{i=1}^3 \frac{1}{2} \boldsymbol{\omega}_i^T \mathbf{J}_i \boldsymbol{\omega}_i \quad (4.115)$$

where  $\mathbf{J}_i$  is the moment of inertia matrix of the  $i$ th bar. The angular velocity  $\boldsymbol{\omega}_i$  of the bar with respect to the inertial frame can be expressed as

$$\boldsymbol{\omega}_i = \boldsymbol{\omega}_i^{c/b} + \boldsymbol{\omega}^{b/o} + \boldsymbol{\omega}^{o/i}. \quad (4.116)$$

Both  $\boldsymbol{\omega}^{b/o}$  and  $\boldsymbol{\omega}^{o/i}$  are derived in the  $\{\mathbf{b}\}$  frame in Section 4.1. Similarly to  $\boldsymbol{\omega}^{o/i}$ , the angular velocity of the bar body frame  $\{\mathbf{c}\}$  with respect to the  $\{\mathbf{b}\}$  frame can be found analytically,

resulting in

$$\boldsymbol{\omega}_i^{c/b} = \begin{bmatrix} 0 \\ -\dot{\delta}_i \\ \dot{\alpha}_i \sin \delta_i \end{bmatrix} = \begin{bmatrix} 0 & 0 \\ 0 & -1 \\ \sin \delta_i & 0 \end{bmatrix} \begin{bmatrix} \dot{\alpha}_i \\ \dot{\delta}_i \end{bmatrix} \quad (4.117)$$

Furthermore,  $\boldsymbol{\omega}^{b/o}$  and  $\boldsymbol{\omega}^{o/i}$  must be rotated into the bar frame  $\{\mathbf{c}\}$  through the rotation  $\mathbf{R}^{cb} = \mathbf{R}_2(\delta_i)\mathbf{R}_3(\alpha_i)$ . The resulting expression for the total angular velocity therefore becomes

$$\begin{aligned} \boldsymbol{\omega}_i = & \begin{bmatrix} 0 & 0 \\ 0 & -1 \\ \sin \delta_i & 0 \end{bmatrix} \begin{bmatrix} \dot{\alpha}_i \\ \dot{\delta}_i \end{bmatrix} + \mathbf{R}_2(\delta_i)\mathbf{R}_3(\alpha_i)\mathbf{S}(\boldsymbol{\theta}) \begin{bmatrix} \dot{\theta}_1 \\ \dot{\theta}_2 \\ \dot{\theta}_3 \end{bmatrix} \\ & + \mathbf{R}_2(\delta_i)\mathbf{R}_3(\alpha_i)\mathbf{R}_1(\theta_1)\mathbf{R}_2(\theta_2)\mathbf{R}_3(\theta_3) \begin{bmatrix} 0 & -\sin \phi & 0 \\ 0 & 0 & 1 \\ 0 & \cos \phi & 0 \end{bmatrix} \begin{bmatrix} \dot{R} \\ \dot{\lambda} \\ \dot{\phi} \end{bmatrix} \end{aligned} \quad (4.118)$$

which, simplifying notation, yields

$$\boldsymbol{\omega}_i = \mathbf{K}_3 \dot{\mathbf{q}}_{(5+2i) \rightarrow (6+2i)} + \mathbf{K}_2 \dot{\mathbf{q}}_{4 \rightarrow 6} + \mathbf{K}_1 \dot{\mathbf{q}}_{1 \rightarrow 3}. \quad (4.119)$$

The terms can be combined into

$$\boldsymbol{\omega}_i = [\mathbf{S}_i(\mathbf{q})] \dot{\mathbf{q}} \quad (4.120)$$

where

$$\begin{aligned} [\mathbf{S}_1(\mathbf{q})] &= [\mathbf{K}_1 \quad \mathbf{K}_2 \quad \mathbf{K}_3 \quad \mathbf{0}_{3 \times 2} \quad \mathbf{0}_{3 \times 2}] \\ [\mathbf{S}_2(\mathbf{q})] &= [\mathbf{K}_1 \quad \mathbf{K}_2 \quad \mathbf{0}_{3 \times 2} \quad \mathbf{K}_3 \quad \mathbf{0}_{3 \times 2}] \\ [\mathbf{S}_3(\mathbf{q})] &= [\mathbf{K}_1 \quad \mathbf{K}_2 \quad \mathbf{0}_{3 \times 2} \quad \mathbf{0}_{3 \times 2} \quad \mathbf{K}_3] \end{aligned} \quad (4.121)$$



Thus, the total rotational kinetic energy of the bars becomes

$$\begin{aligned}
T_R &= \frac{1}{2} \dot{\mathbf{q}}^T [\mathbf{S}_1(\mathbf{q})]^T \mathbf{J}_1 [\mathbf{S}_1(\mathbf{q})] \dot{\mathbf{q}} + \frac{1}{2} \dot{\mathbf{q}}^T [\mathbf{S}_2(\mathbf{q})]^T \mathbf{J}_2 [\mathbf{S}_2(\mathbf{q})] \dot{\mathbf{q}} + \frac{1}{2} \dot{\mathbf{q}}^T [\mathbf{S}_3(\mathbf{q})]^T \mathbf{J}_3 [\mathbf{S}_3(\mathbf{q})] \dot{\mathbf{q}} \\
&= \frac{1}{2} \dot{\mathbf{q}}^T \{ [\mathbf{S}_1(\mathbf{q})]^T \mathbf{J}_1 [\mathbf{S}_1(\mathbf{q})] + [\mathbf{S}_2(\mathbf{q})]^T \mathbf{J}_2 [\mathbf{S}_2(\mathbf{q})] + [\mathbf{S}_3(\mathbf{q})]^T \mathbf{J}_3 [\mathbf{S}_3(\mathbf{q})] \} \dot{\mathbf{q}} \\
&= \frac{1}{2} \dot{\mathbf{q}}^T \left\{ \sum_{i=1}^3 [\mathbf{S}_i(\mathbf{q})]^T \mathbf{J}_i [\mathbf{S}_i(\mathbf{q})] \right\} \dot{\mathbf{q}} \tag{4.122}
\end{aligned}$$

where  $\mathbf{J}_i = \text{diag}[\frac{m_i L_i^2}{12}, \frac{m_i L_i^2}{12}, 0]$ .

### Total Kinetic Energy

Recall the expression from Equation (2.21) for the total kinetic energy of the system:

$$T = \sum_{i=0}^3 \{T_T + T_R\}_i \tag{4.123}$$

Substituting in the expressions for the kinetic energies derived for the base and the three bars, the kinetic energy becomes

$$\begin{aligned}
T &= \frac{1}{2} \dot{\mathbf{q}}^T [\mathbf{P}_0(\mathbf{q})]^T \mathbf{M}_0 [\mathbf{P}_0(\mathbf{q})] \dot{\mathbf{q}} + \frac{1}{2} \dot{\mathbf{q}}^T [\mathbf{S}_0(\mathbf{q})]^T \mathbf{J}_0 [\mathbf{S}_0(\mathbf{q})] \dot{\mathbf{q}} \\
&\quad + \frac{1}{2} \dot{\mathbf{q}}^T \left\{ \sum_{i=1}^3 [\mathbf{P}_i(\mathbf{q})]^T \mathbf{M}_i [\mathbf{P}_i(\mathbf{q})] \right\} \dot{\mathbf{q}} + \frac{1}{2} \dot{\mathbf{q}}^T \left\{ \sum_{i=1}^3 [\mathbf{S}_i(\mathbf{q})]^T \mathbf{J}_i [\mathbf{S}_i(\mathbf{q})] \right\} \dot{\mathbf{q}} \tag{4.124}
\end{aligned}$$

$$= \frac{1}{2} \dot{\mathbf{q}}^T \left\{ \sum_{i=0}^3 [\mathbf{P}_i(\mathbf{q})]^T \mathbf{M}_i [\mathbf{P}_i(\mathbf{q})] + \sum_{i=0}^3 [\mathbf{S}_i(\mathbf{q})]^T \mathbf{J}_i [\mathbf{S}_i(\mathbf{q})] \right\} \dot{\mathbf{q}} \tag{4.125}$$

$$= \frac{1}{2} \dot{\mathbf{q}}^T \mathbf{M}(\mathbf{q}) \dot{\mathbf{q}} \tag{4.126}$$

which is in the form desired for implementing Lagrange's method.

### 4.2.2 Generalized Gravitational Force

Start with a general expression for the generalized forces on the entire system:

$$\mathbf{Q}_g = \sum_{i=0}^3 \left[ \left( \frac{\partial \dot{\mathbf{r}}_i}{\partial \dot{\mathbf{q}}} \right)^T \mathbf{F}_{g_i} \right] + \sum_{i=0}^3 \left[ \left( \frac{\partial \boldsymbol{\omega}_i}{\partial \dot{\mathbf{q}}} \right)^T \mathbf{M}_{g_i} \right] \quad (4.127)$$

where  $\dot{\mathbf{r}}_i$  and  $\boldsymbol{\omega}_i$  are the translational and angular velocities of the  $i$ th body. The gravitational forces and moments,  $\mathbf{F}_{g_i}$  and  $\mathbf{M}_{g_i}$ , were previously found to be [34, 35]

$$\mathbf{F}_{g_i} = -\frac{\mu m}{R^2} \mathbf{o}_r - \frac{3\mu}{2R^4} [\text{tr}(\mathbf{J}_i) - 5\mathbf{o}_r^T \mathbf{J}_i \mathbf{o}_r] \mathbf{o}_r - \frac{3\mu}{R^4} \mathbf{J}_i \mathbf{o}_r \quad (4.128)$$

$$\mathbf{M}_{g_i} = \frac{3\mu}{R^3} \mathbf{o}_r^\times \mathbf{J}_i \mathbf{o}_r, \quad (4.129)$$

where  $\mathbf{o}_r$  is a unit vector that points along the direction of orbital radius vector  $\mathbf{r}_0$ , which also coincides with the third axis of the orbital frame  $\{\mathbf{o}\}$ . Following a process similar to that taken for the base, the generalized velocities for the  $i$ th body are

$$\frac{\partial \dot{\mathbf{r}}_i}{\partial \dot{\mathbf{q}}} = [\mathbf{P}_i(\mathbf{q})]. \quad (4.130)$$

A similar process is used to find that

$$\frac{\partial \boldsymbol{\omega}_i}{\partial \dot{\mathbf{q}}} = [\mathbf{S}_i(\mathbf{q})]. \quad (4.131)$$

Combining the above expressions, the generalized gravitational forces on the base become

$$\mathbf{Q}_g = \sum_{i=0}^3 [\mathbf{P}_i(\mathbf{q})]^T \mathbf{F}_{g_i} + \sum_{i=0}^3 [\mathbf{S}_i(\mathbf{q})]^T \mathbf{M}_{g_i}. \quad (4.132)$$

### 4.2.3 Tensegrity Elastic Potential Energy

Recall from Section 2.3 that the Jacobian of the elastic potential energy over the generalized coordinates is

$$\nabla_{\mathbf{q}} V_e = \mathbf{A}(\mathbf{q})\mathbf{F} \quad (4.133)$$

and that the elements of  $\mathbf{A}(\mathbf{q})$  are

$$A_{kj} = \frac{\partial l_j}{\partial q_k}, \quad k = 1, \dots, N, \quad j = 1, \dots, E. \quad (4.134)$$

Many of the most interesting solutions of tensegrity structures are those derived from a symmetrical configuration, like the one shown in Figure 4.9. One such example is the configuration chosen where[21]

$$[\alpha_1 \quad \delta_1 \quad \alpha_2 \quad \delta_2 \quad \alpha_3 \quad \delta_3]^T = [\alpha \quad \delta \quad \alpha + \frac{4\pi}{3} \quad \delta \quad \alpha + \frac{2\pi}{3} \quad \delta]^T \quad (4.135)$$

From this, the matrix  $\mathbf{A}(\mathbf{q})$  becomes

$$\mathbf{A}(\mathbf{q}) = \begin{bmatrix} \mathbf{0}_{6 \times 6} \\ \bar{\mathbf{A}} \end{bmatrix}, \quad (4.136)$$

where the matrix  $\bar{\mathbf{A}}$  is defined as

$$\bar{\mathbf{A}}|_{\mathbf{q}_d} = \begin{bmatrix} 0 & 0 & A_1 & A_2 & 0 & 0 \\ 0 & 0 & 0 & 0 & A_1 & A_2 \\ A_1 & A_2 & 0 & 0 & 0 & 0 \\ A_5 & A_6 & A_3 & A_4 & 0 & 0 \\ 0 & 0 & A_5 & A_6 & A_3 & A_4 \\ A_3 & A_4 & 0 & 0 & A_5 & A_6 \end{bmatrix} \quad (4.137)$$

and

$$\begin{aligned}
A_1 &= 2Lb \sin \alpha \sin \delta \\
A_2 &= -2Lb \cos \alpha \cos \delta \\
A_3 &= L \sin \delta (2b \sin \alpha - \sqrt{3}L \sin \delta) \\
A_4 &= L \cos \delta (3L \sin \delta - 2b \cos \alpha) \\
A_5 &= L \sin \delta (b \sin \alpha + \sqrt{3}L \sin \delta - \sqrt{3}b \cos \alpha) \\
A_6 &= L \cos \delta (3L \sin \delta - b \cos \alpha - \sqrt{3}b \sin \alpha).
\end{aligned} \tag{4.138}$$

#### 4.2.4 Tensegrity Prestressed Equilibrium

To maintain the integrity of the tensegrity structure, all the tendons must remain in a continuous state of tension. It is beneficial to choose some static equilibrium configuration such that this condition is met - this is what will be referred here as prestressability.[8]

Recall that the equations of motion of the system are

$$\frac{d}{dt}(\nabla_{\dot{\mathbf{q}}}T) - \nabla_{\mathbf{q}}T = -\nabla_{\mathbf{q}}V_e + \mathbf{Q}_g + \mathbf{Q}_t. \tag{4.139}$$

For analyzing a static system, however, all time-derivative terms go to zero, and thus the equations for the statics of the tensegrity structure become

$$\nabla_{\mathbf{q}}V_e = \mathbf{Q}_g + \mathbf{Q}_t \tag{4.140}$$

which is equivalent to

$$\begin{bmatrix} \mathbf{0}_{6 \times 6} \\ \bar{\mathbf{A}} \end{bmatrix} \mathbf{F} = \mathbf{Q}_g + \begin{bmatrix} \bar{\mathbf{Q}}_t \\ \mathbf{0}_{6 \times 6} \end{bmatrix} \mathbf{u}. \tag{4.141}$$

This equation can be split in two, and for the prestressability analysis, the portion that is important is

$$\bar{\mathbf{A}}\mathbf{F} = \bar{\mathbf{Q}}_g \tag{4.142}$$

where  $\bar{\mathbf{Q}}_g = \mathbf{Q}_{g_{7 \rightarrow 12}}$  corresponds to the last six elements of the vector of generalized gravitational forces and  $\mathbf{F}$  is the vector of tendon forces. Once again, to satisfy the condition of prestressability, all the tendons must be in tension, namely

$$F_j > 0 \text{ for } j = 1, \dots, 6, \tag{4.143}$$

where  $F_j$  is the element of the vector  $\mathbf{F}$  corresponding to the  $j$ th tendon (see Figure 4.8 for assigned labels).

Further simplifications can be made by recalling the small angle approximation made in Section 4.1, which is also implying that the body frame  $\{\mathbf{b}\}$  of the base and the orbital frame  $\{\mathbf{o}\}$  are approximately coincident.

Taking these simplifications into account, and substituting in the angles from the equilibrium configuration from Equation (4.135), the expression for  $\bar{\mathbf{Q}}_g$  is found to be

$$\bar{\mathbf{Q}}_g = [0 \quad Q_G \quad 0 \quad Q_G \quad 0 \quad Q_G]^T, \tag{4.144}$$

where

$$Q_G = \frac{GM_{\oplus}L^3\rho \cos \delta \sin \delta}{4(R_{\oplus} + h)^3}.$$

The resulting static equilibrium equation for the tensegrity structure is

$$[0 \quad Q_G \quad 0 \quad Q_G \quad 0 \quad Q_G]^T = \bar{\mathbf{A}} [F_1 \quad F_2 \quad F_3 \quad F_4 \quad F_5 \quad F_6]^T \tag{4.145}$$

which, solving for the forces, becomes:

$$[F_1 \ F_2 \ F_3 \ F_4 \ F_5 \ F_6]^T = \bar{\mathbf{A}}^{-1} [0 \ Q_G \ 0 \ Q_G \ 0 \ Q_G]^T.$$

Once again, substituting in the equilibrium configuration from Equation (4.135) yields the following expressions for the forces:

$$F_1 = F_2 = F_3 = \frac{GM_{\oplus}L^2\rho}{4(R_{\oplus} + h)^3} \frac{\cos \alpha \cos \delta}{(\sqrt{3}b - 6L \sin \alpha \sin \delta)} \quad (4.146)$$

and

$$F_4 = F_5 = F_6 = \frac{GM_{\oplus}L^2\rho}{4(R_{\oplus} + h)^3} \frac{\sin \alpha \sin \delta}{(\sqrt{3}b - 6L \sin \alpha \sin \delta)}. \quad (4.147)$$

Recall from Equation (4.143) that tensile forces in the tendons must always be positive so as to not let the tendons go slack. Since the constants in Equations (4.146) and (4.147) are all already positive, the sections of the above equations must meet the condition

$$\frac{\cos \alpha \cos \delta}{(\sqrt{3}b - 6L \sin \alpha \sin \delta)} > 0 \quad \text{and} \quad \frac{\sin \alpha \sin \delta}{(\sqrt{3}b - 6L \sin \alpha \sin \delta)} > 0. \quad (4.148)$$

In order for these inequalities to hold, the numerator and denominator of each must both be negative, or both positive. Following this, the conditions that must be met are:

$$\text{(Case 1)} \quad \cos \alpha \cos \delta > 0 \quad \text{and} \quad \sin \alpha \sin \delta > 0$$

$$\text{(Case 2)} \quad \cos \alpha \cos \delta < 0 \quad \text{and} \quad \sin \alpha \sin \delta < 0.$$

Consider first Case 1. The physical limitations of the tensegrity system cause the bar orientation angles to be constrained to  $\alpha \in [0, 2\pi)$  and  $\delta \in (0, \pi/2)$ . Within this range,  $\cos \delta$

and  $\sin \delta$  are always positive, thus the limits of  $\alpha$  fall within the first quadrant:  $\alpha \in (0, \pi/2)$ . Since the numerators are positive, the denominator ( $\sqrt{3}b - 6L \sin \alpha \sin \delta$ ) must also be greater than zero. Solving for  $\alpha$  yields

$$\sin \alpha < \frac{\sqrt{3}b}{6L \sin \delta}. \quad (4.149)$$

A visualization of the solution of this inequality is provided in Figure 4.10. Since  $\sin \delta$  is always positive, the value of  $\sqrt{3}b/(6L \sin \delta)$  falls in the first two quadrants, or in the positive  $y$  space. Note that if  $\sqrt{3}b/(6L \sin \delta) \geq 1$ , then Inequality (4.149) is satisfied for all  $\alpha$  since  $\sin \alpha \leq 1$  always. For the case where  $\sqrt{3}b/(6L \sin \delta) < 1$ , the maximum angle is found to be  $\alpha_{max} = \arcsin(\sqrt{3}b/(6L \sin \delta))$ , which can be measured upward from either the positive or negative  $x$ -axis. However, since  $\alpha \in [0, \pi/2)$ ,  $\alpha$  cannot fall in any quadrants but the first, and so  $\alpha_{max}$  must be measured from the positive  $x$ -axis. The limit of  $\alpha$  for this case becomes,

$$\alpha \in \left( 0, \arcsin \left( \frac{\sqrt{3}b}{6L \sin \delta} \right) \right) \quad \text{for} \quad \frac{\sqrt{3}b}{6L \sin \delta} < 1. \quad (4.150)$$

Now for Case 2, where the numerators are negative:  $\cos \alpha \cos \delta < 0$  and  $\sin \alpha \sin \delta < 0$ . Again,  $\cos \delta$  and  $\sin \delta$  are always positive, the Case 2 inequalities are reduced to  $\cos \alpha < 0$  and  $\sin \alpha < 0$ . For these to be valid,  $\alpha \in (\pi, 3\pi/2)$  which corresponds to the third quadrant. The denominators must be of the same sign, so in this case ( $\sqrt{3}b - 6L \sin \alpha \sin \delta$ )  $< 0$ . Solving for  $\sin \alpha$  gives

$$\sin \alpha > \frac{\sqrt{3}b}{6L \sin \delta}. \quad (4.151)$$

As in the previous case,  $\sin \delta$  is always positive, and so the value of  $\sqrt{3}b/(6L \sin \delta)$  falls again

in the top two quadrants. The inequality states that the value of  $\sin \alpha$  must fall above the  $\sqrt{3}b/(6L \sin \delta)$ . This, however, clashes with the previous limits of  $\sin \alpha$ , which states that  $\sin \alpha < 0$ . Thus, this case is invalid for all  $\alpha$ .

The conditions for the prestressed equilibrium configurations can therefore be summarized as follows:

If  $\delta \in (0, \pi/2)$  and

$$\alpha \in (0, \alpha_{max}) \quad \text{where} \quad \alpha_{max} = \begin{cases} \frac{\pi}{2}, & \text{for } \frac{\sqrt{3}b}{6L \sin \delta} \geq 1 \\ \arcsin\left(\frac{\sqrt{3}b}{6L \sin \delta}\right), & \text{for } \frac{\sqrt{3}b}{6L \sin \delta} < 1 \end{cases}$$

then  $F_j > 0$ , thus satisfying Equation (4.143).

For visualization purposes, the forces are plotted against  $\alpha$  and  $\delta$  in Figures 4.11 and 4.12, where  $\alpha \in [0, 2\pi)$  and  $\delta \in (0, \pi/2)$ , and the values for the constants are shown in Table 4.1, where the linear density  $\rho$  is calculated by assuming a steel bar with a 5 mm radius. Only positive  $F$  values are shown in the plots. Note that the only range where all forces are positive is when  $\delta \in (0, \pi/2)$  and  $\alpha \in [0, \arcsin(\sqrt{3}b/(6L \sin \delta))$ .



Parameter	Value
$R_{\oplus}$	$6878 \times 10^3 m$
$M_{\oplus}$	$5.972 \times 10^{24} kg$
$G$	$6.67 \times 10^{-11} m^3 kg^{-1} s^{-2}$
$h$	$200 \times 10^3 m$
$L$	$30 m$
$b$	$10 m$
$\rho$	$0.6283 kg m^{-1}$

Table 4.1: Parameter values for simulation.

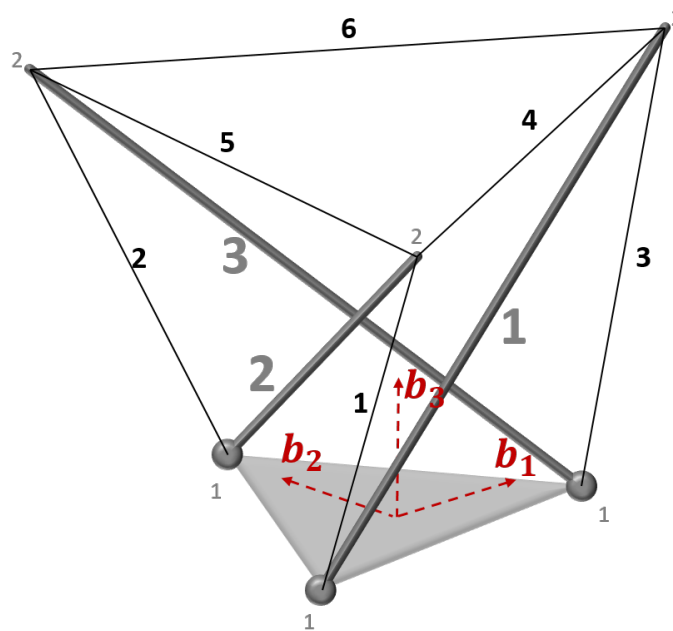


Figure 4.8: Assigned indices to bars and tendons that make up the 3-bar tensegrity structure. A tendon force  $F_j$  means a tendon force in the  $j$ th tendon, according to this diagram.[8]

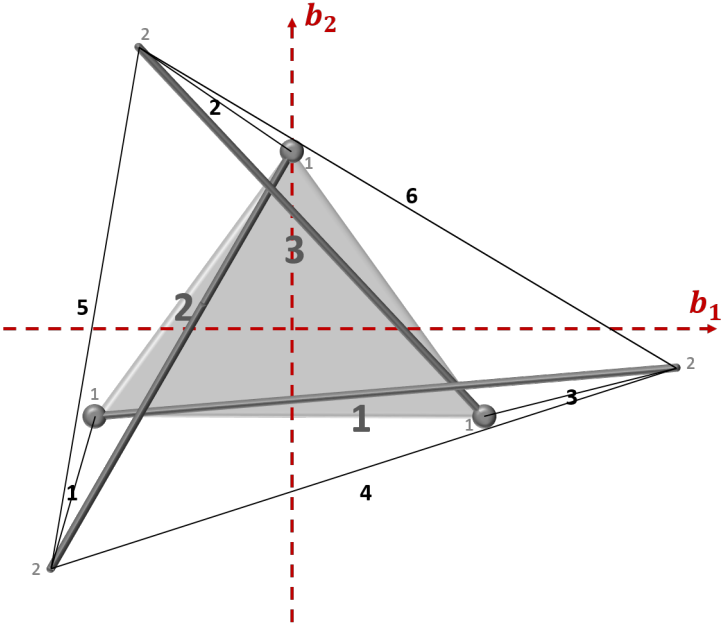


Figure 4.9: Top view looking down along  $b_3$  axis of 3-bar tensegrity structure. The symmetry of the structure is apparent.[8]

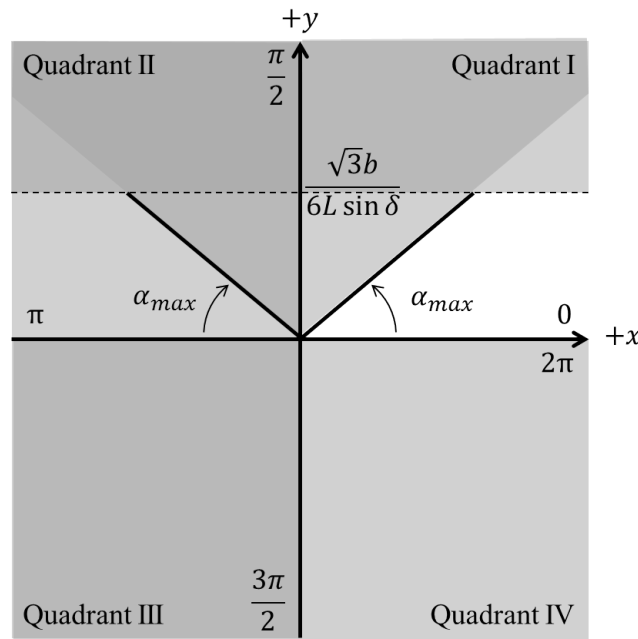


Figure 4.10: For a chosen  $\delta$  that falls between 0 and  $\pi$ , and the symmetric configuration suggested, the limits of  $\alpha$  are depicted above. Note the fairly small range of  $\alpha$  for which the tensegrity structure will meet the conditions of prestressability (i.e. all tendons in a state of stress).

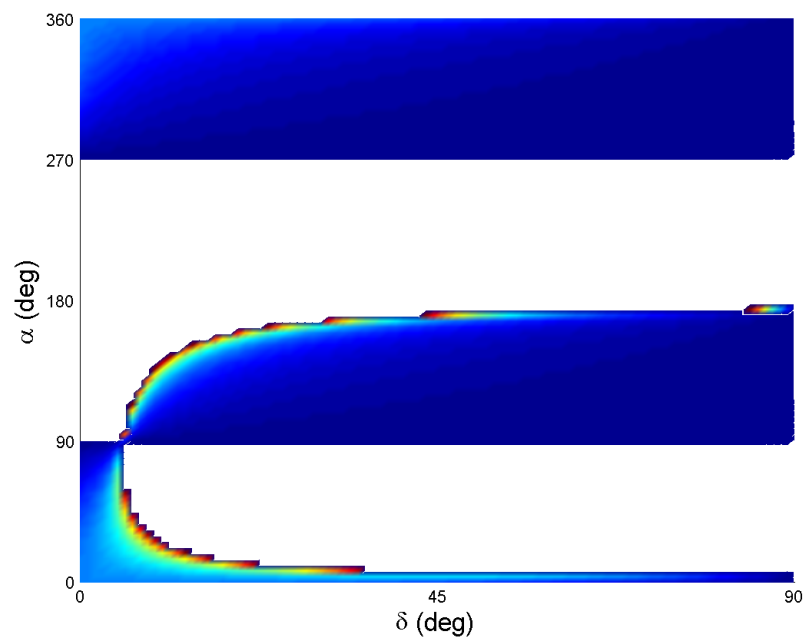


Figure 4.11: Plot of area where tensions in the vertical three tendons  $F_{1,2,3}$  are positive. If an angle  $\alpha$  or  $\delta$  is chosen outside this shaded region, the tendon will be slack and the tensegrity structure will risk collapse.

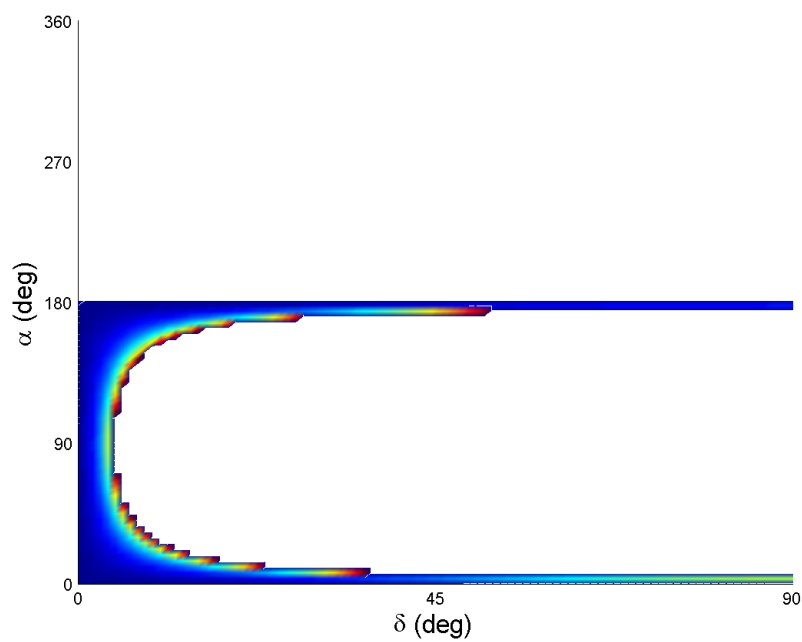


Figure 4.12: Plot of area where tensions in the top three horizontal tendons  $F_{4,5,6}$  are positive. If an angle  $\alpha$  or  $\delta$  is chosen outside this shaded region, the tendon will be slack and the tensegrity structure will risk collapse.

### 4.2.5 Desired Configuration

Recall the generalized coordinates of a three-bar tensegrity spacecraft:

$$\mathbf{q} = [R \ \lambda \ \phi \ \theta_1 \ \theta_2 \ \theta_3 \ \alpha_1 \ \delta_1 \ \alpha_2 \ \delta_2 \ \alpha_3 \ \delta_3]^T \quad (4.152)$$

The spacecraft is to follow a circular equatorial orbit, such that

$$\phi = \frac{\pi}{2} \quad (4.153)$$

and  $R$  is constant. It follows that the angular velocity of the base about the Earth will be equal to

$$\dot{\lambda} = n = \sqrt{\mu/R^3} \quad (4.154)$$

The attitude of the spacecraft is maintained in a synchronous orbit, shown in Figure 4.13, by setting the Euler angles to zero so that  $\{\mathbf{b}\}$  remains coincident with  $\{\mathbf{o}\}$ :

$$\theta_1 = 0, \quad \theta_2 = 0, \quad \theta_3 = 0 \quad (4.155)$$

Lastly, the desired orientation of the bars that make up the tensegrity structure is a symmetrical configuration that was chosen from the discussion on prestressability:

$$[\alpha_1 \ \delta_1 \ \alpha_2 \ \delta_2 \ \alpha_3 \ \delta_3]^T = \left[ \alpha \ \delta \ \alpha + \frac{4\pi}{3} \ \delta \ \alpha + \frac{2\pi}{3} \ \delta \right]^T, \quad (4.156)$$

where  $\alpha$  and  $\delta$  are chosen such that the tensegrity structure meets prestressability conditions; in this numerical analysis, values of  $\alpha = \delta = \pi/12$  are chosen. Thus, the array of generalized coordinates for this desired configuration,  $\mathbf{q}_d$ , becomes

$$\mathbf{q}_d = \left[ R \ \lambda(t) \ \frac{\pi}{2} \ 0 \ 0 \ 0 \ \frac{\pi}{12} \ \frac{\pi}{12} \ \frac{\pi}{12} + \frac{4\pi}{3} \ \frac{\pi}{12} \ \frac{\pi}{12} + \frac{2\pi}{3} \ \frac{\pi}{12} \right]^T. \quad (4.157)$$

The symmetric configuration of the tensegrity structure is controlled by adjusting the rest lengths  $r_i$  of the tendons. The orbit and attitude are maintained by means of thrusters  $u_i$  attached to the base that generate forces and moments about the principal axes of the base. The array of controls  $\mathbf{u}$  is

$$\mathbf{u} = [u_1 \ u_2 \ u_3 \ u_4 \ u_5 \ u_6 \ r_1 \ r_2 \ r_3 \ r_4 \ r_5 \ r_6]^T. \quad (4.158)$$

All the bars that make up the tensegrity system are assumed to be of length  $L$  and mass  $m_b$ , and the tendons have stiffness  $k$ . The bars are connected to the base in such a way that the connection points fall on the corners of an equilateral triangle of sides  $b$  inscribed into the top face of the base. The first and second dimensions of the base are

$$D_1 = b \quad \text{and} \quad D_2 = \frac{\sqrt{3}}{2}b. \quad (4.159)$$

Taking into account these chosen parameters, the equations of motion of the desired configuration are

$$\mathbf{C}(\mathbf{q}_d, \dot{\mathbf{q}}_d)\dot{\mathbf{q}}_d = -\nabla_{\mathbf{q}}V_e(\mathbf{q}_d) + \mathbf{Q}_g(\mathbf{q}_d) + \mathbf{Q}_t(\mathbf{q}_d) \quad (4.160)$$

where

$$\dot{\mathbf{q}}_d = [0 \ \dot{\lambda}(t) \ 0 \ 0 \ 0 \ 0 \ 0 \ 0 \ 0 \ 0 \ 0 \ 0]^T. \quad (4.161)$$

Consider first the elastic potential energy term, which recall can be written as

$$\nabla_{\mathbf{q}}V_e(\mathbf{q}_d) = \mathbf{A}(\mathbf{q}_d)\mathbf{F} = \begin{bmatrix} \mathbf{0}_{6 \times 6} \\ \bar{\mathbf{A}}|_{\mathbf{q}_d} \end{bmatrix} \mathbf{F}. \quad (4.162)$$



The matrix  $\bar{\mathbf{A}}$  evaluated at  $\mathbf{q}_d$  is

$$\bar{\mathbf{A}}|_{\mathbf{q}_d} = \begin{bmatrix} 0 & 0 & a_1 & a_2 & 0 & 0 \\ 0 & 0 & 0 & 0 & a_1 & a_2 \\ a_1 & a_2 & 0 & 0 & 0 & 0 \\ a_5 & a_6 & a_3 & a_4 & 0 & 0 \\ 0 & 0 & a_5 & a_6 & a_3 & a_4 \\ a_3 & a_4 & 0 & 0 & a_5 & a_6 \end{bmatrix}, \quad (4.163)$$

where

$$\begin{aligned} a_1 &= -1/2 Lb(\sqrt{3} - 2) \\ a_2 &= -1/2 Lb(\sqrt{3} + 2) \\ a_3 &= -1/4 L(3L + 3b - 2\sqrt{3}L - 2\sqrt{3}b) \\ a_4 &= -1/4 L(4b - 3L + 2\sqrt{3}b) \\ a_5 &= -1/4 L(3L - 2b - 2\sqrt{3}L + 2\sqrt{3}b) \\ a_6 &= -1/4 L(2b - 2L + 2\sqrt{3}b) \end{aligned}$$

The array of tendon forces  $\mathbf{F}$  is also evaluated at  $\mathbf{q}_d$  to be

$$\mathbf{F} = [F_1 \ F_2 \ F_3 \ F_4 \ F_5 \ F_6]^T \quad (4.164)$$

where

$$F_j = \begin{cases} -\frac{k}{r_j}(r_j - \sqrt{L^2 - 1/2 Lb + 2b^2}) & \text{for } j = 1, 2, 3 \\ -\frac{k}{r_j}(r_j - 1/2 \sqrt{6L^2 - 3\sqrt{3}L^2 + 4b^2 - 2\sqrt{3}Lb}) & \text{for } j = 4, 5, 6 \end{cases} \quad (4.165)$$

Now consider the generalized force vector of the thruster controls,  $\mathbf{Q}_t$ , which evaluated at  $\mathbf{q}_d$  is

$$\mathbf{Q}_t(\mathbf{q}_d) = \begin{bmatrix} \bar{\mathbf{Q}}_t|_{\mathbf{q}_d} \\ \mathbf{0}_{6 \times 6} \end{bmatrix} \mathbf{u}. \quad (4.166)$$

where

$$\bar{\mathbf{Q}}_t|_{\mathbf{q}_d} = \begin{bmatrix} \cos \lambda & \sin \lambda & 0 & 0 & 0 & 0 \\ -R \sin \lambda & R \cos \lambda & 0 & 0 & 0 & -1 \\ 0 & 0 & 1 & 0 & 1 & 0 \\ 0 & 0 & 0 & 1 & 0 & 0 \\ 0 & 0 & 0 & 0 & 1 & 0 \\ 0 & 0 & 0 & 0 & 0 & 1 \end{bmatrix} \quad (4.167)$$

Finally, Equation (4.162) and (4.166) are substituted into Equation (4.160) to yield

$$\mathbf{C}_d = - \begin{bmatrix} \mathbf{0}_{6 \times 6} \\ \bar{\mathbf{A}}|_{\mathbf{q}_d} \end{bmatrix} \mathbf{F} + \mathbf{Q}_g(\mathbf{q}_d) + \begin{bmatrix} \bar{\mathbf{Q}}_t|_{\mathbf{q}_d} \\ \mathbf{0}_{6 \times 6} \end{bmatrix} \mathbf{u} \quad (4.168)$$

where  $\mathbf{C}_d = \mathbf{C}(\mathbf{q}_d, \dot{\mathbf{q}}_d)\dot{\mathbf{q}}_d$  and  $\mathbf{Q}_g(\mathbf{q}_d) = [Q_{g1} \quad Q_{g2} \quad \dots \quad Q_{g12}]^T$ . The equation can be separated into the following two expressions

$$(\mathbf{C}_d)_{1 \rightarrow 6} = \mathbf{Q}_g(\mathbf{q}_d)_{1 \rightarrow 6} + \bar{\mathbf{Q}}_t|_{\mathbf{q}_d} \mathbf{u} \quad (4.169)$$

and

$$(\mathbf{C}_d)_{7 \rightarrow 12} = -\bar{\mathbf{A}}|_{\mathbf{q}_d} \mathbf{F} + \mathbf{Q}_g(\mathbf{q}_d)_{7 \rightarrow 12} \quad (4.170)$$

where  $\mathbf{Q}_g(\mathbf{q}_d)_{1 \rightarrow 6}$  and  $\mathbf{Q}_g(\mathbf{q}_d)_{7 \rightarrow 12}$  correspond, respectively, to the first six and last six elements of  $\mathbf{Q}_g(\mathbf{q}_d)$ , and  $(\mathbf{C}_d)_{1 \rightarrow 6}$  and  $(\mathbf{C}_d)_{7 \rightarrow 12}$  to the first six and last six elements of  $\mathbf{C}_d$ .

The required tendon rest lengths and thruster controls necessary to keep the system in the desired configuration depend on the longitude angle  $\lambda$  and its time derivative  $\dot{\lambda}$ . In order to numerically analyze this effect, values were chosen for the orbital and structural parameters of the system, listed in Table 4.1. Additionally, recall that the value of  $\dot{\lambda}$  for a circular equatorial orbit is  $\dot{\lambda} = \sqrt{\mu/R^3}$ .

Evaluated at the above parameters and the desired configuration, the resulting vector of gravitational effects is

$$\mathbf{Q}_g = [-1.2456e5 \ 0 \ 0 \ 0 \ 0 \ 0 \ 0 \ -0.119 \ 0 \ -0.119 \ 0 \ -0.119]^T N. \quad (4.171)$$

In this configuration, the  $\alpha_i$  angles of the bars do not have an effect on the gravitational forces on the system. Since the spacecraft is moving in a circular orbit, the angles  $\lambda$  and  $\phi$  also do not contribute. Finally, since the spacecraft is forced into a synchronous orbit, such that the Euler angles are set to zero, the contribution of these angles to the gravity force are also nil.

The synchronous nature of the spacecraft's orbit about the Earth is maintained primarily by the control torque  $u_4$  of  $-0.2818 Nm$  about the  $\mathbf{o}_\phi$  axis (the axis normal to the plane of the orbit) that preserves the system's orientation with respect to the Earth's surface, so as to follow the behavior shown in Figure 4.13. By maintaining this orbit and orientation, and assuming a spherical Earth, the system will remain in a gravity field of equal strength and direction as it revolves around the Earth. Thus, the gravity effect will be equal across all the bars that make up the tensegrity structure. The resulting rest lengths of the vertical

tendons  $(r_1, r_2, r_3)$  are all equal to  $28.97\text{ m}$ ; the rest lengths of the top tendons  $(r_4, r_5, r_6)$  are  $4.57\text{ m}$ . These rest lengths yield elongations  $\varepsilon$  of  $0.183\text{ m}$  and  $0.0167\text{ m}$  for the vertical and top tendons, respectively. Since the elongations are all of positive sign, the tendons do not go slack, and so the tensegrity structure remains stressed throughout its orbit. These thruster controls and rest lengths make up the controls  $\mathbf{u}_d$  necessary to maintain the system's desired configuration.

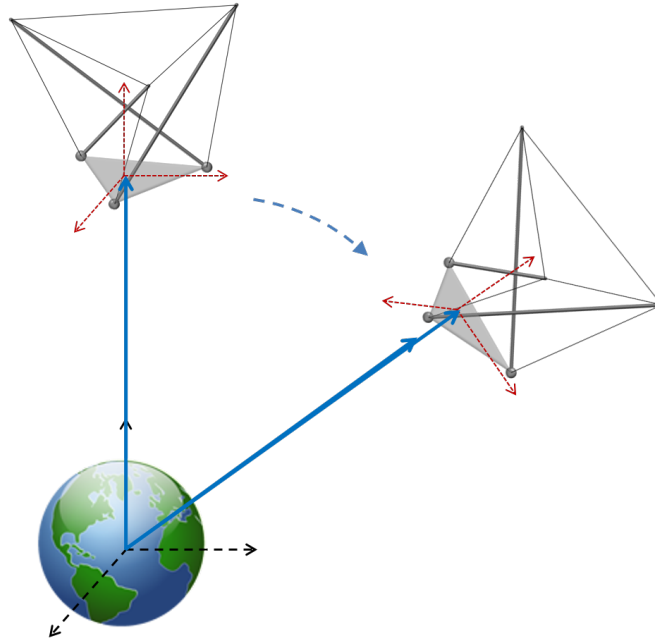


Figure 4.13: Desired orbit configuration chosen for tensegrity spacecraft. The orbit is a synchronous one, meaning that the same face of the spacecraft (the bottom of the base) is always pointed along the negative orbital radius vector (i.e. pointed towards the earth). This also means the body frame of the base  $\{\mathbf{b}\}$  coincides with the orbital frame  $\{\mathbf{o}\}$  (the Euler angles relating the two are all zero). If the spacecraft is in a circular orbit about an assumed-spherical Earth, this means that the spacecraft will be subject to the same gravitational forces throughout its orbit.

### 4.2.6 LQR Control

Recall the equations of motion for the 3-bar tensegrity spacecraft:

$$\mathbf{M}(\mathbf{q})\ddot{\mathbf{q}} + \mathbf{C}(\mathbf{q}, \dot{\mathbf{q}})\dot{\mathbf{q}} + (\nabla_{\mathbf{q}}V_e(\mathbf{q}, \mathbf{u}) - \mathbf{Q}_g(\mathbf{q}) - \mathbf{Q}_t(\mathbf{q}, \mathbf{u})) = 0$$

where the generalized coordinates are

$$\mathbf{q} = [R \ \lambda \ \phi \ \theta_1 \ \theta_2 \ \theta_3 \ \alpha_1 \ \delta_1 \ \alpha_2 \ \delta_2 \ \alpha_3 \ \delta_3]^T \quad (4.172)$$

and the controls are

$$\mathbf{u} = [u_1 \ u_2 \ u_3 \ u_4 \ u_5 \ u_6 \ r_1 \ r_2 \ r_3 \ r_4 \ r_5 \ r_6]^T \quad (4.173)$$

Linearizing about the desired configuration yields the linearized second order system

$$\tilde{\mathbf{M}}\delta\ddot{\mathbf{q}} + \tilde{\mathbf{C}}\delta\dot{\mathbf{q}} + \tilde{\mathbf{K}}\delta\mathbf{q} + \tilde{\mathbf{B}}\delta\mathbf{u} = 0, \quad (4.174)$$

where  $\delta\mathbf{q} = \mathbf{q} - \mathbf{q}_d$ .

Recall from Section 3.2 that this second order system can be converted into the first order form:

$$\dot{\mathbf{x}} = \tilde{\mathbf{A}}\mathbf{x} + \tilde{\mathbf{B}}\mathbf{u}, \quad \mathbf{x}(0) = \mathbf{x}_d, \quad (4.175)$$

whose response is controlled by choosing a control law  $\mathbf{u} = -\mathbf{K}\mathbf{x}$  that minimizes the cost function

$$V = \int_0^{\infty} (\mathbf{x}^T \mathbf{Q} \mathbf{x} + \mathbf{u}^T \mathbf{R} \mathbf{u}) dt, \quad (4.176)$$

Letting  $\mathbf{x} = [\delta\mathbf{q} \ \delta\dot{\mathbf{q}}]^T$  and  $\mathbf{u} = \delta\mathbf{u}$ , and choosing both  $\mathbf{Q}$  and  $\mathbf{R}$  to be equal to identity, the response of the system under the LQR control is generated about the desired configuration

below:

$$\mathbf{q}_d = [R \quad \lambda(t) \quad 0 \quad 0 \quad 0 \quad 0 \quad \frac{\pi}{12} \quad \frac{\pi}{12} \quad \frac{17\pi}{12} \quad \frac{\pi}{12} \quad \frac{3\pi}{4} \quad \frac{\pi}{12}] \quad (4.177)$$

$$\dot{\mathbf{q}}_d = [0 \quad \dot{\lambda} \quad 0 \quad 0 \quad 0 \quad 0 \quad 0 \quad 0 \quad 0 \quad 0 \quad 0 \quad 0] \quad (4.178)$$

$$\ddot{\mathbf{q}}_d = [0 \quad 0 \quad 0 \quad 0 \quad 0 \quad 0 \quad 0 \quad 0 \quad 0 \quad 0 \quad 0 \quad 0] \quad (4.179)$$

In order to determine how different elements of the system affected the others, the system was perturbed in two manners. The first was by inducing a displacement on the Euler angles (i.e. the attitude angles of the base) of  $\delta\theta_1 = \delta\theta_2 = \delta\theta_3 = 1^\circ$ , while the initial displacement of the orientation angles of the bars from their desired configuration was set to zero ( $\delta\alpha_i = \delta\delta_i = 0^\circ$ ). Figure 4.14 shows the response of the base as it slowly returns to its equilibrium configuration under guidance of the thruster controls on the base. What is interesting to note is the effect that the response of the base has on the dynamics of the bars that are attached to it, shown in Figure 4.15. As the base is first displaced, it causes the bars to jerk away from their equilibrium configuration. As the controls kick in, they follow a similar oscillatory pattern as the base, until they zero out at the equilibrium.

The next perturbation chosen was that of the bars. The attitude of the base was left at its equilibrium configuration, but the bars were displaced by some amount from their equilibrium. To better see the response of the bars, the different displacements were chosen for their displacement angles; specifically:  $\delta\alpha_1 = \delta\delta_1 = 0.1^\circ$ ,  $\delta\alpha_2 = \delta\delta_2 = 0.2^\circ$ , and  $\delta\alpha_3 = \delta\delta_3 = 0.3^\circ$ . The bars are quickly brought back to their equilibrium configuration, as shown in Figure 4.19. On the other hand, the base, shown in Figure 4.18, is in a state of perpetual

minor oscillation: this is due to the constant corrections employed by the thruster controls as the spacecraft moves through its orbit. Notice that the limits on the vertical axis are quite small, which is the reason why this oscillatory response can be seen. There is a slight increase in the oscillation amplitude early on, which corresponds to the early motion of the bars as they return to equilibrium. Then the base returns to a steady oscillation about its equilibrium.

Applying this linear control law to the original nonlinear system yields similarly favorable results. Figures 4.22 and 4.23 show the response of the nonlinear system under the desired configuration and control; that is,  $\mathbf{q} = \mathbf{q}_d$  and  $\mathbf{u} = \mathbf{u}_d$ . In this case, the bars are disturbed by a  $\delta\alpha$  and  $\delta\delta$  of  $1^\circ$ . Note that under these controls, the system remains in a state of neutral stability, where the response oscillates about the desired configuration  $\mathbf{q}_d$  but never converges to that equilibrium nor becomes unstable. Disturbing the system (in this case, the same perturbation that was applied to the linearized system; namely,  $\delta\alpha_1 = \delta\delta_1 = 0.1^\circ$ ,  $\delta\alpha_2 = \delta\delta_2 = 0.2^\circ$ , and  $\delta\alpha_3 = \delta\delta_3 = 0.3^\circ$ ) and applying the linear control law developed using LQR *does* return the system to its equilibrium, as shown in Figures 4.24 and 4.25. Because it is a linear control being applied to a nonlinear system, this control will only work for small disturbances of the nonlinear system from its equilibrium. Larger disturbances will cause the system to become unstable.



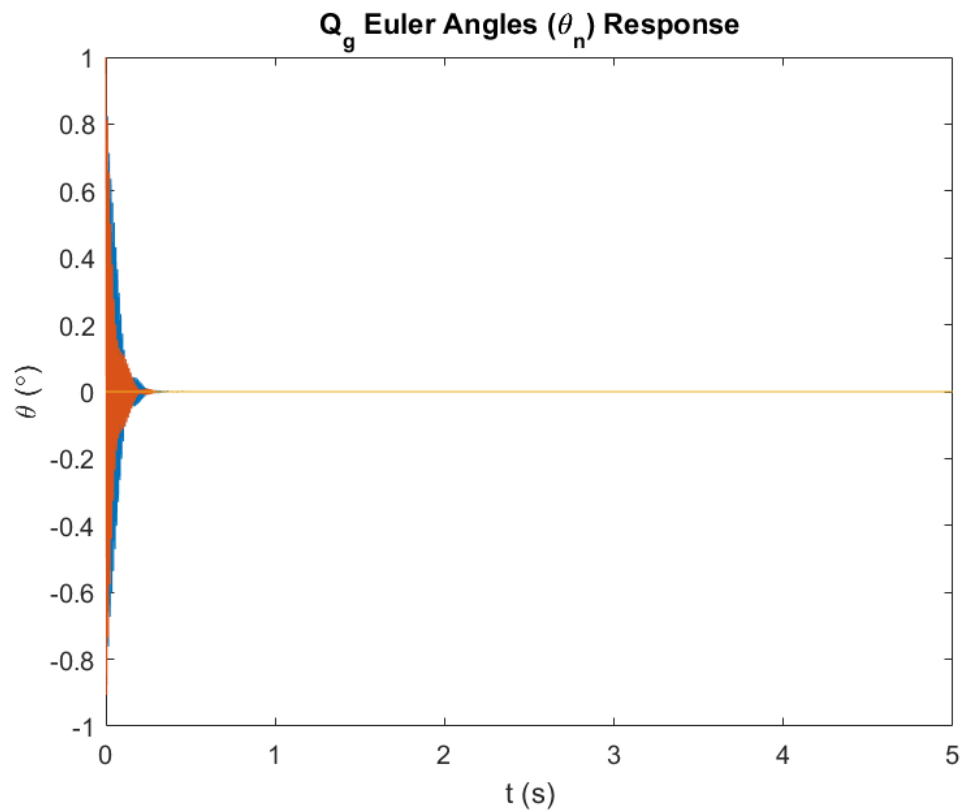


Figure 4.14: Response for the base attitude angles  $\theta_1, \theta_2, \theta_3$  for their perturbation from equilibrium of  $1^\circ$ . The base is quickly returned to equilibrium by the thruster controls.

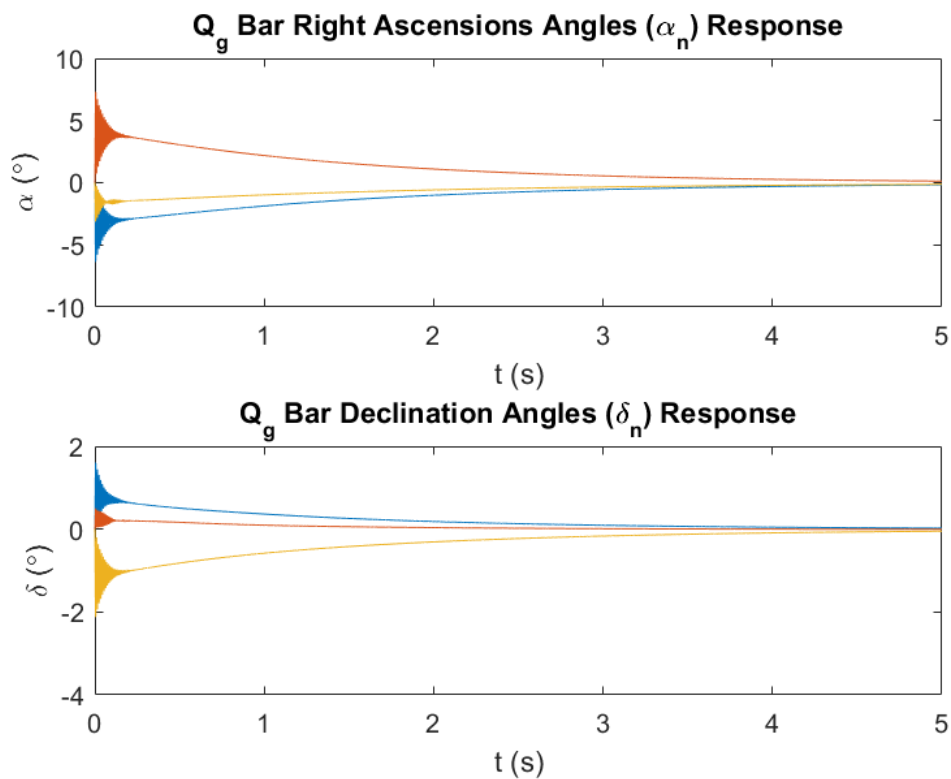


Figure 4.15: Response for the bar orientation angles  $\alpha_{1,2,3}$  and  $\delta_{1,2,3}$  for the perturbed attitude angles. Although the bars are not initially perturbed, their motion is affected by the oscillation of the base. Note how the response of the bars follows that of the base. When the base finally stills about its equilibrium, it is no longer affecting the bars, and therefore the bars stop oscillating as well.

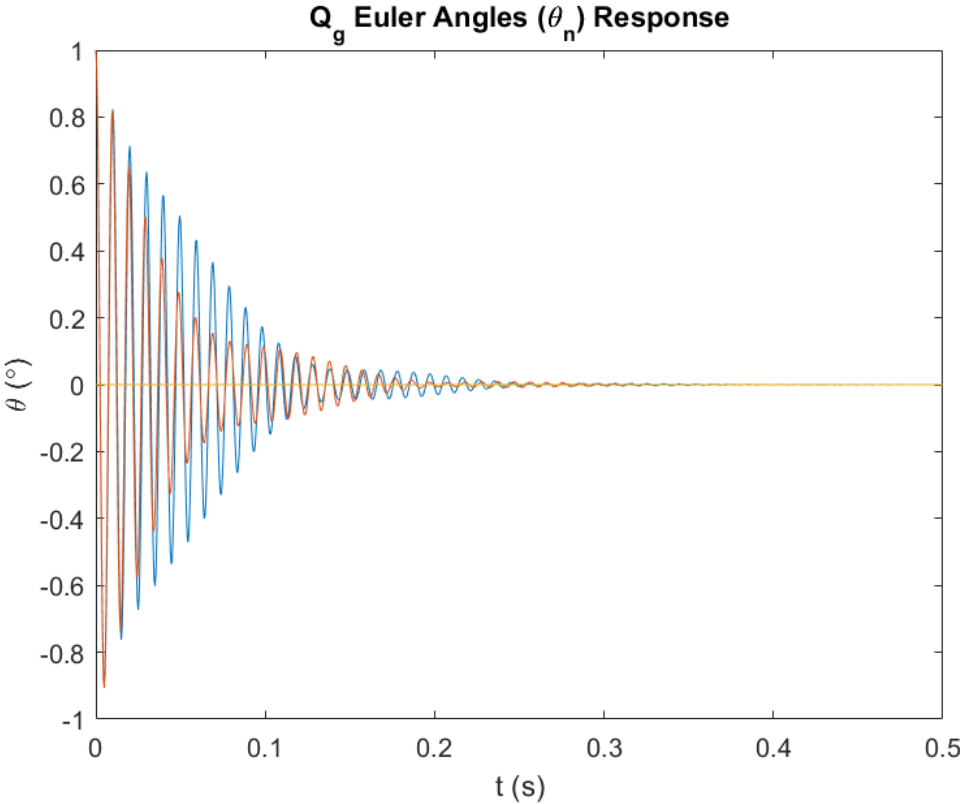


Figure 4.16: Zoomed into initial response of Figure 4.14.

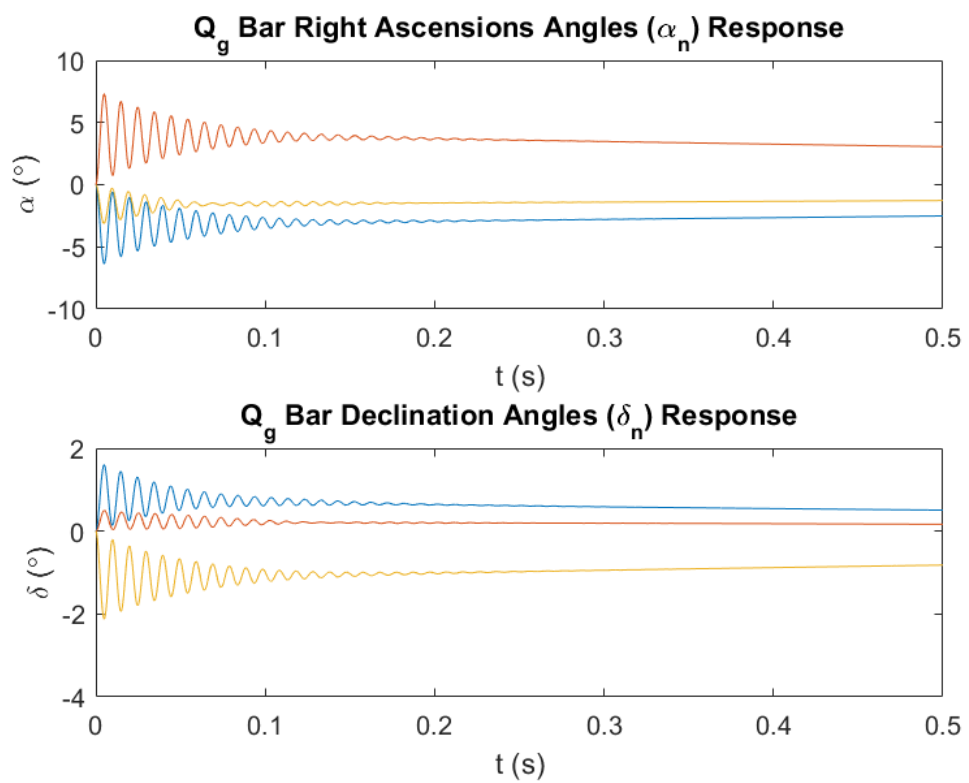


Figure 4.17: Zoomed into initial response of Figure 4.15.

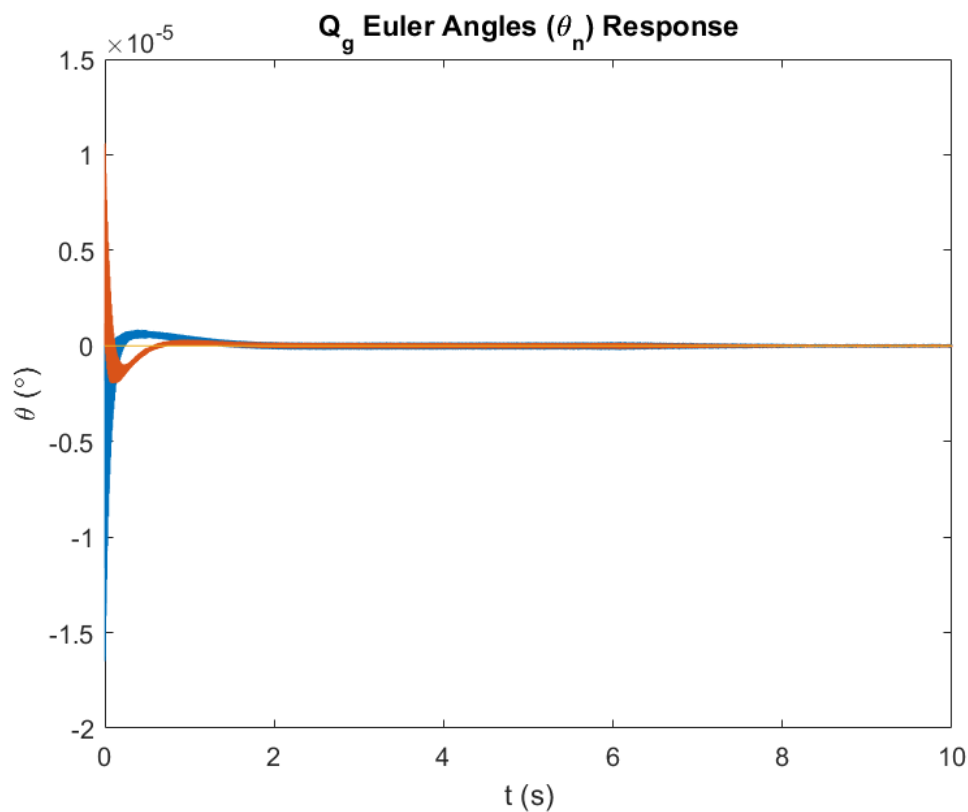


Figure 4.18: Response for the base attitude angles  $\theta_1$ ,  $\theta_2$ ,  $\theta_3$  for the perturbed bar orientation angles. The steady state response of the base is a continuous oscillation about its equilibrium, which is due to the thruster controls constantly making minute adjustments to the base as it moves about the Earth. The increase in amplitude towards the beginning of the time frame is due to the movement of the bars upon the base, as they work to return from their initial perturbation back to their equilibrium state.

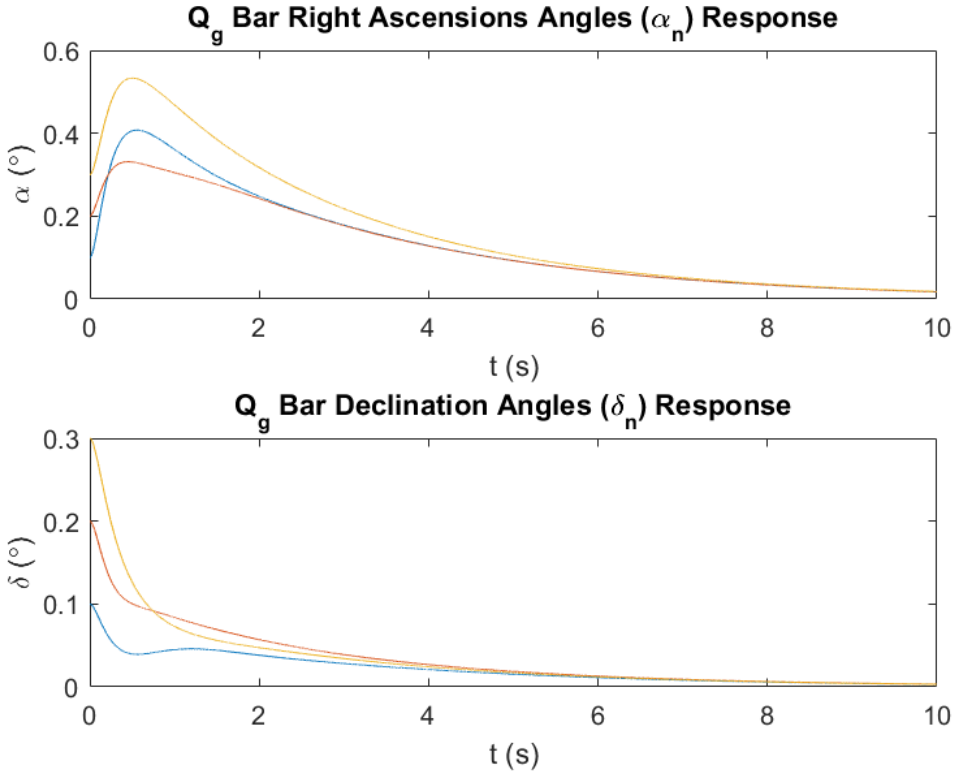


Figure 4.19: Response for  $\alpha_{1,2,3}$  and  $\delta_{1,2,3}$  for a perturbation of  $\{0.1, 0.2, 0.3\}^\circ$ , respectively. The bars are quickly returned to their equilibrium configuration.

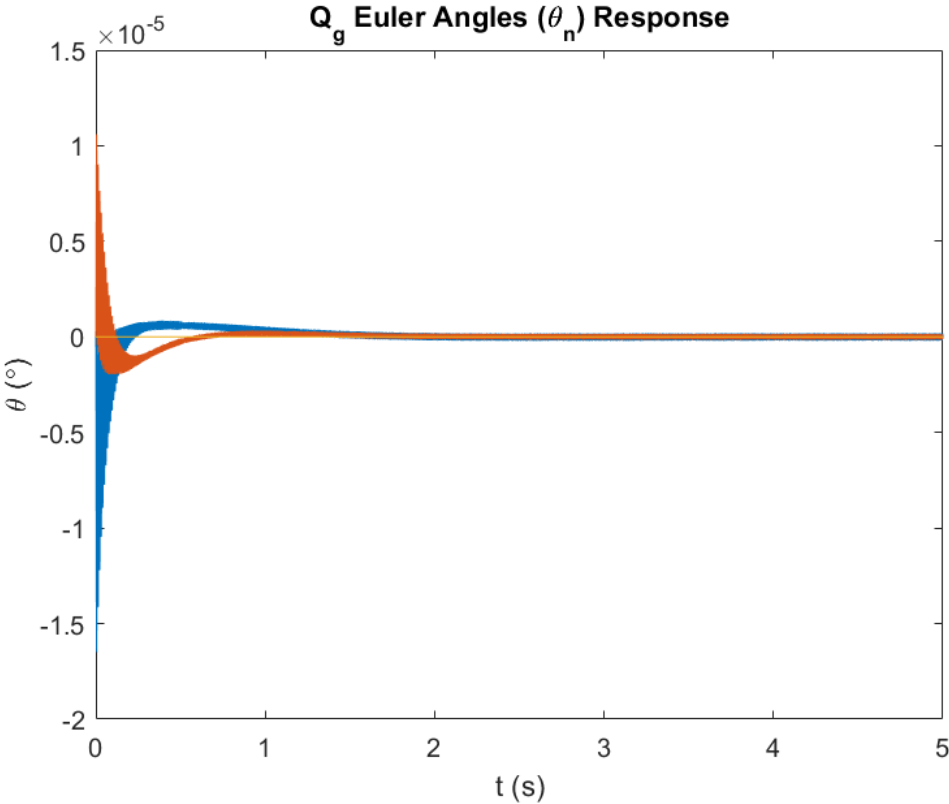


Figure 4.20: Zoomed into initial response of Figure 4.18.

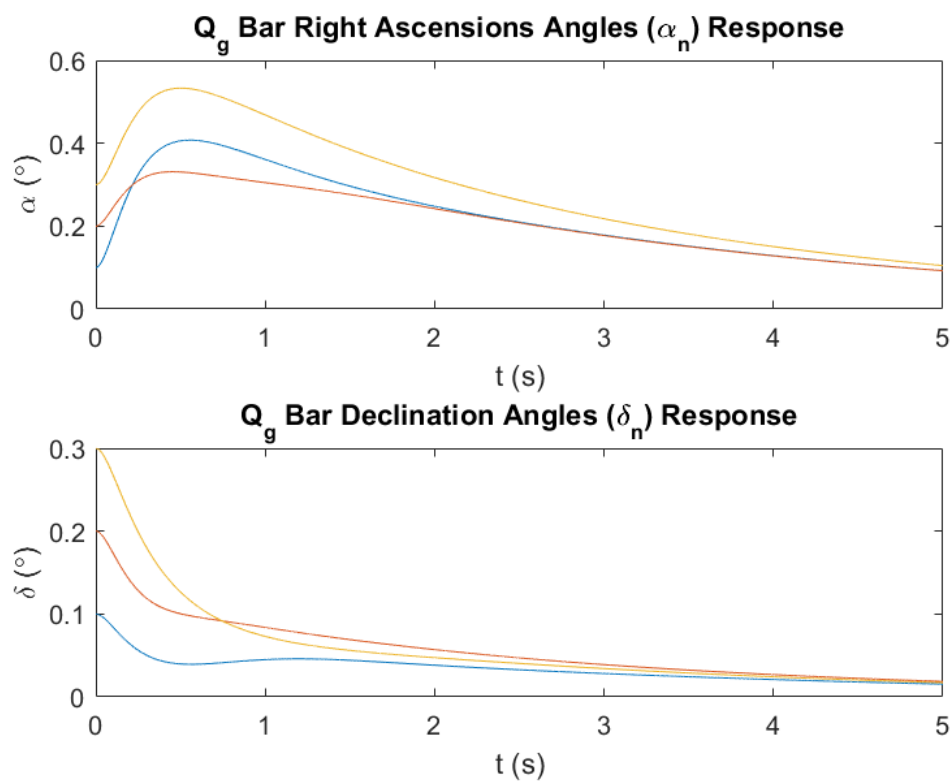


Figure 4.21: Zoomed into initial response of Figure 4.19.



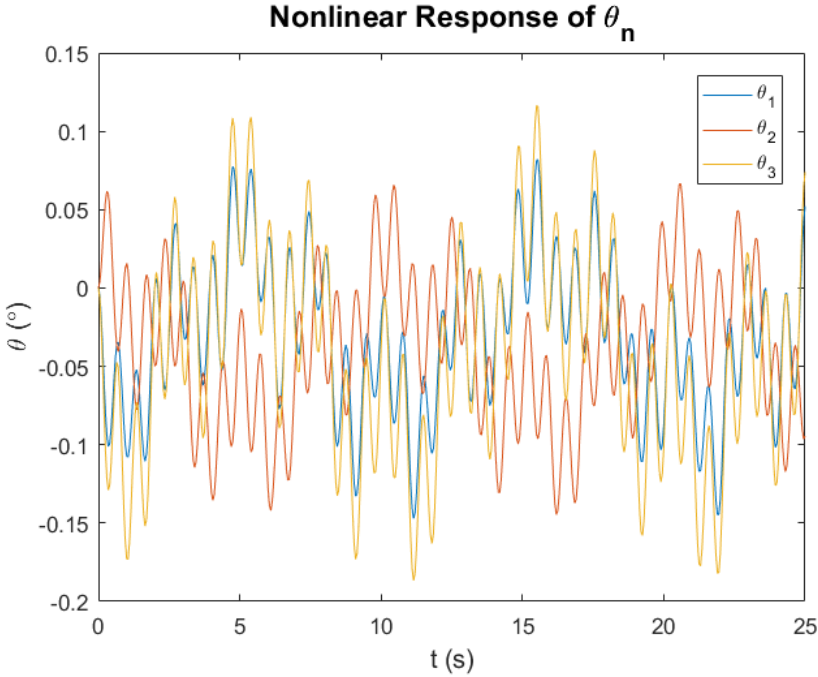


Figure 4.22: Response for the base attitude angles  $\theta_1, \theta_2, \theta_3$  at the desired configuration. The sharper oscillations are due to the response of the bars that sit atop the base.

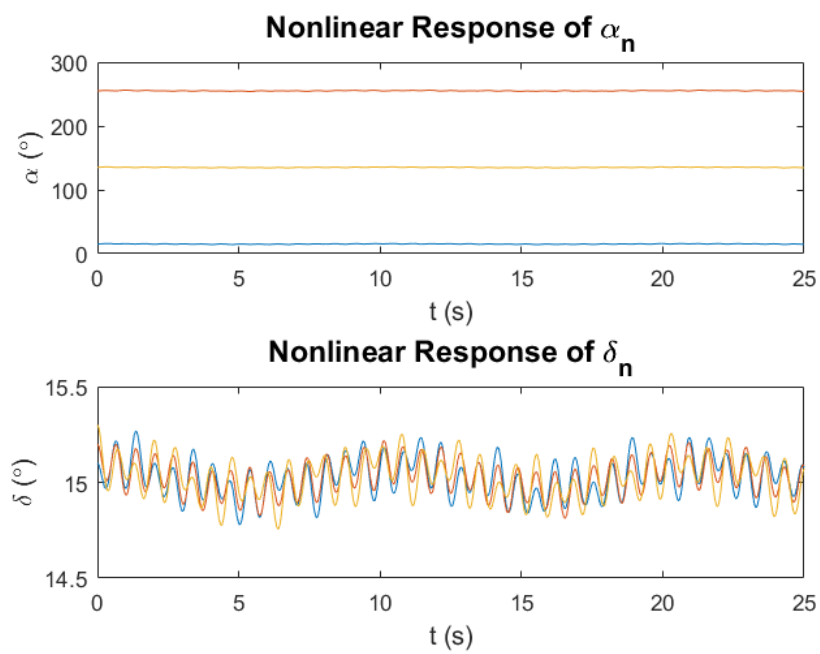


Figure 4.23: Response for the bar orientation angles  $\alpha_{1,2,3}$  and  $\delta_{1,2,3}$  at the desired configuration. Note that the bars oscillate along with the oscillating base.

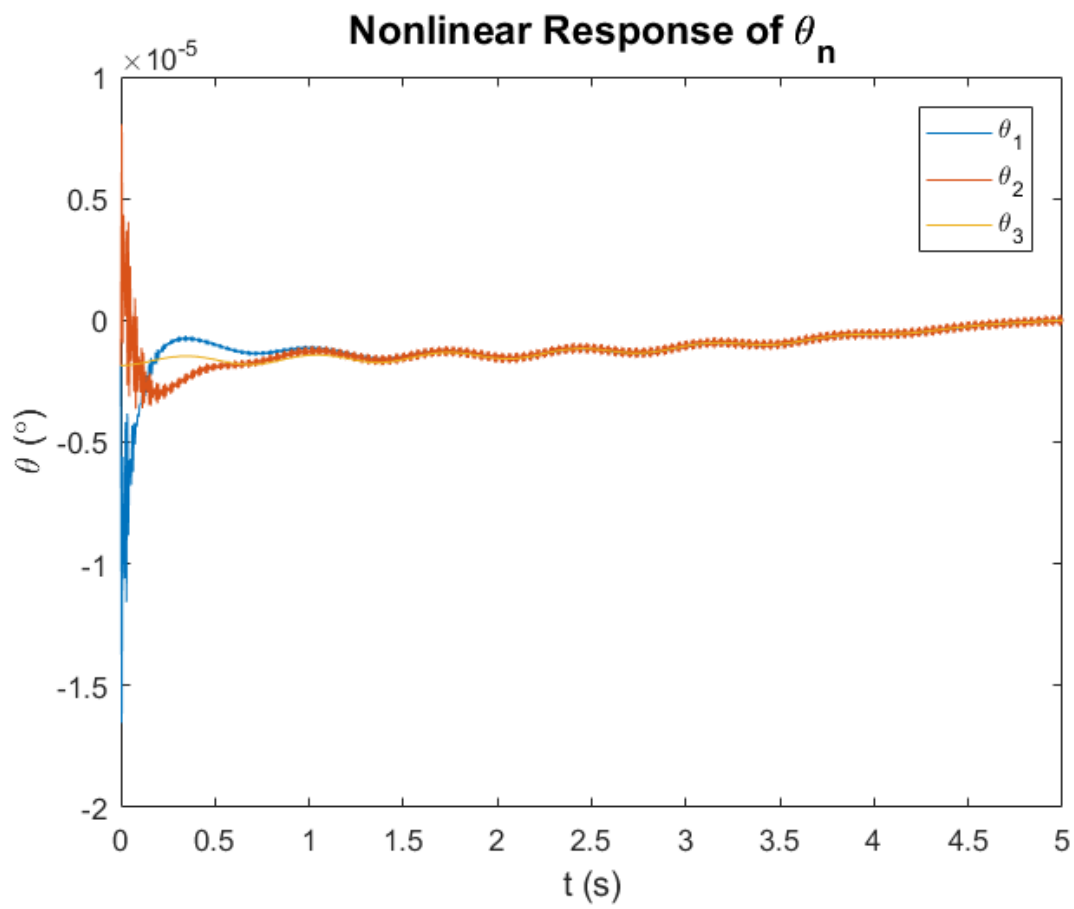


Figure 4.24: Nonlinear response for the base attitude angles  $\theta_1, \theta_2, \theta_3$  due to the perturbed bars under the LQR control law.

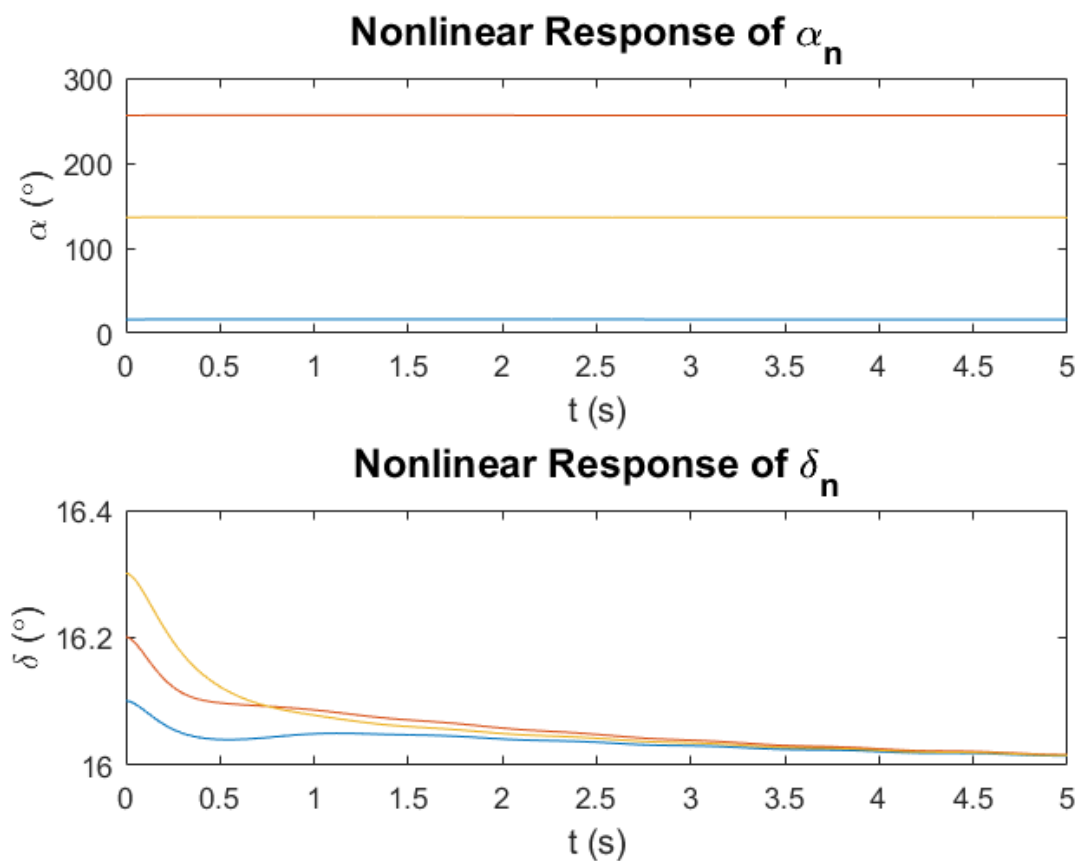


Figure 4.25: Nonlinear response for the bar orientation angles  $\alpha_{1,2,3}$  and  $\delta_{1,2,3}$  perturbed from the desired configuration by  $\{0.1, 0.2, 0.3\}^{\circ}$  for the first, second, and third bar angles, respectively. Note that the bars oscillate along with the oscillating base.

### 4.3 6-Bar Tensegrity Structure

This section derives the dynamics of the 6-bar tensegrity spacecraft depicted in Figure 4.26.

Begin by considering the bar shown in Figure 4.27. The position vector of the base mass center in the Earth-centered inertial frame  $\{\mathbf{i}\}$  is

$$\mathbf{R} = R \begin{bmatrix} \cos \lambda \cos \phi \\ \sin \lambda \cos \phi \\ \sin \phi \end{bmatrix}. \quad (4.180)$$

The rotation matrix from  $\{\mathbf{i}\}$  to the trajectory frame  $\{\mathbf{o}\}$  is

$$\mathbf{R}^{oi} = \mathbf{R}_2(\pi/2 - \phi)\mathbf{R}_3(\lambda). \quad (4.181)$$

The rotation matrix from the base body frame  $\{\mathbf{b}\}$  to  $\{\mathbf{o}\}$  is

$$\mathbf{R}^{ob} = \mathbf{R}_3(\theta_3)\mathbf{R}_2(\theta_2)\mathbf{R}_1(\theta_1) \quad (4.182)$$

The position vector between the mass centers of the base and the  $i$ th bar is

$$\mathbf{r}_i^b = \overline{\mathbf{BA}}_i + \overline{\mathbf{A}_i\mathbf{C}_i}. \quad (4.183)$$

For bars 1 through 3, which are attached to the surface of the base,  $\overline{\mathbf{BA}}_i$  will be constant:

$$\overline{\mathbf{BA}}_1^b = \frac{1}{2} \begin{bmatrix} -D_1 \\ -D_2 \\ D_3 \end{bmatrix} \quad \overline{\mathbf{BA}}_2^b = \frac{1}{2} \begin{bmatrix} 0 \\ D_2 \\ D_3 \end{bmatrix} \quad \overline{\mathbf{BA}}_3^b = \frac{1}{2} \begin{bmatrix} D_1 \\ -D_2 \\ D_3 \end{bmatrix}. \quad (4.184)$$

For bars 4 through 6, the  $\overline{\mathbf{BA}}_{4 \rightarrow 6}$  can be expressed in the base frame  $\{\mathbf{b}\}$  as

$$\overline{\mathbf{BA}}_4^b = \frac{1}{2} \begin{bmatrix} x_4 \\ -y_4 \\ x_4 \end{bmatrix} \quad \overline{\mathbf{BA}}_5^b = \frac{1}{2} \begin{bmatrix} x_5 \\ y_5 \\ z_5 \end{bmatrix} \quad \overline{\mathbf{BA}}_6^b = \frac{1}{2} \begin{bmatrix} x_6 \\ y_6 \\ z_6 \end{bmatrix}, \quad (4.185)$$

where  $x_i$ ,  $y_i$ , and  $z_i$  change with time.

The vector from the bar ends to the center of mass of the bars is given for the  $i$ th bar by

$\overline{\mathbf{A}_i \mathbf{C}_i}$  in the  $\{\mathbf{b}\}$  frame as

$$\overline{\mathbf{A}_i \mathbf{C}_i}^b = \frac{L_i}{2} \begin{bmatrix} \cos \alpha_i \sin \delta_i \\ \sin \alpha_i \sin \delta_i \\ \cos \delta_i \end{bmatrix}. \quad (4.186)$$

The angles  $\alpha_i$  and  $\delta_i$  define the orientation of the bar with respect to the  $\{\mathbf{b}\}$  frame. Defining a new body frame  $\{\mathbf{c}\}$  centered on each bar mass center and aligned with the bar principal axes, the transformation to  $\{\mathbf{c}\}$  from the base frame is

$$\mathbf{R}^{cb} = \mathbf{R}_2(\delta_i) \mathbf{R}_3(\alpha_i). \quad (4.187)$$

A set of independent generalized coordinates can be extracted from the above analysis for the base and three bars, and consolidated into the vector

$$\mathbf{q} = [R \ \lambda \ \phi \ \theta_1 \ \theta_2 \ \theta_3 \ x_4 \ y_4 \ z_4 \ x_5 \ y_5 \ z_5 \ x_6 \ y_6 \ z_6 \ \dots \\ \alpha_1 \ \delta_1 \ \alpha_2 \ \delta_2 \ \alpha_3 \ \delta_3 \ \alpha_4 \ \delta_4 \ \alpha_5 \ \delta_5 \ \alpha_6 \ \delta_6]^T \quad (4.188)$$

Choosing to use the force-based approach to determining the gravitational effects on the

system, the dynamics equations of a 3-bar system are

$$\frac{d}{dt}(\nabla_{\dot{\mathbf{q}}}T) - \nabla_{\mathbf{q}}T = -\nabla_{\mathbf{q}}V_e + \mathbf{Q}_g + \mathbf{Q}_t. \quad (4.189)$$

The following sections derive the kinetic energy  $T$ , the gravitational generalized forces  $\mathbf{Q}_g$ , and the elastic potential energy  $V_e$  of this system. The thruster generalized forces were found in Section 4.1.

### 4.3.1 Kinetic Energy

For a system consisting of a base and six bars, the total kinetic energy is

$$T = \sum_{i=0}^6 \{T_T + T_R\}_i \quad (4.190)$$

where  $i = 0$  corresponds to the base and  $i = 1, 2, 3, 4, 5, 6$  to the six bars that make up the tensegrity structure. The kinetic energy for the base was already derived in Section 4.1; the following sections derive the kinetic energy for the three bars.

#### Bars Translational Kinetic Energy

The translational kinetic energy is

$$T_T = \sum_{i=1}^6 \frac{1}{2} \dot{\mathbf{r}}_i^T \mathbf{M}_i \dot{\mathbf{r}}_i, \quad (4.191)$$

where  $\mathbf{M}_i = m_i \mathbb{I}_{3 \times 3}$  is the mass matrix,  $m_i$  being the mass of the  $i$ th bar. The vector  $\dot{\mathbf{r}}_i$  of the bar is the translational velocity of the center of mass of the  $i$ th bar with respect to the

origin of the Earth inertial frame, and is equal to

$$\dot{\mathbf{r}}_i = \dot{\mathbf{r}}_0 + \overline{\mathbf{BC}}_i. \quad (4.192)$$

**TIER I** The derivation for the previous 3-bar system can be adapted to the lower level of the 6 bar system:

$$\begin{aligned} \dot{\mathbf{r}}_{i=1 \rightarrow 3} &= [\mathbf{r}_{0_R} \quad \mathbf{r}_{0_\lambda} + \mathbf{R}_\lambda^{ib} \overline{\mathbf{BC}}_i^b \quad \mathbf{r}_{0_\phi} + \mathbf{R}_\phi^{ib} \overline{\mathbf{BC}}_i^b \quad \mathbf{R}_{\theta_1}^{ib} \overline{\mathbf{BC}}_i^b \quad \mathbf{R}_{\theta_2}^{ib} \overline{\mathbf{BC}}_i^b \quad \mathbf{R}_{\theta_3}^{ib} \overline{\mathbf{BC}}_i^b \dots \\ &\mathbf{0}_{3 \times 9} \quad [\mathbf{W}]_i] \dot{\mathbf{q}} \end{aligned} \quad (4.193)$$

where

$$\begin{aligned} [\mathbf{W}]_1 &= [\mathbf{R}^{ib} \overline{\mathbf{A}}_1 \mathbf{C}_{1\alpha_1}^b \quad \mathbf{R}^{ib} \overline{\mathbf{A}}_1 \mathbf{C}_{1\delta_1}^b \quad \mathbf{0}_{3 \times 2} \quad \mathbf{0}_{3 \times 2} \quad \mathbf{0}_{3 \times 6}] \\ [\mathbf{W}]_2 &= [\mathbf{0}_{3 \times 2} \quad \mathbf{R}^{ib} \overline{\mathbf{A}}_2 \mathbf{C}_{2\alpha_2}^b \quad \mathbf{R}^{ib} \overline{\mathbf{A}}_2 \mathbf{C}_{2\delta_2}^b \quad \mathbf{0}_{3 \times 2} \quad \mathbf{0}_{3 \times 6}] \\ [\mathbf{W}]_3 &= [\mathbf{0}_{3 \times 2} \quad \mathbf{0}_{3 \times 2} \quad \mathbf{R}^{ib} \overline{\mathbf{A}}_3 \mathbf{C}_{3\alpha_3}^b \quad \mathbf{R}^{ib} \overline{\mathbf{A}}_3 \mathbf{C}_{3\delta_3}^b \quad \mathbf{0}_{3 \times 6}] \end{aligned} \quad (4.194)$$

**TIER II** Now derive the translational velocity of the bars in the second tier. Begin with

$$\dot{\mathbf{r}}_{i=4 \rightarrow 6} = \dot{\mathbf{r}}_0 + \overline{\mathbf{BC}}_i = \dot{\mathbf{r}}_0 + \overline{\mathbf{BA}}_i + \overline{\mathbf{A}_i \mathbf{C}_i}. \quad (4.195)$$

Note that  $\dot{\mathbf{r}}_i$  is in the inertial reference frame. The following rotation matrix is used to rotate vectors expressed in the  $\{\mathbf{b}\}$  frame to the inertial frame:

$$\mathbf{R}^{ib} = \mathbf{R}^{io} \mathbf{R}^{ob} \mathbf{R}^{bs} = \mathbf{R}_3^T(\lambda) \mathbf{R}_2^T(\pi/2 - \phi) \mathbf{R}_3(\theta_3) \mathbf{R}_2(\theta_2) \mathbf{R}_1(\theta_1). \quad (4.196)$$

Incorporating this rotation into the expression for  $\dot{\mathbf{r}}_i$  and employing the chain rule for differential equations yields

$$\dot{\mathbf{r}}_{i=4 \rightarrow 6} = \dot{\mathbf{r}}_0 + \mathbf{R}^{ib} \frac{d}{dt}(\overline{\mathbf{BA}}_i^b) + \frac{d}{dt}(\mathbf{R}^{ib}) \overline{\mathbf{BA}}_i^b + \frac{d}{dt}(\mathbf{R}^{ib}) \overline{\mathbf{A}_i \mathbf{C}_i}^b + \mathbf{R}^{ib} \frac{d}{dt}(\overline{\mathbf{A}_i \mathbf{C}_i}^b). \quad (4.197)$$



The time derivative of the rotation matrix  $\mathbf{R}^{ib}$  is

$$\frac{d}{dt}\mathbf{R}^{ib} = \dot{\lambda}\mathbf{R}_{\lambda}^{ib} + \dot{\phi}\mathbf{R}_{\phi}^{ib} + \dot{\theta}_1\mathbf{R}_{\theta_1}^{ib} + \dot{\theta}_2\mathbf{R}_{\theta_2}^{ib} + \dot{\theta}_3\mathbf{R}_{\theta_3}^{ib} \quad (4.198)$$

where  $\mathbf{R}_{*}^{ib}$  is the partial derivative of the rotation matrix  $\mathbf{R}^{ib}$  with respect to the variable

(\*)). The time derivatives of the vectors  $\overline{\mathbf{BA}}_i$  and  $\overline{\mathbf{A}_i\mathbf{C}_i}$  are

$$\frac{d}{dt}(\overline{\mathbf{BA}}_i^b) = \dot{x}_i\overline{\mathbf{BA}}_{ix_i}^b + \dot{y}_i\overline{\mathbf{BA}}_{iy_i}^b + \dot{z}_i\overline{\mathbf{BA}}_{iz_i}^b \quad (4.199)$$

and

$$\frac{d}{dt}(\overline{\mathbf{A}_i\mathbf{C}_i}^b) = \dot{\alpha}_i\overline{\mathbf{A}_i\mathbf{C}_i}_{\alpha_i}^b + \dot{\delta}_i\overline{\mathbf{A}_i\mathbf{C}_i}_{\delta_i}^b, \quad (4.200)$$

where  $\overline{\mathbf{BA}}_{ix_i}^b$ ,  $\overline{\mathbf{BA}}_{iy_i}^b$ , and  $\overline{\mathbf{BA}}_{iz_i}^b$  are the partial derivatives of  $\overline{\mathbf{BA}}_i^b$  with respect to  $x_i$ ,  $y_i$ , and  $z_i$  for the  $i$ th bar, and  $\overline{\mathbf{A}_i\mathbf{C}_i}_{\alpha_i}^b$  and  $\overline{\mathbf{A}_i\mathbf{C}_i}_{\delta_i}^b$  are the partial derivatives of  $\overline{\mathbf{A}_i\mathbf{C}_i}^s$  with respect to  $\alpha_i$  and  $\delta_i$ . Substituting expressions and collecting terms yields

$$\begin{aligned} \dot{\mathbf{r}}_{i=4 \rightarrow 6} &= [\mathbf{r}_{0R} \quad \mathbf{r}_{0\lambda} + \mathbf{R}_{\lambda}^{is}\overline{\mathbf{BC}}_i^b \quad \mathbf{r}_{0\phi} + \mathbf{R}_{\phi}^{ib}\overline{\mathbf{BC}}_i^b \quad \mathbf{R}_{\theta_1}^{ib}\overline{\mathbf{BC}}_i^b \quad \mathbf{R}_{\theta_2}^{ib}\overline{\mathbf{BC}}_i^b \quad \mathbf{R}_{\theta_3}^{ib}\overline{\mathbf{BC}}_i^b \quad \dots \\ &[\mathbf{X}]_i \quad [\mathbf{W}]_i] \dot{\mathbf{q}} \end{aligned} \quad (4.201)$$

where

$$\begin{aligned} [\mathbf{X}]_4 &= [\mathbf{R}^{ib}\overline{\mathbf{BA}}_{4x_4}^b \quad \mathbf{R}^{ib}\overline{\mathbf{BA}}_{4y_4}^b \quad \mathbf{R}^{ib}\overline{\mathbf{BA}}_{4z_4}^b \quad \mathbf{0}_{3 \times 3} \quad \mathbf{0}_{3 \times 3}] \\ [\mathbf{X}]_5 &= [\mathbf{0}_{3 \times 3} \quad \mathbf{R}^{ib}\overline{\mathbf{BA}}_{5x_5}^b \quad \mathbf{R}^{ib}\overline{\mathbf{BA}}_{5y_5}^b \quad \mathbf{R}^{ib}\overline{\mathbf{BA}}_{5z_5}^b \quad \mathbf{0}_{3 \times 3}] \\ [\mathbf{X}]_6 &= [\mathbf{0}_{3 \times 3} \quad \mathbf{0}_{3 \times 3} \quad \mathbf{R}^{ib}\overline{\mathbf{BA}}_{6x_6}^b \quad \mathbf{R}^{ib}\overline{\mathbf{BA}}_{6y_6}^b \quad \mathbf{R}^{ib}\overline{\mathbf{BA}}_{6z_6}^b] \end{aligned} \quad (4.202)$$

and

$$[\mathbf{W}]_4 = [\mathbf{0}_{3 \times 6} \quad \mathbf{R}^{is}\overline{\mathbf{A}_4\mathbf{C}_4}_{\alpha_4}^s \quad \mathbf{R}^{is}\overline{\mathbf{A}_4\mathbf{C}_4}_{\delta_4}^s \quad \mathbf{0}_{3 \times 2} \quad \mathbf{0}_{3 \times 2}]$$

$$[\mathbf{W}]_5 = [\mathbf{0}_{3 \times 6} \quad \mathbf{0}_{3 \times 2} \quad \mathbf{R}^{is} \overline{\mathbf{A}_5 \mathbf{C}_{5\alpha_5}^s} \quad \mathbf{R}^{is} \overline{\mathbf{A}_5 \mathbf{C}_{5\delta_5}^s} \quad \mathbf{0}_{3 \times 2}] \quad (4.203)$$

$$[\mathbf{W}]_6 = [\mathbf{0}_{3 \times 6} \quad \mathbf{0}_{3 \times 2} \quad \mathbf{0}_{3 \times 2} \quad \mathbf{R}^{is} \overline{\mathbf{A}_6 \mathbf{C}_{6\alpha_6}^s} \quad \mathbf{R}^{is} \overline{\mathbf{A}_6 \mathbf{C}_{6\delta_6}^s}]$$

**COMBINE TIERS** Recall that the time derivative of the position vector  $\dot{\mathbf{r}}_i$  can be written as

$$\dot{\mathbf{r}}_i = [\mathbf{P}_i(\mathbf{q})] \dot{\mathbf{q}} \quad (4.204)$$

which is substituted into Eq. (4.191) to yield the total translational kinetic energy

$$\begin{aligned} T_T &= \frac{1}{2} \dot{\mathbf{q}}^T [\mathbf{P}_1(\mathbf{q})]^T \mathbf{M}_1 [\mathbf{P}_1(\mathbf{q})] \dot{\mathbf{q}} + \frac{1}{2} \dot{\mathbf{q}}^T [\mathbf{P}_2(\mathbf{q})]^T \mathbf{M}_2 [\mathbf{P}_2(\mathbf{q})] \dot{\mathbf{q}} \dots \\ &\quad + \frac{1}{2} \dot{\mathbf{q}}^T [\mathbf{P}_3(\mathbf{q})]^T \mathbf{M}_3 [\mathbf{P}_3(\mathbf{q})] \dot{\mathbf{q}} + \frac{1}{2} \dot{\mathbf{q}}^T [\mathbf{P}_4(\mathbf{q})]^T \mathbf{M}_4 [\mathbf{P}_4(\mathbf{q})] \dot{\mathbf{q}} \dots \\ &\quad + \frac{1}{2} \dot{\mathbf{q}}^T [\mathbf{P}_5(\mathbf{q})]^T \mathbf{M}_5 [\mathbf{P}_5(\mathbf{q})] \dot{\mathbf{q}} + \frac{1}{2} \dot{\mathbf{q}}^T [\mathbf{P}_6(\mathbf{q})]^T \mathbf{M}_6 [\mathbf{P}_6(\mathbf{q})] \dot{\mathbf{q}} \\ &= \frac{1}{2} \dot{\mathbf{q}}^T \{ [\mathbf{P}_1(\mathbf{q})]^T \mathbf{M}_1 [\mathbf{P}_1(\mathbf{q})] + [\mathbf{P}_2(\mathbf{q})]^T \mathbf{M}_2 [\mathbf{P}_2(\mathbf{q})] + [\mathbf{P}_3(\mathbf{q})]^T \mathbf{M}_3 [\mathbf{P}_3(\mathbf{q})] \dots \\ &\quad + [\mathbf{P}_4(\mathbf{q})]^T \mathbf{M}_4 [\mathbf{P}_4(\mathbf{q})] + [\mathbf{P}_5(\mathbf{q})]^T \mathbf{M}_5 [\mathbf{P}_5(\mathbf{q})] + [\mathbf{P}_6(\mathbf{q})]^T \mathbf{M}_6 [\mathbf{P}_6(\mathbf{q})] \} \dot{\mathbf{q}} \\ &= \frac{1}{2} \dot{\mathbf{q}}^T \left\{ \sum_{i=1}^6 [\mathbf{P}_i(\mathbf{q})]^T \mathbf{M}_i [\mathbf{P}_i(\mathbf{q})] \right\} \dot{\mathbf{q}} \quad (4.205) \end{aligned}$$

### Bars Rotational Kinetic Energy

The total rotational energy of the bars is expressed as

$$T_R = \sum_{i=1}^3 \frac{1}{2} \boldsymbol{\omega}_i^T \mathbf{J}_i \boldsymbol{\omega}_i \quad (4.206)$$

where  $\mathbf{J}_i$  is the moment of inertia matrix of the  $i$ th bar.

The rotational velocity of the first tier bars have previously been derived to be

$$\begin{aligned}
 \boldsymbol{\omega}_{i=1 \rightarrow 3} = & \begin{bmatrix} 0 & 0 \\ 0 & -1 \\ \sin \delta_i & 0 \end{bmatrix} \begin{bmatrix} \dot{\alpha}_i \\ \dot{\delta}_i \end{bmatrix} + \mathbf{R}_2(\delta_i) \mathbf{R}_3(\alpha_i) \mathbf{S}(\boldsymbol{\theta}) \begin{bmatrix} \dot{\theta}_1 \\ \dot{\theta}_2 \\ \dot{\theta}_3 \end{bmatrix} \dots \\
 & + \mathbf{R}_2(\delta_i) \mathbf{R}_3(\alpha_i) \mathbf{R}_1^T(\theta_1) \mathbf{R}_2^T(\theta_2) \mathbf{R}_3^T(\theta_3) \begin{bmatrix} 0 & 0 & 0 \\ 0 & 0 & \cos \phi \\ 0 & -1 & 0 \end{bmatrix} \begin{bmatrix} \dot{R} \\ \dot{\lambda} \\ \dot{\phi} \end{bmatrix} \quad (4.207)
 \end{aligned}$$

which, simplifying notation, yields

$$\boldsymbol{\omega}_{i=1 \rightarrow 6} = \mathbf{K}_3 \dot{\mathbf{q}}_{(14+2i) \rightarrow (15+2i)} + \mathbf{K}_2 \dot{\mathbf{q}}_{4 \rightarrow 6} + \mathbf{K}_1 \dot{\mathbf{q}}_{1 \rightarrow 3}. \quad (4.208)$$

The terms can be combined into

$$\boldsymbol{\omega}_{i=1 \rightarrow 6} = [\mathbf{S}_i(\mathbf{q})] \dot{\mathbf{q}} \quad (4.209)$$

where

$$\begin{aligned}
 [\mathbf{S}_1(\mathbf{q})] &= [\mathbf{K}_1 \quad \mathbf{K}_2 \quad \mathbf{0}_{3 \times 12} \quad \mathbf{K}_3 \quad \mathbf{0}_{3 \times 2} \quad \mathbf{0}_{3 \times 2} \quad \mathbf{0}_{3 \times 6}] \\
 [\mathbf{S}_2(\mathbf{q})] &= [\mathbf{K}_1 \quad \mathbf{K}_2 \quad \mathbf{0}_{3 \times 12} \quad \mathbf{0}_{3 \times 2} \quad \mathbf{K}_3 \quad \mathbf{0}_{3 \times 2} \quad \mathbf{0}_{3 \times 6}] \quad (4.210)
 \end{aligned}$$

$$\begin{aligned}
 [\mathbf{S}_3(\mathbf{q})] &= [\mathbf{K}_1 \quad \mathbf{K}_2 \quad \mathbf{0}_{3 \times 12} \quad \mathbf{0}_{3 \times 2} \quad \mathbf{0}_{3 \times 2} \quad \mathbf{K}_3 \quad \mathbf{0}_{3 \times 6}] \\
 [\mathbf{S}_4(\mathbf{q})] &= [\mathbf{K}_1 \quad \mathbf{K}_2 \quad \mathbf{0}_{3 \times 12} \quad \mathbf{0}_{3 \times 6} \quad \mathbf{K}_3 \quad \mathbf{0}_{3 \times 2} \quad \mathbf{0}_{3 \times 2}] \\
 [\mathbf{S}_5(\mathbf{q})] &= [\mathbf{K}_1 \quad \mathbf{K}_2 \quad \mathbf{0}_{3 \times 12} \quad \mathbf{0}_{3 \times 6} \quad \mathbf{0}_{3 \times 2} \quad \mathbf{K}_3 \quad \mathbf{0}_{3 \times 2}] \quad (4.211)
 \end{aligned}$$

$$[\mathbf{S}_6(\mathbf{q})] = [\mathbf{K}_1 \quad \mathbf{K}_2 \quad \mathbf{0}_{3 \times 12} \quad \mathbf{0}_{3 \times 6} \quad \mathbf{0}_{3 \times 2} \quad \mathbf{0}_{3 \times 2} \quad \mathbf{K}_3]$$

Thus, the total rotational kinetic energy of the bars becomes

$$\begin{aligned}
T_R &= \frac{1}{2} \dot{\mathbf{q}}^T [\mathbf{S}_1(\mathbf{q})]^T \mathbf{J}_1 [\mathbf{S}_1(\mathbf{q})] \dot{\mathbf{q}} + \frac{1}{2} \dot{\mathbf{q}}^T [\mathbf{S}_2(\mathbf{q})]^T \mathbf{J}_2 [\mathbf{S}_2(\mathbf{q})] \dot{\mathbf{q}} \dots \\
&+ \frac{1}{2} \dot{\mathbf{q}}^T [\mathbf{S}_3(\mathbf{q})]^T \mathbf{J}_3 [\mathbf{S}_3(\mathbf{q})] \dot{\mathbf{q}} + \frac{1}{2} \dot{\mathbf{q}}^T [\mathbf{S}_4(\mathbf{q})]^T \mathbf{J}_4 [\mathbf{S}_4(\mathbf{q})] \dot{\mathbf{q}} \dots \\
&+ \frac{1}{2} \dot{\mathbf{q}}^T [\mathbf{S}_5(\mathbf{q})]^T \mathbf{J}_5 [\mathbf{S}_5(\mathbf{q})] \dot{\mathbf{q}} + \frac{1}{2} \dot{\mathbf{q}}^T [\mathbf{S}_6(\mathbf{q})]^T \mathbf{J}_6 [\mathbf{S}_6(\mathbf{q})] \dot{\mathbf{q}} \quad (4.212)
\end{aligned}$$

$$\begin{aligned}
&= \frac{1}{2} \dot{\mathbf{q}}^T \{ \mathbf{S}_b(\mathbf{q}) \}_1^T \mathbf{J}_1 [\mathbf{S}_1(\mathbf{q})] + [\mathbf{S}_2(\mathbf{q})]^T \mathbf{J}_2 [\mathbf{S}_2(\mathbf{q})] + [\mathbf{S}_3(\mathbf{q})]^T \mathbf{J}_3 [\mathbf{S}_3(\mathbf{q})] \dots \\
&+ \mathbf{S}_b(\mathbf{q}) \}_4^T \mathbf{J}_4 [\mathbf{S}_4(\mathbf{q})] + [\mathbf{S}_5(\mathbf{q})]^T \mathbf{J}_5 [\mathbf{S}_5(\mathbf{q})] + [\mathbf{S}_6(\mathbf{q})]^T \mathbf{J}_6 [\mathbf{S}_6(\mathbf{q})] \} \dot{\mathbf{q}} \quad (4.213)
\end{aligned}$$

$$= \frac{1}{2} \dot{\mathbf{q}}^T \left\{ \sum_{i=1}^6 [\mathbf{S}_i(\mathbf{q})]^T \mathbf{J}_i [\mathbf{S}_i(\mathbf{q})] \right\} \dot{\mathbf{q}} \quad (4.214)$$

where  $\mathbf{J}_i = \text{diag}[\frac{m_i L_i^2}{12}, \frac{m_i L_i^2}{12}, 0]$ .

### Total Kinetic Energy

Recall the expression from Equation (2.21) for the total kinetic energy of the system:

$$T = \sum_{i=0}^3 \{ T_T + T_R \}_i \quad (4.215)$$

Substituting in the expressions for the kinetic energies derived for the base and the three bars, the kinetic energy becomes

$$\begin{aligned}
T &= \frac{1}{2} \dot{\mathbf{q}}^T [\mathbf{P}_0(\mathbf{q})]^T \mathbf{M}_0 [\mathbf{P}_0(\mathbf{q})] \dot{\mathbf{q}} + \frac{1}{2} \dot{\mathbf{q}}^T [\mathbf{S}_0(\mathbf{q})]^T \mathbf{J}_0 [\mathbf{S}_0(\mathbf{q})] \dot{\mathbf{q}} \dots \\
&+ \frac{1}{2} \dot{\mathbf{q}}^T \left\{ \sum_{i=1}^6 [\mathbf{P}_i(\mathbf{q})]^T \mathbf{M}_i [\mathbf{P}_i(\mathbf{q})] \right\} \dot{\mathbf{q}} + \frac{1}{2} \dot{\mathbf{q}}^T \left\{ \sum_{i=1}^6 [\mathbf{S}_i(\mathbf{q})]^T \mathbf{J}_i [\mathbf{S}_i(\mathbf{q})] \right\} \dot{\mathbf{q}} \quad (4.216)
\end{aligned}$$

$$= \frac{1}{2} \dot{\mathbf{q}}^T \left\{ \sum_{i=0}^6 [\mathbf{P}_i(\mathbf{q})]^T \mathbf{M}_i [\mathbf{P}_i(\mathbf{q})] + \sum_{i=0}^6 [\mathbf{S}_i(\mathbf{q})]^T \mathbf{J}_i [\mathbf{S}_i(\mathbf{q})] \right\} \dot{\mathbf{q}} \quad (4.217)$$

$$= \frac{1}{2} \dot{\mathbf{q}}^T \mathbf{M}(\mathbf{q}) \dot{\mathbf{q}} \quad (4.218)$$

which is in the form desired for implementing Lagrange's method.

### 4.3.2 Generalized Gravitational Forces

Start with a general expression for the generalized forces on the entire system:

$$\mathbf{Q}_g = \sum_{i=0}^6 \left[ \left( \frac{\partial \dot{\mathbf{r}}_i}{\partial \dot{\mathbf{q}}} \right)^T \mathbf{F}_{g_i} \right] + \sum_{i=0}^6 \left[ \left( \frac{\partial \boldsymbol{\omega}_i}{\partial \dot{\mathbf{q}}} \right)^T \mathbf{M}_{g_i} \right] \quad (4.219)$$

where  $\dot{\mathbf{r}}_i$  and  $\boldsymbol{\omega}_i$  are the translational and angular velocities of the  $i$ th body. The gravitational forces and moments,  $\mathbf{F}_{g_i}$  and  $\mathbf{M}_{g_i}$ , were previously found to be [34, 35]

$$\mathbf{F}_{g_i} = -\frac{\mu m}{R^2} \mathbf{o}_r - \frac{3\mu}{2R^4} [\text{tr}(\mathbf{J}_i) - 5\mathbf{o}_r^T \mathbf{J}_i \mathbf{o}_r] \mathbf{o}_r - \frac{3\mu}{R^4} \mathbf{J}_i \mathbf{o}_r \quad (4.220)$$

$$\mathbf{M}_{g_i} = \frac{3\mu}{R^3} \mathbf{o}_r^\times \mathbf{J}_i \mathbf{o}_r, \quad (4.221)$$

where  $\mathbf{o}_r$  is a unit vector that points along the direction of orbital radius vector  $\mathbf{r}_0$ , which also coincides with the third axis of the orbital frame  $\{\mathbf{o}\}$ . Following a process similar to that taken for the base, the generalized velocities for the  $i$ th body are

$$\frac{\partial \dot{\mathbf{r}}_i}{\partial \dot{\mathbf{q}}} = [\mathbf{P}_i(\mathbf{q})]. \quad (4.222)$$

A similar process is used to find that

$$\frac{\partial \boldsymbol{\omega}_i}{\partial \dot{\mathbf{q}}} = [\mathbf{S}_i(\mathbf{q})]. \quad (4.223)$$

Combining the above expressions, the generalized gravitational forces on the base become

$$\mathbf{Q}_g = \sum_{i=0}^6 [\mathbf{P}_i(\mathbf{q})]^T \mathbf{F}_{g_i} + \sum_{i=0}^6 [\mathbf{S}_i(\mathbf{q})]^T \mathbf{M}_{g_i}. \quad (4.224)$$

### 4.3.3 Tensegrity Elastic Potential Energy

The gradient of the elastic potential energy with respect to the generalized coordinates was previously derived as

$$\nabla_{\mathbf{q}} V_e = \mathbf{A}(\mathbf{q}) \mathbf{F}. \quad (4.225)$$

For a six bar system, not only does  $\mathbf{A}(\mathbf{q})$  depend on the orientation angles of the bars, but also on the position of the three bars in the top tier. The resulting matrix is

$$\mathbf{A}(\mathbf{q}) = \begin{bmatrix} \mathbf{0}_{12 \times 15} \\ \bar{\mathbf{A}} \end{bmatrix}. \quad (4.226)$$

The elements of  $\bar{\mathbf{A}}$  are

$$A_{kj} = \frac{\partial l_j}{\partial q_k}, \quad k = 15, \dots, 27, \quad j = 1, \dots, 12 \quad (4.227)$$

where  $l_j$  represents the length of the  $j$ th tendon. The vector  $\mathbf{F}$  of the force in the  $j$ th elastic tendons is defined by

$$F_j = \frac{k_j}{r_j} (l_j - r_j) \quad (4.228)$$

where  $k_j$  is the stiffness of the  $j$ th tendon and  $r_j$  are the rest lengths of the tendons, which also serve as the controls for the tensegrity structure.

### 4.3.4 Desired Configuration

Recall the generalized coordinates for a six-bar system:

$$\mathbf{q} = [R \ \lambda \ \phi \ \theta_1 \ \theta_2 \ \theta_3 \ x_4 \ y_4 \ z_4 \ x_5 \ y_5 \ z_5 \ x_6 \ y_6 \ z_6 \ \dots \\ \alpha_1 \ \delta_1 \ \alpha_2 \ \delta_2 \ \alpha_3 \ \delta_3 \ \alpha_4 \ \delta_4 \ \alpha_5 \ \delta_5 \ \alpha_6 \ \delta_6]^T \quad (4.229)$$

Constrict the spacecraft to follow a circular equatorial orbit, where

$$\phi = 90^\circ \quad (4.230)$$

and  $R$  is constant. Let the angular velocity of the base about the Earth be constant:

$$\dot{\lambda} = n = \sqrt{\mu/R^3} \quad (4.231)$$

Set Euler angles to zero so that  $\{\mathbf{b}\}$  remains coincident with  $\{\mathbf{o}\}$ :

$$\theta_1 = 0, \quad \theta_2 = 0, \quad \theta_3 = 0 \quad (4.232)$$

Choose the positions of the ends of the upper tier bars such that they are symmetric to the lower tier bars; that is:

$$\overline{\mathbf{BA}}_4^b = \frac{1}{2} \begin{bmatrix} -D_1 \\ -D_2 \\ Z \end{bmatrix} \quad \overline{\mathbf{BA}}_5^b = \frac{1}{2} \begin{bmatrix} 0 \\ D_2 \\ Z \end{bmatrix} \quad \overline{\mathbf{BA}}_6^b = \frac{1}{2} \begin{bmatrix} D_1 \\ -D_2 \\ Z \end{bmatrix} \quad (4.233)$$

where  $Z$  is the height of the end of the bars above the center of mass of the base, and are equal to each other. Choose  $Z$  such that it falls between the height of the lower tier bars and the maximum height of the tensegrity system, which is twice the height of the bars.

$$D_3/2 + L \cos \delta < Z < D_3/2 + 2L \cos \delta \quad (4.234)$$

where the value of  $\delta$  is discussed below. Choosing an arbitrary  $Z$  that meets these limits,

$$Z = D_3/2 + 3/2L \cos \delta \tag{4.235}$$

Lastly, the desired orientation of the bars that make up the tensegrity structure is chosen to have a symmetrical configuration. The lower three bars have the same declination  $\delta$ , and their right ascension is shifted by  $2\pi/3$ . [8] The  $\alpha$  of the upper bars is similarly shifted; the declination angle of all three is also equivalent. The resulting desired values for the orientation angles are therefore

$$\begin{aligned} & [\alpha_1 \ \delta_1 \ \alpha_2 \ \delta_2 \ \alpha_3 \ \delta_3 \ \alpha_4 \ \delta_4 \ \alpha_5 \ \delta_5 \ \alpha_6 \ \delta_6]^T \\ &= [\alpha \ \delta \ \alpha + \frac{4\pi}{3} \ \delta \ \alpha + \frac{2\pi}{3} \ \delta \ \alpha \ \pi - \delta \ \alpha + \frac{4\pi}{3} \ \pi - \delta \ \alpha + \frac{2\pi}{3} \ \pi - \delta]^T, \end{aligned} \tag{4.236}$$

where  $\alpha$  and  $\delta$  are chosen such that the tensegrity structure meets prestressability conditions; in this analysis, values of  $\alpha = \delta = \pi/12$  are chosen. Thus, the array of generalized coordinates for this desired configuration,  $\mathbf{q}_d$ , becomes:

$$\begin{aligned} \mathbf{q}_d = & [R \ 0 \ \lambda(t) \ 0 \ 0 \ 0 \ 0 \ 0 \ 0 \ Z \ 0 \ 0 \ Z \ 0 \ 0 \ Z \dots \\ & \frac{\pi}{12} \ \frac{\pi}{12} \ \frac{\pi}{12} + \frac{4\pi}{3} \ \frac{\pi}{12} \ \frac{\pi}{12} + \frac{2\pi}{3} \ \frac{\pi}{12} \dots \\ & \frac{\pi}{12} \ \pi - \frac{\pi}{12} \ \frac{\pi}{12} + \frac{4\pi}{3} \ \pi - \frac{\pi}{12} \ \frac{\pi}{12} + \frac{2\pi}{3} \ \pi - \frac{\pi}{12}]^T. \end{aligned} \tag{4.237}$$

The above derivation of the dynamics for a 6-bar tensegrity system are provided as a rough guide for managing increasingly complex tensegrity systems in a low-Earth gravitational field.



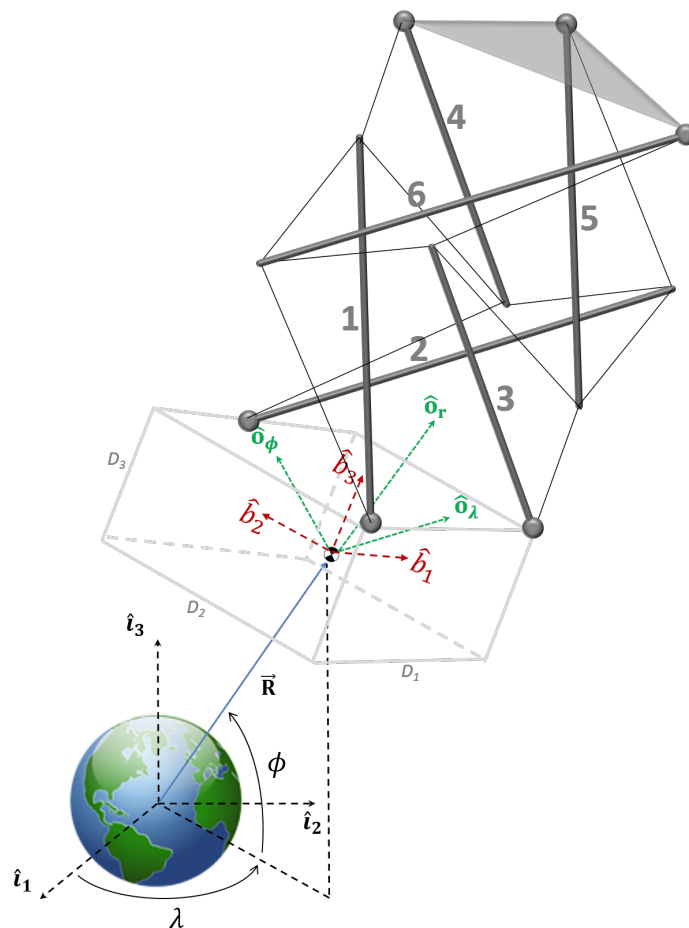


Figure 4.26: A slightly more complex tensegrity structure is one with 6 bars and 12 elastic tendons, where one of the ends of the lower bars are constrained to the base, and one of the ends of the upper bars are constrained to some massless plate. Both the bottom and top connection points form an equilateral triangle of the same size.

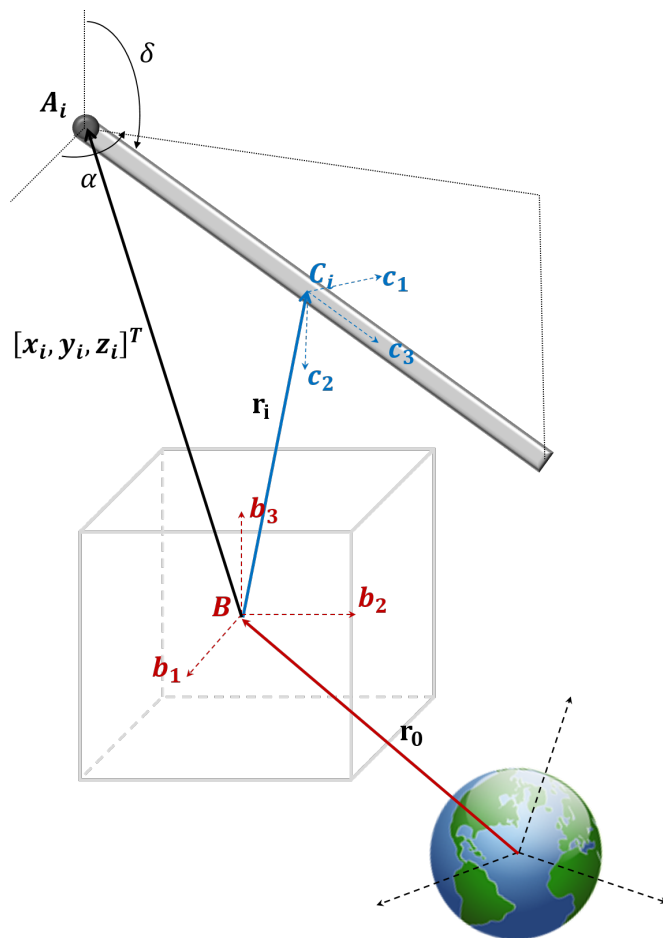


Figure 4.27: Position vectors to the center of mass of a bar not constrained to the base. The position of the bar relative to the base center of mass is given by the vector  $[x_i, y_i, z_i]^t$  that defines the location of one end of the bar. The orientation of the bar is given by the angles  $\alpha_i$  and  $\delta_i$  measured from the axes of the  $\{\mathbf{b}\}$  frame.

# Chapter 5

## Conclusions

This thesis detailed the process for deriving the dynamics of a general tensegrity system that is subject to gravitational forces in an Earth orbit. The gravity forces and moments induced on the individual elements of the system can potentially cause the tensegrity structure to become distorted, and potential methods for avoiding or controlling these distortions were discussed. A linear control was developed that stabilizes the system to some desired equilibrium by adjusting the lengths of the tendons that interconnect the independent bars, as well as controlling the attitude of the spacecraft via force and moment thrusters. Passive control of the spacecraft's attitude via gravity-gradient stabilization was also explored.

As an example following the derivation of the dynamics of a general tensegrity system, the process was applied to a 3-bar system. A prestressed configuration for the tensegrity structure was chosen so as to keep the tendons from going slack, an undesirable possibility

in tensegrity systems that can cause large instabilities in its structure. Linear control of the system shows an eventual return from some perturbed state back to the desired equilibrium. Due to the lack of damping in the tendons, the response was highly oscillatory - as a next step in furthering the research of tensegrity systems in space, it would be beneficial and more realistic to include damping in the dynamic model.

## 5.1 Future Work

Though the general dynamics derived are capable of accounting for orbits of all shapes and radii, the numerical analysis performed was only for a simple equatorial orbit. It would be useful to know how the tensegrity spacecraft would behave, for example, in a highly eccentric orbit. The gravitational force on the spacecraft would be greater at periapsis (closest point in the orbit) than at apoapsis (farthest point), and these constantly changing forces would cause constantly changing distortions in the tensegrity structure.

Another route that can be taken to further research in the field are the other perturbative effects present in low-Earth orbit, particularly that due to atmospheric drag. Whereas gravity acts on the system in the orbit radius direction, drag acts in the orbit velocity direction. Although small, the drag forces on a system that is so inherently flexible can cause the system to distort in a direction opposite to the velocity direction, which may cause tendons to go slack unless a control is designed to counteract the distortions.

It is the author's hope that this thesis provides the backbone for pursuing more in depth

research into orbiting tensegrity spacecraft.

# Bibliography

- [1] K. Snelson, “Needle tower,” 2016. <http://kennethsnelson.net/> (Accessed 24 Oct, 2016).
- [2] G. Castro and M. P. Levy, “Analysis of the georgia dome cable roof,” in *Proceedings of the Eighth Conference of Computing in Civil Engineering and Georgraphic Information Systems Symposium* (B. J. Goodno and J. R. Wright, eds.), (Dallas, TX), American Society of Civil Engineers, June 1992.
- [3] A. Longman and R. E. Skelton, “Skyframe research and development, inc.,” 2017. <https://www.skyframeresearch.com/niac-old-1.html> (Accessed 05 Feb, 2017).
- [4] C. Sultan and R. E. Skelton, “Deployment of tensegrity structures,” *International Journal of Solids and Structures*, 2003.
- [5] P. B. de Selding, “Harris corp.: Muos radio software patch clears hurdle, antenna business booming,” *SpaceNews*, May 2016. <http://spacenews.com/harris-corp-muos-radio-software-patch-certification-imminent-antenna-business-booming/> (Accessed 05 Feb, 2017).

- [6] P. Bely, *The Design and Construction of Large Optical Telescopes*. New York, NY: Springer-Verlag New York Inc., 2003.
- [7] B. Wie, *Space Vehicle Dynamics and Control*. Reston, VA: American Institute of Aeronautics and Astronautics, 1998.
- [8] M. Rye and C. Sultan, “Modeling and control of tensegrity systems under leo gravitational effects,” in *Guidance, Navigation, and Control Conference*, (Boston, MA), American Institute of Aeronautics and Astronautics, August 2013.
- [9] B. Fuller, *Portfolio and ARTNews Annual*, vol. 4. The Art Foundation Press, 1960.
- [10] A. Pugh, *An introduction to tensegrity*. Berkeley, CA: University of California Press, 1976.
- [11] R. E. Skelton and M. C. de Oliveira, *Tensegrity Systems*. New York, NY: Springer, 1 ed., June 2009.
- [12] D. E. Ingber, “Cellular tensegrity: defining new rules of biological design that govern the cytoskeleton,” *Journal of Cell Science*, pp. 613–627, March 1993.
- [13] D. E. Ingber, “Tensegrity i. cell structure and hierarchical systems biology,” *Journal of Cell Science*, pp. 1157–1173, March 2003.
- [14] WilkonsonEyre, “Tensegrity bridge,” 2016. <http://www.wilkinsoneyre.com/projects/tensegrity-bridge> (Accessed 24 Oct, 2016).

- [15] ArchDaily, “Students of ball state construct parametric tensegrity structure for local art fair,” October 2014. <http://www.archdaily.com/553311/students-of-ball-state-construct-parametric-tensegrity-structure-for-local-art-fair> (Accessed 24 Oct, 2016).
- [16] P. Debney, “Why it’s good to be a lightweight,” *STRUCTURE Magazine*, November 2014. <http://www.structuremag.org/?p=7578> (Accessed 05 Feb, 2017).
- [17] A. Paronesso, “The 2002 world cycling center arena aigle, switzerland,” in *International IASS Symposium on “Lightweight Structures in Civil Engineering”*, (Warsaw, Poland), International Association for Shell and Spatial Structures, 2002.
- [18] A. Agongino, V. SunSpiral, and D. Atkinson, “Superball bot tensegrity planetary lander.” <https://ti.arc.nasa.gov/tech/asr/intelligent-robotics/tensegrity/superballbot> (Accessed 24 Oct, 2016).
- [19] A. Agongino, “Best lab uc berkeley,” September 2016. <http://best.berkeley.edu/best-research/best-berkeley-emergent-space-tensegrities-robotics> (Accessed 24 Oct, 2016).
- [20] M. Zhang, X. Geng, J. Bruce, K. Caluwaerts, M. Vespignani, V. SunSpiral, P. Abbeel, and S. Levine, “Deep reinforcement learning for tensegrity robot locomotion,” in *International Conference on Robotics and Automation*, (Singapore), Institute of Electrical and Electronics Engineers, March 2017.
- [21] C. Sultan, “Tensegrity motion control using internal mechanisms,” in *International Conference on Control Applications*, (Saint Petersburg, Russia), Institute of Electrical and Electronics Engineers, July 2009.



- [22] C. Sultan, M. Corless, and R. E. Skelton, “The prestressability problem of tensegrity structures: some analytical solutions,” *International Journal of Solids and Structures*, vol. 38, pp. 5223–5252, July 2001.
- [23] G. Tibert, *Deployable Tensegrity Structures for Space Applications*. PhD thesis, Royal Institute of Technology, Stockholm, Sweden, 2002.
- [24] A. Longman and R. E. Skelton, “Growth-adapted tensegrity structures: A new calculus for the space economy,” 2014. [https://www.nasa.gov/sites/default/files/files/Longman\\_2013\\_PhI\\_Tensegrity.pdf](https://www.nasa.gov/sites/default/files/files/Longman_2013_PhI_Tensegrity.pdf) (Accessed 05 Feb, 2017).
- [25] E. Howell, “Growable spacecraft: A solution to artificial gravity?,” June 2016. <http://www.airspacemag.com/daily-planet/growable-spacecraft-solution-artificial-gravity-180959584> (Accessed 05 Feb, 2017).
- [26] C. Sultan, M. Corless, and R. E. Skelton, “Peak to peak control of an adaptive tensegrity space telescope,” in *Symposium on Smart Structures and Materials*, (Newport Beach, CA), Society of Photographic Instrumentation Engineers, March 1999.
- [27] I. P. Stern, “Deployable reflector antenna with tensegrity support architecture and associated methods,” December 2002. <http://www.sumobrain.com/patents/wipo/Deployable-reflector-antenna-with-tensegrity/WO2002101880A1.pdf> (Accessed 05 Feb, 2017).

- [28] R. E. Freeland, "Survey of deployable antenna concepts," in *Large Space Antenna Systems Technology - 1982*, (Houston, TX), National Aeronautics and Space Administration, November 1982.
- [29] W. K. Belvin, H. H. Edighoffer, and C. L. Herstrom, "Quasi-static shape adjustment of a 15 meter diameter space antenna," in *28th Structures, Structural Dynamics and Materials Conference*, (Monterey, CA), American Institute of Aeronautics and Astronautics, April 1987.
- [30] R. Courant and D. Hilbert, *Methods of Mathematical Physics*, vol. 1. John Wiley & Sons, 1 ed., 1989.
- [31] R. Askey, *Mathematics and Social Utopias in France: Olinde Rodrigues and His Times*. History of Mathematics, American Mathematical Society, 2005.
- [32] R. V. D. Hilst, "Essentials of geophysics." Massachusetts Institute of Technology: MIT OpenCourseWare, 2004. <http://ocw.mit.edu> (Accessed 28 Mar, 2016).
- [33] H. Jeffreys and B. Swirles, *Methods of Mathematical Physics*. Cambridge University Press, 1966.
- [34] T. R. Kane, P. W. Likins, and D. A. Levinson, *Spacecraft Dynamics*. New York, NY: McGraw-Hill, 1983.

- [35] M. Rye and C. Sultan, “Methods for modeling tensegrity dynamics in leo,” in *SciTech Conference*, (Kissimmee, FL), American Institute of Aeronautics and Astronautics, January 2015.